The effect of fouling and concentration polarisation on the performance of an enzyme membrane reactor

Sanders, Neil

Award date:
1990

Awarding institution:
University of Bath

THE EFFECT OF FOULING AND CONCENTRATION POLARISATION ON THE PERFORMANCE OF AN ENZYME MEMBRANE REACTOR

submitted by Neil Sanders
for the degree of PhD
of the University of Bath
1990

Neil Sanders.

ProQuest LLC
789 East Eisenhower Parkway
P.O. Box 1346
Ann Arbor, MI 48106-1346

ABSTRACT

A constant flux ultrafiltration apparatus was used to investigate membrane fouling and polarisation phenomena and their effect on the performance of an enzyme membrane reactor. The specific aspects of membrane fouling and concentration polarisation investigated were:

(a) Protein (bovine serum albumin, BSA) adsorption. Membranes studied were polysulphone hollow fibres and flat sheets and regenerated cellulose flat sheets. Experiments were conducted under conditions of zero flux, and the isotherms obtained provided evidence for multilayer adsorption and also for migration of protein through to the permeate side of the membrane.

(b) Concentration polarisation of BSA was studied under conditions of constant flux; the level of polarisation was measured by reduction in bulk protein concentration. A lumped parameter model which considered the polarised layer to be uniform in concentration and constant in thickness was developed and could, when combined with a mass balance over the different regions of the system, describe the experimentally measured changes in bulk concentration.

(c) Rejection was studied using adenosine 5′ monophosphate (molecular weight 347.2) as a low molecular weight tracer. The presence of adsorbed protein (BSA) strongly affected the observed rejection of tracer, resulting in significant increases in the rejection shown by the 10,000 molecular weight cutoff polysulphone membrane (rejection increased from 15% to 60%).

The performance of the ultrafiltration apparatus when used as an enzyme reactor was evaluated. Hydrolysis of urea by urease was used as a model system. Product concentration was monitored continuously over a range of residence times and feed substrate concentrations. Experimental results were adequately described using continuous stirred tank reactor (CSTR) performance equations based on the kinetic models commonly used to describe enzyme catalysed reactions. The values suggested for substrate rejection were consistent with rejections measured during tracer studies.

Rapid deactivation of urease observed in the membrane reactor was not prevented by the use of standard sulphydryl protection agents and suggested that dynamic exchange between soluble (active) enzyme and adsorbed (inactive) enzyme occurred.

ACKNOWLEDGEMENTS

John Hubble, for untiring and enthusiastic support and advice in his role as supervisor.

John Bishop, for technical expertise and assistance with instrumentation and many of the experimental problems encountered.

Mary Lojkine, for thoroughly reading this thesis and offering constructive criticism.

The School of Chemical Engineering, for providing facilities and equipment.

The Science and Engineering Research Council, for a Quota studentship.

BIOSEP, for a research contract to study protein - membrane interactions.

CONTENTS

CHAPTER 3: PROTEIN - MEMBRANE INTERACTIONS in a CONSTANT FLUX ULTRAFILTRATION APPARATUS

CHAPTER 6: UREA HYDROLYSIS in a CONSTANT FLUX ENZYME MEMBRANE REACTOR: EXPERIMENTAL and CSTR-KINETIC MODELLING

Last Page of Contents

CHAPTER 1

INTRODUCTION

Enzyme Use and Immobilisation

Enzymes have a wide range of uses, from large scale industrial (e.g. cheese making, beer clarification) to therapeutic (e.g. removal of blood clots) (Gacesa and Hubble, 1987). In comparison to chemical catalysts, enzymes are effective at much lower temperatures and can often be highly specific, for example exhibiting selective action on one of a pair of optical isomers. However, loss of enzyme activity is often rather fast, and a half life of 70 days for immobilised glucose isomerase is an example of an exceptionally stable enzyme preparation (Gacesa and Hubble, 1987). In practice limited stability and cost are the main restrictions on the industrial use of enzymes.

Traditionally (mainly in the food industry), enzymes have been used batchwise in free solution and not recovered after use. This practice is acceptable where the enzyme cost is relatively low, and the enzyme may remain in the product. Recent applications of enzymes often require that the enzyme is recovered, both for re-use and to prevent contamination of the product. This has led to the use of immobilised enzymes.

Immobilisation allows the enzyme to be retained, for example in a packed bed, while substrate is passed through and reaction takes place. Immobilisation may be achieved in many ways, including adsorption, entrapment or covalent attachment to a support (Weetal, 1975), and means that catalysis changes from homogeneous (enzyme, substrate and product in solution) to heterogeneous (enzyme on solid; substrate and product in solution). Immobilisation removes the need to separate enzyme from the product, allows continuous processing and can improve productivity in terms of the amount of enzyme used per unit product produced (Cheryan and Mehaia, 1986). In some cases, immobilisation can

improve enzyme stability (Gacesa and Hubble, 1987).

All methods of immobilisation possess disadvantages: There is usually a loss of activity (10% to 90%) associated with immobilising enzymes, when compared to the activity in free solution. The transfer from homogeneous to heterogeneous catalysis creates problems of transport of substrates and products to and from the immobilised enzyme molecules, sometimes causing the reaction to become limited by diffusion of substrate and/or product. Immobilisation can also reduce the accessibility of the active sites of the enzymes to the reacting species, especially if the substrates are large molecules. This phenomenon is known as 'steric hindrance'. The effects of diffusional resistance and steric hindrance can reduce both the apparent activity and the specificity of enzymes. The cost of immobilisation and support materials can be significant. Some support materials lead to high pressure drops and hence operational problems when used in packed beds. The factors affecting the activity of an immobilised enzyme preparation were illustrated schematically by Engasser and Horvath (1976) (Fig 1).

Fig 1. Factors Affecting the Activity of an Immobilised Enzyme Preparation

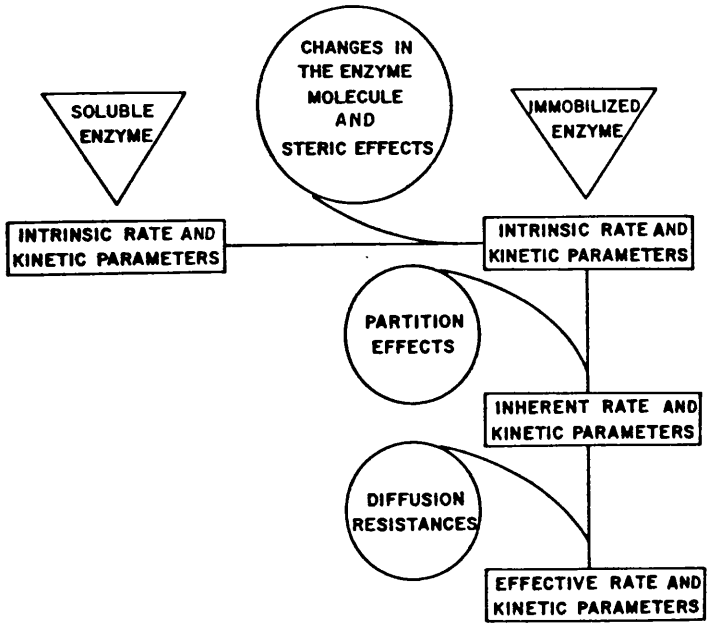

Some industrial uses of immobilised enzymes are (Vos et al, 1987):

Enzyme	Product
aminoacylase	L-amino acids
aspartase	aspartate
fumarase	fumarate
glucose isomerase	high fructose corn syrup
lactase	lactose free whey and milk
penicillin acylase	6-amino penicillanic acid

The enzymes are usually chemically attached to support beads in packed beds.

An additional restriction to further industrial use of enzymes is the requirement for cofactors for many industrially important enzyme reactions. The high cost of cofactors often precludes their use as 'disposable' reagents in batch systems, and commercial use of enymes has hitherto been largely restricted to coenzyme independent systems (Wandrey and Wichmann, 1985). Immobilisation of cofactors in order to retain and regenerate them is therefore of great significance to the future of industrial enzyme use, and there are several commercially significant enzyme reactions with cofactor requirements (Schmidt et al, 1986). Immobilisation of cofactors to traditional insoluble supports has been investigated, and the use of ultrafiltration membranes for immobilisation of both enzymes and cofactors has also received attention. The molecular size of cofactors can be increased by covalent attachment to high molecular weight soluble polymers, for example dextrans or polyethylene glycol. The complex formed is capable of contributing to the enzyme reaction, as well as being retained by an ultrafiltration membrane and regenerated in situ (Wichmann and Wandrey, 1981).

Use of Membranes for Enzyme Immobilisation

Ultrafiltration membranes are artificial, porous filters with pore sizes appropriate for retaining proteins (molecular weight 10^4 to 10^5) whilst allowing the passage of smaller molecules. The use of membranes in enzyme reactors was demonstrated by Blatt et al

(1968) for the hydrolysis of protein. The concept of enzyme membrane reactors is based on the ability of ultrafiltration membranes to retain proteins (enzymes) but allow the passage of products. There are several possible configurations for enzyme membrane reactors, classified by two criteria (Flaschel and Wandrey, 1979) (Fig 2):

-Distribution of enzyme in the reactor. The enzyme is either membrane associated (bound, adsorbed or trapped in the support matrix), or in solution.

-Driving force for products to pass the membrane. This can be either by a pressure gradient (convective) or by a concentration gradient (diffusive).

Fig 2. Classifications of Enzyme Membrane Reactor

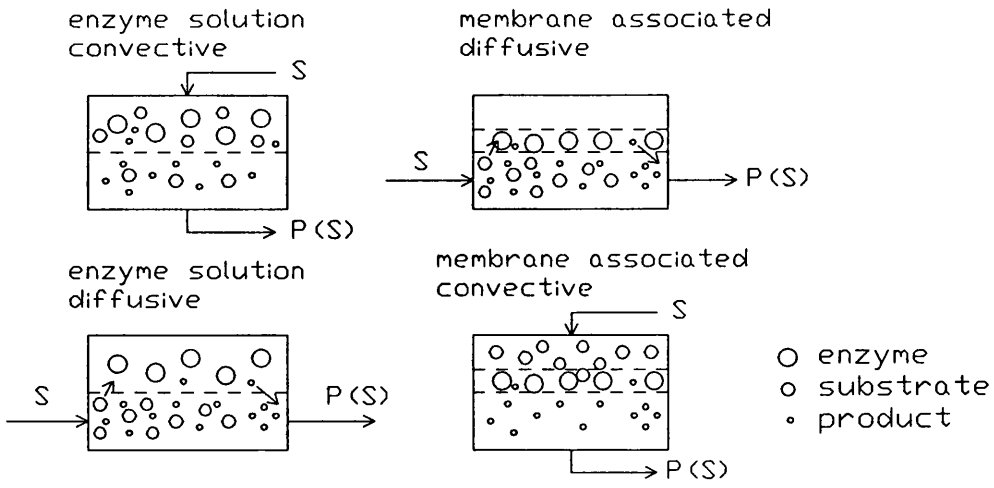

It seems likely that requirements for high throughput and high conversion will favour the convective configurations, at least for larger scale production. Diffusive operation limits the flux of product through the membrane, and requires a much larger membrane area per unit of production. Membrane associated types of reactor will incur costs for attaching the enzyme to the membrane, and the procedure for regenerating the system will be more complex than for enzyme solution reactors. Larger scale production is therefore likely to favour enzyme solution, convective types of membrane reactor.

This does not preclude the use of diffusive membrane reactors, and these have been successfully applied to cell culture for the production of small quantities of very high value products. Immobilised cell reactors have commonly used hollow fibre membrane modules with the cells growing on the shell side, whilst nutrients are supplied and products removed via the fibre lumen (Belfort, 1989; Vorlop and Lehmann, 1981). In the case of very high value products, low diffusional fluxes through the membrane and the difficulty of re-using the membrane modules need not be an insurmountable problem.

The work presented in this thesis has concentrated on enzyme solution convective membrane reactors which seem most appropriate for larger scale, enzyme catalysed reactions (Flaschel and Wandrey, 1979). These reactors have some advantages over other methods of enzyme immobilisation. The use of enzymes in solution will often result in high activity compared to chemical immobilisation, and there is no diffusive resistance to transfer of substrate and product. However, stability in solution may be less than that for chemically immobilised enzymes. In enzyme solution convective membrane reactors, ultrafiltration membranes are used in the same way as in conventional ultrafiltration operations (protein concentration), and the cost of membrane cleaning and replenishing enzyme activity is likely to be low in comparison with chemical immobilisation techniques. Activity decline can be compensated by adding more enzyme during a run, removing the need to reduce throughput to maintain conversion. Enzyme solution convective membrane reactors seem to offer a promising alternative to chemical immobilisation techniques. In addition, they allow immobilisation and in situ regeneration of coenzymes on an industrial scale (Leuchtenberger et al, 1983).

Literature Survey on Membrane Reactors

The literature on membrane reactors is large, and includes a great deal of work on cell culture as opposed to enzyme reactions.

There are several good reviews on membrane reactors:

Flaschel and Wandrey (1979) - classification of types of reactor; membranes for membrane reactors; enzyme characterisation and reactor performance.

Flaschel et al (1983b) - theory, design and operation of membrane reactors. Enzyme, coenzyme dependent and microorganism systems.

Wandrey (1983) - cofactor regeneration in membrane reactors.

Hummel et al (1984) - enzymes and membrane reactors for the synthesis of chiral compounds.

Gekas (1986) - soluble and attached biocatalysts.

Cheryan and Mehaia (1986) - enzymes and microorganisms; cofactor regeneration.

Chang (1987) - enzymes, microorganisms and animal and plant cell culture.

Hanemaaijer et al (1987) - membrane reactor work at the Netherlands dairy institute.

Belfort (1989) - membrane reactors for cell culture.

In order to simplify the treatment of the literature presented here, the survey has been restricted to enzyme membrane reactors. It is largely concerned with the convective, enzyme in solution type, in keeping with the system studied in this work.

Enzyme solution convective membrane reactors have been constructed in many configurations. A common laboratory reactor consists of a stirred vessel with an ultrafiltration membrane in its base, the purpose of the stirrer being to reduce concentration polarisation (Berke et al, 1988; Darnoko et al, 1989). Transmembrane flux is induced by pressurisation with gas or by pumping in more feed solution. Stirred ultrafiltration cells have been used in batch or semi-batch mode (Ohlson et al, 1983) as well as continuous mode. This apparatus has been widely used to investigate the feasibility and/or kinetics of particular reaction systems in membrane reactors, but the small membrane area prevents application on a larger scale. In practice, membrane reactors

usually comprise crossflow membrane modules in conjunction with a continuous stirred tank reactor (CSTR) or a tubular (plug flow) reactor (PFR). Plug flow reactors with recycle to a membrane module were used by Flaschel et al (1983a).

Membrane reactor systems incorporating CSTR or PFR are often referred to as recycle reactors (Cheryan and Mehaia, 1986) as the retentate containing enzyme is recycled back to the reaction vessel from the membrane module. Many different membrane configurations have been used, including:

Hollow fibres (Koyama et al, 1987; Piot et al, 1988; Cheryan and Deeslie, 1983; Bressollier et al, 1988).

Thin channels (Schmid and Wandrey, 1987; Azhar and Hamdy, 1981; Ryu et al, 1972; Gacesa et al, 1983).

Tubular modules (Howaldt et al, 1988; Piot et al, 1988).

Perhaps the simplest form of recycle membrane reactor is one which has only a recycle pump and a membrane module: All the reaction volume is provided by the holdup of pump, membrane module and connecting pipework. The small volume of such systems, especially when based on hollow fibre membranes, makes them attractive for laboratory investigation of membrane reactors (Schmid and Wandrey, 1987). A further advantage is that the presence of a crossflow membrane module brings the operating conditions closer to those in a large scale recycle system than would be the case with a stirred ultrafiltration cell. A closed recycle loop invites operation in constant flux mode, where feed solution is forced into the recycle loop by a constant flow pump, and must exit through the membrane (Turker and Hubble, 1987).

Ultrafiltration is not the only membrane process applied to membrane reactors. The feasibility of dialytic membrane reactors has been demonstrated by Catapano et al (1989) and Williams et al (1989). Product was extracted by dialysis, and reverse osmosis was used to concentrate the product in the dialysate. Inorganic membrane reactors have been used for chemical reactions, an area

which is reviewed by Hsieh (1989). Electrophoresis can allow preferential removal of product from a membrane reactor (Lee and Hong, 1987, 1988; Kitpreechavanich, 1985; Kulbe et al, 1987a, 1987b).

Membrane reactors have been applied to a wide range of reaction systems, a brief summary of which will be presented here.

Production of L-amino acids is an area which has received considerable attention. These reactions require cofactors and have featured in the development of coupled enzyme systems for in-situ regeneration of cofactors. The cofactors are bound to soluble polymers, allowing them to be retained by ultrafiltration membranes (Leuchtenberger et al, 1983; Hummel et al, 1984; Wandrey, 1983; Wandrey et al, 1978; Wichmann et al, 1981; Ohshima et al, 1985, 1989; Fiolitakis and Wandrey, 1983; Bossow and Wandrey, 1987).

Protein hydrolysis has been undertaken in membrane reactors, to produce hydrolysates for improvement of the functional and/or nutritional properties of food products (Blatt et al, 1968; Boudrant and Cheftel, 1976; Cheryan and Deeslie, 1983; Cunningham et al, 1978; Deeslie and Cheryan, 1981a, 1981b, 1982; Iacobucci et al, 1974; Roozen and Pilnik, 1979; Piot et al, 1988; Bresollier et al, 1988). Membrane reactors are an obvious choice for protein hydrolysis as the substrate will be retained until it has been broken down to smaller (amino acid) products, thus permitting high conversions. Protein hydrolysis was one of the first reaction systems to be carried out in a membrane reactor (Blatt et al, 1968). Choice of membrane cutoff may allow the molecular weight distribution of the products to be controlled (Cheryan and Mehaia, 1986).

Starch hydrolysis is of interest for the production of glucose, high fructose sweeteners, brewing syrups and fermentation substrates. As in protein hydrolysis, the large difference in

molecular weight between the substrate and products can be advantageous, but fouling of the membrane is often a problem (Closset et al, 1974; Darnoko et al, 1989). Single pass tubular membrane reactors have been applied to starch hydrolysis; enzyme and substrate are fed through a tubular membrane, so that reaction and separation occur (Closset et al, 1974; Tachauer et al, 1974; Madagavkar et al, 1977; Subramanian, 1976). It is unlikely that this type of reactor will be of commercial significance, due to the low efficiency of enzyme use and the conflicting requirements of high shear and long residence time. More conventional membrane reactors in starch hydrolysis have also been investigated (Azhar and Hamdy, 1981; Butterworth et al, 1970; Darnoko et al, 1989; Marshall and Whelan, 1971; Porter and Michaels, 1972; Matsumura and Hirata, 1989).

Cellulose hydrolysis is of interest because the hydrolysate can be used as a fermentation substrate for alcohol production (Ghose and Kostick, 1970; Hagerdal et al, 1980; Henley et al, 1980; Luchini and Pozzi, 1986; Ohlson et al, 1983, 1984a, 1984b; Porter and Michaels, 1972; Frennesson et al, 1985; Schmid and Wandrey, 1987). Work on cellulose hydrolysis has highlighted one of the problems associated with membrane reactors - that of enzyme deactivation by adsorption (Ohlson et al, 1983).

Sugar hydrolysis has received considerable attention in the membrane reactor literature, partly because it makes a convenient model system and partly because of commercial interest in the hydrolysis of lactose in cheese whey (Bowski et al, 1972; Bowski and Ryu, 1974; Flaschel et al, 1983a; Huffman and Harper, 1982, 1985; Katoh et al, 1978; Miller and Brand, 1980; Norman et al, 1978; Howaldt et al, 1988; Mertens and Huyghebeart, 1987; Lee and Hong, 1987). Several modes of operation of a hollow fibre membrane reactor were investigated by Huffman and Harper (1982), including immobilisation of enzyme by backflushing into the porous support region of the hollow fibres. A single pass tubular membrane reactor was studied and modelled by Katoh et al (1978).

The model was based on solution of the convection-diffusion equations for a permeating tube with reaction and partial rejection of enzyme, substrate and product and provides the basis for a comprehensive mathematical description of enzyme solution convective membrane reactors.

Several other reactions have been carried out in membrane reactors, and are summarised here:

Cellobiose hydrolysis (Hong et al, 1981). A stirred ultrafiltration cell was studied and modelled, the model taking into account the reduction in bulk enzyme concentration due to concentration polarisation. Enzyme deactivation was accelerated at high levels of polarisation. Cellobiose hydrolysis was also investigated by Alfani et al (1990).

Oil (triglyceride) hydrolysis has attracted considerable interest, although most work has concentrated on diffusive operation with the membrane acting as a phase separation barrier (Hoq et al, 1984). An exception is the work by Molinari et al (1988) who performed hydrolysis of olive oil in aqueous solution in an enzyme solution convective membrane reactor with hollow fibre membranes.

Penicillin drug precursors (Ryu et al, 1972; Noworyta, 1989).

Pectin hydrolysis to D-galactouronic acid (Kulbe et al, 1987b).

R-mandelic acid production (Vasic-Racki et al, 1989).

L-aspartic acid production (Koyama et al, 1987).

Xylitol production (Kitpreechavanich, 1985) - using a functionalised membrane.

Urea hydrolysis (Gacesa et al, 1983) was used as a model system for investigating the performance of a membrane reactor. This system has the advantage of producing ammonium ions, whose concentration is easy to measure continuously using ion selective electrodes. Urease is also highly active, very specific and relatively cheap. The urease-urea system is attractive for reactor studies where the fundamentals rather than the reaction

system are being studied.

Modelling of enzyme membrane reactors has been undertaken, but has generally been restricted to consideration of the system as an ideal CSTR together with an enzyme kinetic model (Bowski et al, 1972; Ryu et al, 1972; Deeslie and Cheryan, 1981a; Wichmann et al, 1981). These models have not always been capable of a complete description of system performance over a range of operating conditions. A similar model was used to determine the type of inhibition in a membrane reactor (Alfani et al, 1990). Modifications of CSTR-kinetic models have been made, for example by Hong et al (1981), who calculated the reduction in bulk enzyme concentration due to concentration polarisation. The contribution of the polarised layer to the overall reaction rate was assumed to be negligible. Flaschel et al (1983a) modelled a PFR recycle system as a combination of ideal PFR and CSTR reactors. More complex models for reactions occurring in porous channels have been developed, based on solution of the convection-diffusion equations in two dimensions for each solute (Katoh et al, 1978; Shah and Remmen, 1971). These models have so far been applied only to once-through systems, which are likely to result in inefficient use of enzyme in comparison to a recycle system. Adaptation of such models for recycle membrane reactors would increase the complexity of the solution.

The review of the literature on enzyme solution convective membrane reactors has shown that these reactors have been applied to many commercially significant reaction systems with success. Often, productivity has been high in terms of the amount of product obtained per unit mass of enzyme used. High conversion and long term stability have been achieved, and the feasibility of cofactor immobilisation and in situ regeneration with conjugated enzyme systems has been demonstrated. However, the influence of membrane fouling and spatial solute distribution on reactor performance has received relatively little attention.

Some Aspects of Ultrafiltration Membrane Fouling

Ultrafiltration is, in principle, a screening process, where molecules larger than the pores are rejected and molecules smaller than the pores are transmitted. However, real membranes possess a distribution of pore sizes so that molecules smaller than the nominal molecular weight cutoff (nmwco) of the membrane may be partially rejected, and molecules larger than the nmwco may be partially transmitted. Charge effects are also important, and charged molecules may be preferentially retained or transmitted in comparison to uncharged molecules of the same size. On exposure to solutes, and notably proteins, ultrafiltration membranes become fouled, leading to a reduction in permeability and often to an increase in solute rejection. Fouling is often regarded as the most serious disadvantage of the ultrafiltration process, and has received a great deal of attention in the literature (e.g. Matthiasson, 1985; Fane and Fell, 1987). One example of a recent text on crossflow membrane filtration is the work by Gutman (1987).

Membrane fouling has been defined in different ways, depending on the background of the author concerned. In this work, it has been divided into two categories: The irreversible or slowly reversible interaction of proteins with the membrane is referred to as 'adsorption', and is often accompanied by denaturation of the protein. Reversible polarisation of solutes (proteins or otherwise) towards the membrane due to transmembrane flux is referred to as 'concentration polarisation' or 'deposition'.

The two fouling phenomena of adsorption and polarisation are linked, because polarisation causes an increased concentration at the membrane surface, resulting in an increased 'driving force' for adsorption. In membrane systems where the effect of fouling is being studied, constant flux operation is valuable because at constant flux and crossflow, the degree of concentration polarisation remains the same.

Adsorption of protein (or other) molecules has been assumed to take place within the membrane pores, reducing pore size and therefore causing an increase in solute rejection and a decrease in permeability (Dejmek and Nilsson, 1989; Hanemaaijer et al, 1989). Highly polarised protein layers may present a significant resistance to solute flow, as well as increasing rejection.

Basis of the Project

The aspects of membrane ultrafiltration discussed above may significantly affect the performance of an enzyme membrane reactor. In the enzyme solution convective membrane reactor considered here, the enzyme solution is recirculated across the retentate side of the membrane module and substrate solution is fed into the closed recycle loop, forcing a flux through the membrane. The main implications of membrane fouling on the performance of such a membrane reactor are:

Adsorption: The enzyme (a protein) will initially be present in the reactor in solution after injection into the recycle loop. Adsorption of the enzyme onto the membrane is likely to occur, the extent of which will depend on the degree of concentration polarisation and the particular enzyme and membrane used. Enzyme denaturation, and thus deactivation, is likely to occur upon adsorption (Norde, 1986), thus reducing the total enzyme activity. After the initial adsorption, dynamic exchange of protein between adsorbed and dissolved states may occur (Brash and Samak, 1978), resulting in longer term loss of activity. The degree of protein adsorption is also likely to affect the membrane permeability and rejection properties (Matthiasson, 1983; Hanemaaijer et al, 1989).

Polarisation: Most models of enzyme solution convective membrane reactors have been based on the ideal CSTR, with the inherent assumption that there is no spatial variation of solute concentrations within the reactor volume. Polarisation of enzyme, and possibly substrate and product, could render this assumption

invalid, necessitating a different modelling approach. It may be possible to enhance reactor performance by using polarisation phenomena to cause localised high concentrations of enzyme and substrate near the membrane surface.

Solute Rejection: Rejection of small molecules (molecular weight of the order of 10^2) by previously unused ultrafiltration membranes of nmwco 10^4 is usually very low, so rejection of the products of enzyme reactions is often assumed to be zero (Alfani et al, 1990). However, fouling can lead to increased rejection of solutes by ultrafiltration membranes, and if the rejection increase is significant, the effect on membrane reactor performance could be marked. Product rejection would result in higher steady state product concentrations in the reactor - an important factor for product inhibited reactions. Substrate rejection would increase the operating substrate concentration, the effect of which would depend on the degree of substrate inhibition of the reaction. The amount of substrate lost through the membrane, and the choice of membrane cutoff for a given reaction system will both be determined by the effect of fouling on solute rejection.

In the forgoing discussion, some of the important consequences of membrane fouling on the performance of enzyme membrane reactors have been identified as being due to the fouling phenomena of adsorption, polarisation and changes in solute rejection. This project comprises detailed investigations if these phenomena, together with work on a model reacting system (urease-urea) in a membrane reactor to assess the effects of fouling.

Use of a constant flux ultrafiltration cell (Turker and Hubble, 1987) removes the complication of polarisation changing with time. Solute-membrane interactions are magnified by using a hollow fibre membrane module with a high membrane area : system volume ratio for much of the work. The hydrolysis of urea with urease, although of limited commercial importance, has several advantages

(product concentration measurement, activity, cost), and makes a suitable reaction system for the investigation of membrane reactor performance.

Summary

Membrane reactors offer a means of enzyme immobilisation with some advantages over enzymes chemically immobilised onto packed beds. In particular, a membrane reactor with enzyme in solution and convective transmembrane flux can offer low preparation costs and the possibility of high activity and selectivity because the enzyme is used in solution. Cofactor retention and regeneration can be achieved, and volumetric throughput is potentially high in comparison with diffusive membrane reactors. Membrane fouling will be a significant factor affecting the performance of such a reactor, and the purpose of this project is to qualify and quantify the effects of fouling.

A constant flux ultrafiltration apparatus is an appropriate means of investigating a membrane reactor, as the polarisation conditions will remain constant. A large membrane area in comparison with the system volume is advantageous as it magnifies the effect of solute-membrane interactions. Urease-urea is attractive as a model reaction system, because the product concentration may be easily and continuously measured.

The fouling phenomena likely to affect the performance of a membrane reactor are protein adsorption, concentration polarisation and changes in rejection of smaller solutes. This investigation into the effects of the above phenomena on reactor performance comprises studies of adsorption, polarisation and solute rejection in isolation. Information gained from these studies, together with a characterisation of the performance of the system as a membrane reactor, should improve the understanding of the effects of membrane fouling on an enzyme membrane reactor.

REFERENCES

Alfani, F.; Gallifuoco, A.; Cantarella, M.
"Study of Michaelis-Menten kinetics with linear type product inhibition in ultrafiltration membrane reactors: Mathematical model, experimental and data correlation".
The Chem. Eng. J., 43 (1990) B43-B51.

Azhar, A.; Hamdy, M.K.
"Alcohol fermentation of sweet potato. Membrane reactor in enzymatic hydrolysis".
Biotechnol. Bioeng., 23 (1981) 1297-1307.

Belfort, G.
"Membranes and bioreactors: a technical challenge to biotechnology".
Biotechnol. Bioeng., 33 (1989) 1047-1066.

Berke, W.; Schuz, H.-J.; Wandrey, C.; Morr, M.; Denda, G.; Kula, M.-R.
"Continuous regeneration of ATP in enzyme membrane reactor for enzymatic syntheses".
Biotechnol. Bioeng., 32 (1988) 130-139.

Blatt, W.F.; Hudson, B.G.; Robinson, S.M.; Zipilivan, E.M.
"A modified ultrafiltration cell for separating the products of hydrolysis".
Anal. Biochem., 22 (1968) 161-165.

Bossow, B.; Wandrey, C.
"Continuous enzymatically catalysed production of L-leucine from the corresponding racemic hydroxy acid".
Ann. N.Y. Acad. Sci., 506 (Biochem. Eng. 5) (1987) 325-336.

Boudrant, J.; Cheftel, C.
"Continuous proteolysis with a stabilised protease. II. Continuous experiments".
Biotechnol. Bioeng., 18 (1976) 1735-1749.

Bowski, L.; Shah, P.M.; Ryu, D.Y.; Vieth, W.R.
"Process simulation of sucrose hydrolysis on invertase in a continuous flow stirred tank / UF reaction system".
Biotechnol. Bioeng. Symp. Ser., 3 (1972) 229-239.

Bowski, L.; Ryu, D.Y.
"Determination of invertase activity during ultrafiltration".
Biotechnol. Bioeng., 16 (1974) 697-699.

Brash, J.L.; Samak, Q.M.
"Dynamics of interactions between human albumin and polyethylene surface".
J. Colloid Interface Sci., 65 (1978) 495-504.

Bressollier, Ph.; Petit, J.M.; Julien, R.
"Enzyme hydrolysis of plasma proteins in a CSTR ultrafiltration reactor: performances and modeling".
Biotechnol. Bioeng., 31 (1988) 650-658.

Butterworth, T.A.; Wang, D.I.C.; Sinskey, A.J.
"Application of ultrafiltration for enzyme retention during continuous enzymatic reaction".
Biotechnol. Bioeng., 12 (1970) 615-631.

Catapano, G.; Williams, T.E.; Klein, E.; Ward, R.A.
"A dialytic membrane reactor for the reduction of product inhibition in the processing of natural substrates".
6th Int. Symp. Membr. Sci. Ind., Tubingen (1989) 151-154.

Chang, H.N.
"Membrane bioreactors: Engineering aspects".
Biotechnol. Adv., 5 (1987) 129-145.

Cheryan, M.; Deeslie, W.D.
"Soy protein hydrolysis in membrane reactors".
J. Am. Oil Chem. Soc., 60 (1983) 1112-1115.

Cheryan, M.; Mehaia, M.A.
"Membrane Bioreactors".
Bioprocess Technol. 1 (Membrane Separations in Biotechnology) (1986) 255-301.

Closset, G.P.; Cobb, J.T.; Shah, Y.T.
"Study of performance of a tubular membrane reactor for an enzyme catalysed reaction".
Biotechnol. Bioeng., 16 (1974) 345-360.

Cunningham, S.D.; Cater, C.M.; Mattil, K.F.
"Cottonseed protein modification in an ultrafiltration cell".
J. Food. Sci., 43 (1978) 1477-1480.

Darnoko, D.; Cheryan, M.; Artz, W.E.
"Saccharification of cassava starch in an ultrafiltration reactor".
Enzyme. Microb. Technol., 11 (1989) 154-159.

Deeslie, W.D.; Cheryan, M.
"A CSTR-hollow fibre system for continuous hydrolysis of proteins. Performance and kinetics".
Biotechnol. Bioeng., 23 (1981a) 2257-2271.

Deeslie, W.D.; Cheryan, M.
"Continuous enzymatic modification of proteins in an ultrafiltration reactor".
J. Food Sci., 46 (1981b) 1035-1042.

Deeslie, W.D.; Cheryan, M.
"A CSTR-hollow fibre system for continuous hydrolysis of proteins. Factors affecting long term stability of the reactor".
Biotechnol. Bioeng., 24 (1982) 69-82.

Dejmek, P.; Nilsson, J.L.
"Flux based measures of adsorption to ultrafiltration membranes".
J. Membr. Sci., 40 (1989) 189-197.

Engasser, J.M.; Horvath, C.
"Diffusion and kinetics with immobilized enzymes".
in Applied Biochemistry and Bioengineering V1 (Immobilized Enzyme Principles), eds. Wingard, L.B. et al, Academic, New York (1976) 127-220.

Fane, A.G.; Fell, C.J.D.
"A review of fouling and fouling control in ultrafiltration".
Desalination, 62 (1987) 117-136.

Fiolitakis, E.; Wandrey, C.
"Reaction technology of the enzymatically catalysed production of L-alanine".
Enzyme Technology - 3rd Rotenburg Ferment. Symp. (1983).

Flaschel, E.; Raetz, E.; Renken, A.
"Development of a tubular recycle membrane reactor for continuous operation with soluble enzymes".
Enzyme Technology, ed. Lafferty, R. (Rotenberg Fermen. Symp.) (1983a) 285-295.

Flaschel, E.; Wandrey, C.; Kula, M.-R.
"Ultrafiltration for the separation of biocatalysts".
Adv. Biochem. Eng. Biotechnol., 26 (1983b) 73-142.

Flaschel, E.; Wandrey, C.
"Membrane reactors".
Dechema Monographs, 84 (1724-1731) (1979) 337-366.

Frennesson, I.; Tragardh, G.; Hahn-Hagerdal, B.
"An ultrafiltration membrane reactor for obtaining experimental reaction rates at defined concentrations of inhibiting sugars".
Biotechnol. Bioeng., 27 (1985) 1328-1334.

Gacesa, P.; Eisenthal, R.; England, R.
"Immobilization of urease within a thin channel ultrafiltration cell".
Enzyme Microb. Technol., 5 (1983) 191-195.

Gacesa, P.; Hubble, J.
"Enzyme Technology".
Open University Press, Milton Keynes, 1987.

Gekas, V.C.
"Artificial membranes as carriers for the immobilisation of biocatalysts".
Enzyme Microb. Technol., 8 (1986) 450-460.

Ghose, T.K.; Kostick, J.A.
"A model for continuous enzymatic saccharification of cellulose with simultaneous removal of glucose syrup".
Biotechnol. Bioeng., 12 (1970) 921-946.

Gutman, R.G.
"Membrane filtration: the technology of pressure driven crossflow processes".
IOP Publishing Ltd, Bristol, 1987.

Hagerdal, B.; Lopez-Leiva, M.; Mattiasson, B.
"Membrane technology applied to bioconversion of macromolecular substrates and upgrading of products".
Desalination, 35 (1980) 365-373.

Hanemaaijer, J.H.; Stadhouders, J.; Visser, S.
"Fermentations and enzyme conversions in membrane reactors".
Proc. 4th Eur. Congr. Biotechnol., 1 (1987) 145.

Hanemaaijer, J.H.; Robbertsen, T.; Boomgaard, T.; Gunnink, J.W.
"Fouling of ultrafiltration membranes. The role of protein adsorption and salt precipitation".
J. Membr. Sci., 40 (1989) 199-217.

Henley, R.G.; Yang, R.Y.K.; Greenfield, P.F.
"Enzymatic saccharification of cellulose in membrane reactors".
Enzyme Microb. Technol., 2 (1980) 206-208.

Hong, J.; Tsao, G.T.; Wankat, P.C.
"Membrane reactor for enzymatic hydrolysis of cellobiose".
Biotechnol. Bioeng., 23 (1981) 1501-1516.

Hoq, M.M.; Yamane, T.; Shimizu, S.; Funada, T.; Ishida, S.
"Continuous synthesis of glycerides by lipase in a microporous membrane reactor".
J. Am. Oil Chem. Soc., 61 (1984) 776-781.

Howaldt, M.; Gottlob, A.; Kulbe, K.D.; Chmiel, H.
"Simultaneous conversion of glucose/fructose mixtures in a membrane reactor".
Ann. N.Y. Acad. Sci., 542 (Enzyme Eng. 9) (1988) 400-405.

Hsieh, H.P.
"Inorganic membrane reactors - a review".
AIChE Symp. Ser., 85 (No 268, Membrane Reactor Technol.) (1989) 53-67.

Huffman-Reichenbach, L.; Harper, W.J.
"Beta-galactosidase retention by hollow fiber membranes".
J. Dairy Sci., 65 (1982) 887-898.

Huffman, L.; Harper, W.J.
"Lactose hydrolysis in batch and hollow fiber membrane reactors".
N.Z. J. Dairy Sci. Technol., 20 (1985) 57-63.

Hummel, W.; Schuette, H.; Kula, M.-R.
"New enzymes for the synthesis of chiral compounds".
Ann. N.Y. Acad. Sci., 434 (1984) 194-205.

Iacobucci, G.A.; Myers, M.J.; Emi, S.; Myers, D.V.
"Large scale continuous production of soybean protein hydrolysate in a constant flux membrane reactor".
Proc. 4th Int. Congr. Food Sci. Technol., 5 (1974) 83-95.

Katoh, S.; Yanagida, T.; Sada, E.
"Performance of a membrane-type enzyme reactor utilizing ultrafiltration".
J. Chem. Eng. Japan, 11 (1978) 143-146.

Kitpreechavanich, V.; Nishio, N.; Hayashi, M.; Nagai, S.
"Regeneration and retention of NADP(H) for xylitol production in an ionized membrane reactor".
Biotechnol. Lett., 7 (1985) 657-662.

Koyama, Y.; Shimazaki, K.; Akashi, K.; Kawahara, Y.;
Kubota, K.; Yoshii, H.
"Production of L-aspartic acid by membrane reactor".
Proc. 4th Int. Congr. Biotechnol. 1 (1987) 119.

Kulbe, K.D.; Schwab, U.; Gudernatsch, W.
"Enzyme-catalyzed production of mannitol and gluconic acid".
Ann. N.Y. Acad. Sci., 506 (Biochem. Eng. 5) (1987a) 552-568.

Kulbe, K.D.; Heinzler, A.; Knopki, G.
"Enzymatic synthesis of L-ascorbic acid via D-uronic acids; membrane -reactor integrated recovery of D-galactouronic acid from pectin hydrolysates".
Ann. N.Y. Acad. Sci., 506 (Biochem. Eng. 5) (1987b) 543-550.

Lee, C.K.; Hong, J.
"Enzyme reaction in a membrane cell coupled with electrophoresis".
Ann. N.Y. Acad. Sci., 506 (Biochem. Eng. 5) (1987) 499-510.

Lee, C.K.; Hong, J.
"Membrane reactor coupled with electrophoresis for enzymatic production of aspartic acid".
Biotechnol. Bioeng., 32 (1988) 647-654.

Leuchtenberger, W.; Karrenbauer, M.; Plocker, U.
"Scale-up of an enzyme membrane reactor process for the manufacture of L-enantiomeric compounds".
Ann. N.Y. Acad. Sci., 434 (1983) 78-86.

Luchini, P.; Pozzi, A.
"Unsteady state behaviour of enzyme membrane reactors with substrate rejection".
J. Membr. Sci., 27 (1986) 263-274.

Madagavkar, A.M.; Shah, Y.T.; Cobb, J.T.
"Hydrolysis of starch in a membrane reactor".
Biotechnol. Bioeng., 19 (1977) 1719-1726.

Marshall, J.J.; Whelan, W.J.
"A new approach to the use of enzymes in starch technology".
Chem. Ind., (1971) 701-702.

Matsumura, M.; Hirata, J.
"Continuous simultaneous saccharification and fermentation of raw starch in a membrane reactor".
J. Chem. Technol. Biotechnol., 46 (1989) 313-326.

Matthiasson, E.
"The role of macromolecular adsorption in fouling of ultrafiltration membranes".
J. Membr. Sci., 16 (1983) 23-36.

Matthiasson, E.
"Fouling in membrane filtration".
in Fouling and Cleaning in Food Processing, eds. Lund, D. et al, Univ. Madison, Wi, USA (1985) 429-448.

Mertens, B.; Huyghebeart, A.
"Lactose hydrolysis in an enzymatic membrane reactor".
Milchwissenschaft, 42 (1987) 640-645.

Miller, J.J.; Brand, J.C.
"Enzymic lactose hydrolysis".
Food Technol. Australia, 32 (1980) 144, 146-147.

Molinari, R.; Drioli, E.; Barbieri, G.
"Membrane reactor in fatty acid production".
J. Membr. Sci., 36 (1988) 525-534.

Norde, W.
"Adsorption of proteins from solution at the solid-liquid interface".
Adv. Colloid and Interface Sci., 25 (1986) 267-340.

Norman, B.E.; Severinsen, S.G.; Nielsen, T.; Wagner, J.
"Enzymatic treatment of whey permeate with recovery of enzyme by ultrafiltration".
World Galaxy for the World Dairy Ind., 7 (1978) 20-23.

Noworyta, A.
"Immobilization of enzymes in membrane bioreactor".
6th Int. Symp. Synth. Membr. Sci. Ind., Tubingen (1989) 375-378.

Ohlson, I.; Tragardh, G.; Hahn-Hagerdal, B.
"Recirculation of cellulolytic enzymes in an ultrafiltration membrane reactor".
Acta Chemica Scandinavica, 37 (1983) 737-738.

Ohlson, I.; Tragardh, G.; Hahn-Hagerdal, B.
"Enzymatic hydrolysis of sodium hydroxide pretreated sallow in an ultrafiltration membrane reactor".
Biotechnol. Bioeng., 26 (1984a) 647-653.

Ohlson, I.; Tragardh, G.; Hahn-Hagerdal, B.
"Evaluation of UF and RO in a cellulose saccharification process".
Desalination, 51 (1984b) 93-101.

Ohshima, T.; Wandrey, C.; Kula, M.-R.; Soda, K.
"Improvement for L-leucine production in a continuously operated membrane reactor".
Biotechnol. Bioeng., 27 (1985) 1616-1618.

Ohshima, T.; Wandrey, C.; Conrad, D.
"Continuous production of 3-fluoro-L-alanine with alanine dehydrogenase".
Biotechnol. Bioeng., 34 (1989) 394-397.

Piot, J.-M.; Guillochon, D.; Leconte, D.
"Application of ultrafiltration to the preparation of defined hydrolysates of bovine haemoglobin".
J. Chem. Technol. Biotechnol., 42 (1988) 147-156.

Porter, M.C.; Michaels, A.S.
"Membrane ultrafiltration: Part 5; a useful adjunct for fermentative and enzymatic processing of foods".
Chem. Technol. (1972) 56-61.

Roozen, J.P.; Pilnik, W.
"Enzymatic protein hydrolysis in a membrane reactor related to taste properties".
Enzyme. Microb. Technol., 1 (1979) 122-124.

Ryu, D.Y.; Bruno, C.F.; Lee, B.K.; Venkatasubramanian, K.
"Microbial penicillin amidohydrolase and the performance of a continuous enzyme reactor system".
Proc. IFS: Ferment. Technol. Today (1972) 307-314.

Schmid, G.; Wandrey, C.
"Investigation of the action mechanism of a cellodextrin glucohydrolase using soluble cellodextrins as substrates".
Ann. N.Y. Acad. Sci., 506 (Biochem. Eng. 5) (1987) 642-648.

Schmidt, E.; Bossow, B.; Wichmann, R.; Wandrey, C.
"The enzyme membrane reactor - an alternative approach for continuous operation with enzymes".
Kem. Ind., 35 (1986) 71-77.

Shah, Y.T., Remmen, T.
"Radial mass transfer effects in a porous wall tubular reactor".
Int. J. Heat Mass Transfer, 14 (1971) 2109-2124.

Subramanian, T.V.
"Hydrolysis of starch by a mixture of enzymes in a membrane reactor".
Biotechnol. Bioeng., 18 (1976) 1473-1478.

Tachauer, E.; Cobb, J.T.; Shah, Y.T.
"Hydrolysis of starch by a mixture of enzymes in a membrane reactor".
Biotechnol. Bioeng., 16 (1974) 545-550.

Turker, M.; Hubble, J.
"Membrane fouling in a constant flux ultrafiltration cell".
J. Membr. Sci., 34 (1987) 267-281.

Vasic-Racki, D.; Jonas, M.; Wandrey, C.; Hummel, W.; Kula, M.-R.
"Continuous R-mandelic acid production in an enzyme membrane reactor".
Applied Microbiol. Biotechnol., 31 (1989) 215-222.

Vorlop, J.; Lehmann, J.
"Scale-up of bioreactors for fermentation of mammalian cell cultures with special reference to oxygen supply and microcarrier mixing".
Chem. Eng. Technol., 11 (1981) 171-.

Vos, H.J.; Groen, D.J.; Potters, J.J.M.; Luyben, K.Ch.A.M.
"Reactor development for immobilised enzyme reactor systems".
Proc. 4th Int. Congr. Biotechnol., 1 (1987) 188-190.

Wandrey, C.
"Enzyme membrane reactor systems".
Biotechnol. 83, Proc. Int. Conf. Commer. Appl. Implic. Biotechnol. (1983) 577-588.

Wandrey, C.; Flaschel, E.; Schugerl, K.
"Use of soluble enzymes in continuous reactor operation by means of hollow fiber ultrafiltration membranes".
Ger. Chem. Eng., 1 (1978) 39-43.

Wandrey, C.; Wichmann, R.
"Coenzyme regeneration in membrane reactors".
Biotechnology Series 5 (1985) Ch8 177-208.

Weetal, H.H.
"Immobilised enzymes and their application in the food and beverage industry".
Process Biochem., 10(6) (1975) 3-12, 22, 30.

Wichmann, R.; Wandrey, C.; Buckmann, A.F.; Kula, M.-R.
"Continuous enzymatic transformation in an enzyme membrane reactor with simultaneous NAD(H) regeneration".
Biotechnol. Bioeng., 23 (1981) 2789-2802.

Williams, T.E.; Catapano, G.; Klein, E.; Ward, R.A.
"Reduction of product inhibition by use of an enzyme membrane reactor in the processing of natural substrates".
AIChE Symp. Ser., 85 (No 268, Membrane Reactor Technol.) (1989) 1-9.

Last Page of Chapter 1

CHAPTER 2

CONSTANT FLUX ULTRAFILTRATION APPARATUS

ABSTRACT

The apparatus used in this work was based on the constant flux principle (Turker and Hubble, 1987). A closed recycle loop incorporated the retentate region and a circulating pump. A second pump forced feed solution into the recycle loop, thus inducing a transmembrane flowrate (flux). The use of positive displacement pumps for feed and recycle (crossflow) meant that at constant pump settings, the polarisation conditions remained constant. Constant polarisation is a valuable tool when studying solute-membrane interactions, as it means that the solute concentration at the membrane surface does not change.

The apparatus incorporated on-line measurement of pressure, concentration and flowrate in both retentate (recycle) and permeate streams. The problem of measuring low permeate flowrates necessitated the development of a novel flowmeter (Bishop and Sanders, 1989). Permeate flow measurements were logged over a variable time interval by a microcomputer, which also controlled some of the instruments. Data logging software was developed to allow continuous, visual display of measured parameters in both graphical and tabular form. Data logged to disc was subsequently manipulated, plotted and compared with model predictions using a commercial spreadsheet package. Hence the apparatus developed as part of this project allowed comprehensive, automatic monitoring of a membrane reactor and transfer of the data obtained to presentation form without any manual manipulation.

GENERAL DESCRIPTION of EQUIPMENT

The apparatus used for this work was based on the constant flux ultrafiltration cell (Turker and Hubble, 1987; Gacesa et al, 1983). In the alternative system, operating at constant pressure, the increase in membrane resistance with time due to fouling results in a decreasing flux, thus changing the degree of concentration polarisation. Constant polarisation conditions are important in studies where the linked effects of polarisation and solute-membrane interactions are to be investigated.

The constant flux apparatus remained approximately the same over the four areas of experimental work undertaken, namely protein adsorption, measurement of concentration polarisation, rejection of small solutes and enzyme reaction. Minor changes and additions to the apparatus were necessary for some of the work, for example the use of ammonium selective electrodes for monitoring enzyme reactions. The basic apparatus will be described here, and specific changes for parts of the work will be described in the relevant chapters.

The general layout of the constant flux apparatus (Fig 1) was as follows (individual items of equipment are described later). The closed recycle loop incorporated the retentate side of the membrane module (either hollow fibre or flat sheet). The liquid in the recycle loop was circulated by a pump to provide crossflow. Transmembrane flow (flux) was induced by a second pump feeding liquid into the recycle loop. To ensure that the liquid in the permeate region was well mixed, circulation was maintained using a peristaltic pump.

Recycle (retentate) rate was measured with a turbine flowmeter, and permeate flowrate was measured with a 'time of flight' bubble flowmeter. Three pressure transducers measured pressure drop along the retentate side of the membrane module and the average transmembrane pressure drop. Temperature in the recycle loop was

measured with a platinum resistance probe. Retentate absorbance was measured with an ultraviolet spectrophotometer, allowing solute concentrations to be determined.

Fig 1. Constant Flux Ultrafiltration Apparatus.

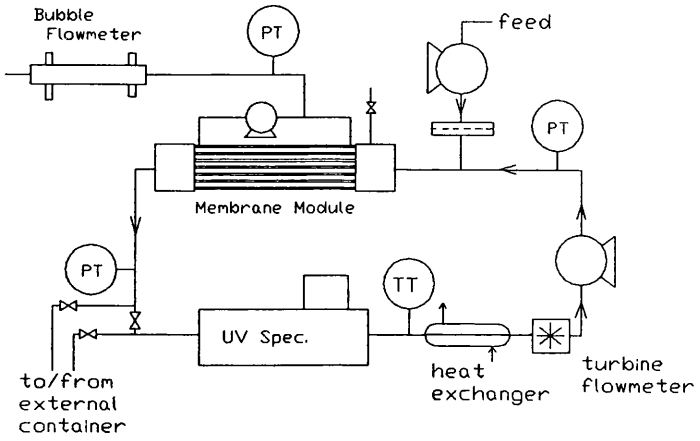

All the above measurement devices were connected via signal conditioning devices and an analogue-to-digital converter to a microcomputer for graphical and numerical display of data. The computer allowed conversion of raw data using polynomial fits to calibration curves, as well as hard copy and logging to disc. The recorded data was manipulated, plotted and compared with model results using a spreadsheet package.

DETAILED DESCRIPTION of EQUIPMENT

Membrane Module: Amicon polysulphone hollow fibre membranes were used for the majority of the work. Two models were used:

H1P10-8: 0.2mm i.d., 1000 fibres per module, 800 cm^2 nominal area, maximum pressure 15 psig.

H1P10-20: 0.5mm i.d., 250 fibres per module, 600 cm^2 nominal area, maximum pressure 25 psig.

Piping was connected to the modules via push-on end caps, sealed by 'O' rings.

An alternative membrane module was used for part of the work on protein adsorption. The second module was a Millipore 'Minitan' unit with flat polysulphone or regenerated cellulose membranes bonded to plastic plates. The plates were separated by elastomer spacer/gaskets which formed the retentate channels. The membrane plates and spacers were clamped in a stainless steel housing which incorporated the piping connections.

Recycle (Crossflow) Pump: A gear pump with a variable speed drive (Flowgen V.015.12/2030) was used for most of the work. Flowrates ranged from 5 to 300 $ml.min^{-1}$ and the delivery was smooth. The recirculation rate at constant pump setting was not affected by changes in the recycle loop design or the feed pump setting. A diaphragm metering pump was used as a recycle pump for some of the adsorption and polarisation work. Two heads operating 180° out of phase gave a maximum flowrate of 600 $ml.min^{-1}$ at a frequency of 200 min^{-1}. The flow was pulsatile and was affected by changes in feed flowrate and recycle loop design, such that careful monitoring of the recycle flowmeter reading was required.

Feed Pump: A peristaltic pump with variable speed control (Watson-Marlow 501U) and small diameter (1.6mm i.d.) tubing, which was capable of developing the required constant flowrates at pressures of up to 30psig. Feed solutions were passed through a

50μm prefilter before passing into the recycle loop, to remove particles that might block the ends of the hollow fibres.

Permeate Circulation Pump: A small peristaltic pump (Watson-Marlow 101U/R) with fairly large (3mm i.d.) tubing. This pump was also used for backflushing during cleaning (see later).

Recycle Flowmeter: Turbine flowmeter (Litre Meter LM25GN). The six bladed turbine rotated in the liquid flow and the magnets in each blade caused a pulse of current as they passed a coil. A subroutine in the data logging and display program determined the time taken for a fixed number of pulses, from which the recycle flow was calculated (Fig 2).

Fig 2. Turbine Flowmeter Calibration Curve

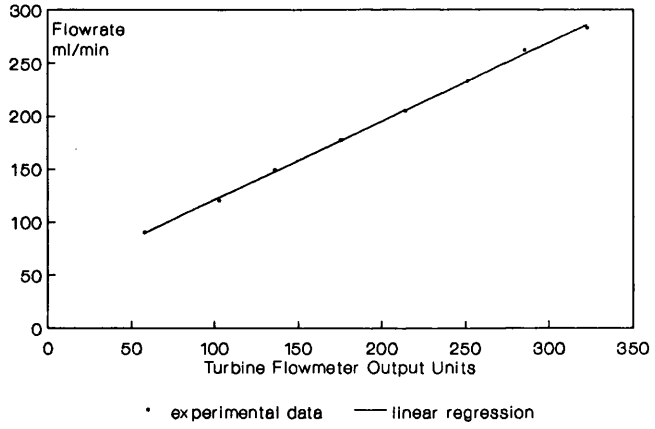

Permeate Flowmeter: The time of flight bubble flowmeter (Fig 1, page 2.12) was developed and constructed in the School of Chemical Engineering (Bishop and Sanders, 1989 - appendix to this chapter; Heinemann and Howell, 1987). A bubble of gas, generated by an electrolytic cell, was introduced into a capillary tube through which the permeate flowed. Infra red sender-detectors placed at either end of the capillary detected the passage of the bubble and allowed the time taken for it to pass along the tube to be measured. This was correlated to the permeate flowrate (Fig 3).

A subroutine in the data logging program controlled the current to the electrolytic cell using the information from a third detector mounted directly above the gas injection nozzle. The subroutine also provided results, as time of flight, to the main program. The bubble flowmeter was shown during this work to be capable of reliable, accurate performance over extended periods, and flowrates from 2 to 45 $ml.min^{-1}$ could be measured with a 2.5 mm diameter capillary.

Fig 3. Bubble Flowmeter Calibration Curve.

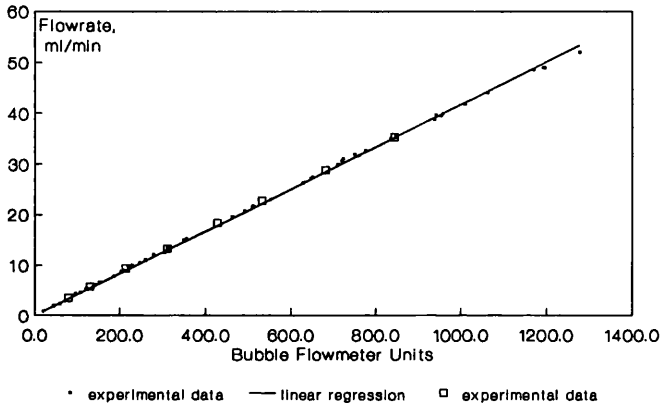

Fig 4. Sample Pressure Transducer Calibration Curve.

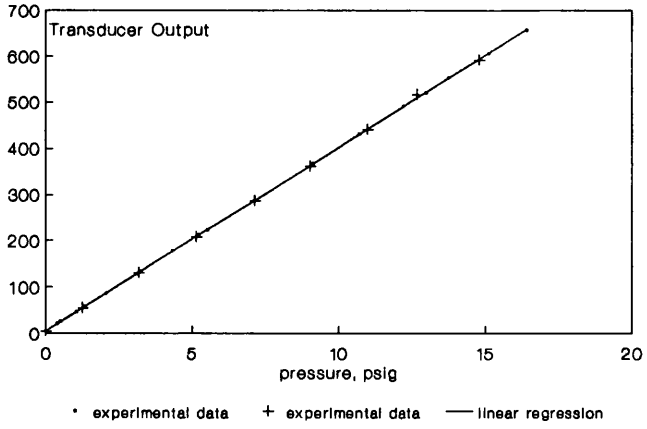

Pressure Transducers: Data Instruments Mediamate MM50 with stainless steel contact parts, reading gauge pressure from 0 to 50

psig. Power supply and signal conditioning equipment for the transducers was designed and constructed in the School of Chemical Engineering. The calibration curve is shown in Fig 4.

Temperature Probe: Philips PT100 platinum resistance probe, housed in a glass flow-through holder and secured with elastomer compression fittings. Signal conditioning equipment was designed and constructed in the School of Chemical Engineering.

Recycle UV Spectrophotometer: Cecil CE2272 linear ultraviolet spectrophotometer. A quartz flow-through cell with a light path of about 1mm allowed the instrument to be calibrated at 280nm for measurement of BSA concentrations of up to ≅ 27 $g.l^{-1}$ (Fig 5).

Fig 5. UV Spectrophotometer Calibration Curve.

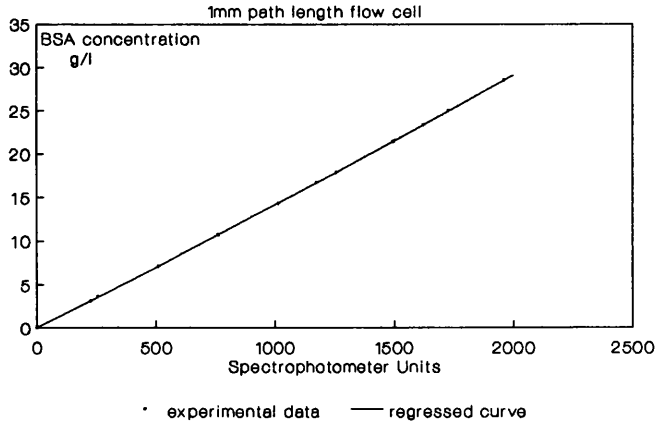

Analogue-Digital Converter and Computer: Signals from all the above measurement devices were passed to a BBC 'B' microcomputer via an analogue-to-digital converter (Kratos Instem 'Linkon') and an Electroplan communications adapter. Data stored on the BBC microcomputer was passed to an IBM compatible personal computer using a file transfer package (Kermit), which allowed subsequent manipulation with a spreadsheet.

Data Display and Logging Program: The program performed the following tasks (Fig 6):

Control of, and data gathering from, the bubble (permeate) flowmeter.

Data gathering from the turbine (recycle) flowmeter, pressure transducers, temperature probe, and spectrophotometer.

Graphical display of data in chart recorder fashion, to provide at-a-glance assessment of progress.

On-line production of hard copy of data.

Recording of data onto disk for later analysis.

Fig 6. Flowchart of Data Logging and Display Program

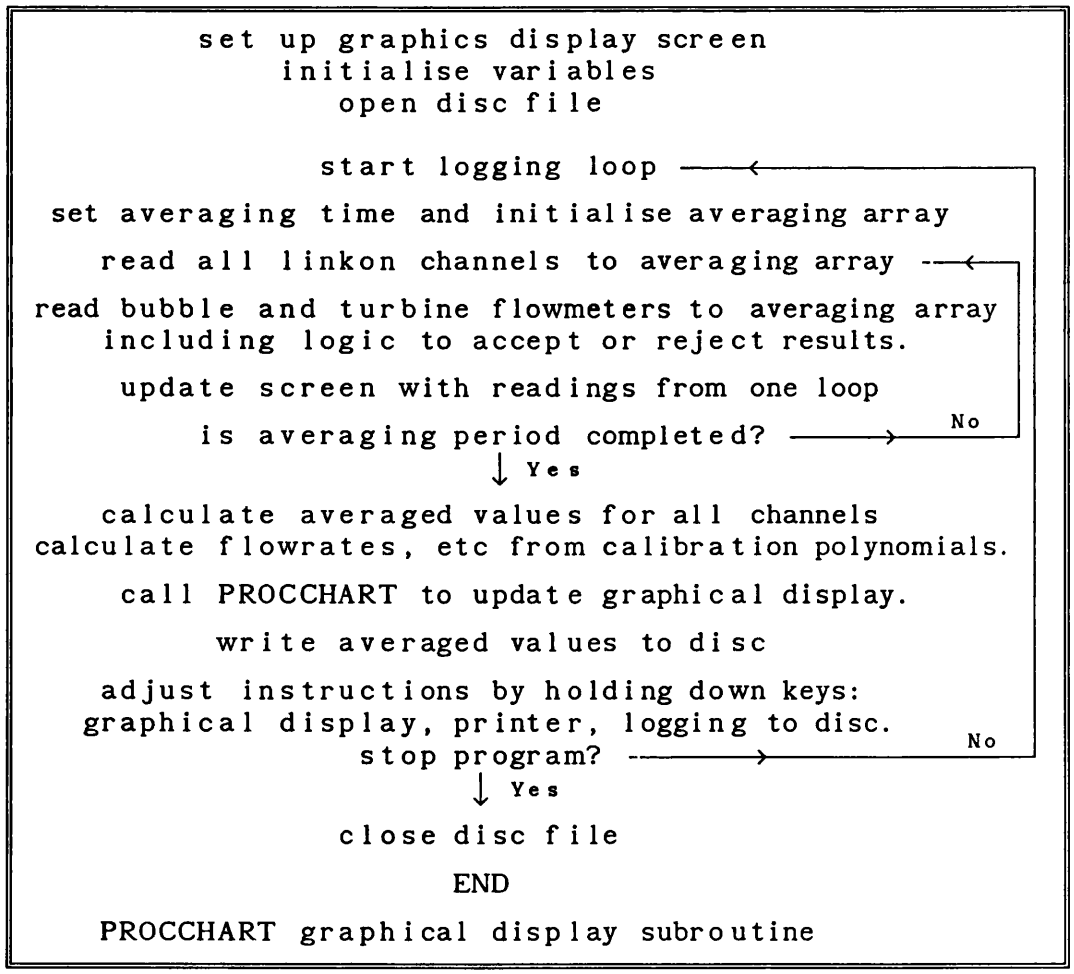

Data from each instrument was read in turn in a closed loop, and reading data once from all instruments took about 5 sec. Readings

from the turbine and bubble flowmeters were discarded if they were equal to zero, because a zero reading indicated that there was no new result available from the instrument. After a specified, variable period of time (the averaging period), the readings for each instrument were averaged. Flowrates, etc. were calculated using polynomials fitted to calibration data for each instrument. The graphical display was updated and the new set of data was recorded onto floppy disc and sent to the printer. The program then returned to reading data. Careful choice of the averaging period allowed optimum smoothing of data at an acceptable reporting frequency.

Operation of the Constant Flux Rig

Operational protocols were specific to the type of investigation being undertaken, and are described in the relevant chapters. It is appropriate to describe the membrane cleaning procedure here, as it remained the same throughout the work.

Membrane Cleaning

The membrane was backflushed with 1.5 litres of 0.1M NaOH, whilst a crossflow of the backflushed solution through the fibre lumen was maintained. Circulation from a container external to the recycle loop was via valved connecting pipes (Fig 1). The recycle loop was then thoroughly rinsed with distilled water and closed, after which 1 litre of distilled water was fed through the membrane via the feed pump. The recycle loop was then flushed out with buffer, and buffer was fed through the membrane until the flux-pressure relationship stabilised. The cleaning procedure described here was found (Sanders and Hubble, 1990; this thesis, Chapter 3) to give reproducible results for successive adsorption experiments, suggesting that the majority of protein fouling was removed.

REFERENCES

Bishop, J.T.; Sanders, N.
"Bubble flowmeter for measurement of low permeate flows in ultrafiltration".
Biotechnol. Techniques, 3 (1989) 101-106.

Gacesa, P.; Eisenthal, R.; England, R.
"Immobilization of urease within a thin channel ultrafiltration cell".
Enzyme. Microb. Technol., 5 (1983) 191-195.

Heinemann, P.; Howell, J.A.
"On-line monitoring of flux and rejection during microfiltration of protein solution".
Separation in Biotechnology, eds. Verrall, M.S.; Hudson, M.J., Chichester, UK, (1987) 397-404.

Sanders, N.; Hubble, J.
"Protein-membrane interactions in a constant flux ultrafiltration cell".
BIOSEP RR15, 1990.

Turker, M.; Hubble, J.
"Membrane fouling in a constant flux ultrafiltration cell".
J. Membrane Sci., 34 (1987) 267-281.

APPENDIX to CHAPTER 2. Bubble Flowmeter Paper

Biotechnology Techniques Vol 3 No 2 101-106 (1989)
Received as revised December 7

BUBBLE FLOWMETER FOR MEASUREMENT OF LOW PERMEATE FLOWS IN ULTRAFILTRATION

John T. Bishop and Neil Sanders*
School of Chemical Engineering,
University of Bath,
Claverton Down, Bath, BA2 7AY, UK.

SUMMARY

Low permeate flow rates on a laboratory ultrafiltration rig have been measured using the transit time principle in a bubble flowmeter. The flowmeter is controlled and the results recorded by microcomputer. Flow rates of 1 to 50 $ml.min^{-1}$ may be measured with a 2.5mm diameter capillary.

INTRODUCTION

The measurement of permeate flow rates in microporous membrane research presents considerable difficulties. The small membrane area of many laboratory and pilot scale membrane systems results in low permeate flow rates. Thus conventional methods of flow measurement such as turbines or orifice meters are frequently unsuitable. The initial flux decline in ultrafiltration is often large, hence requirements for flowmeters often include high turndown ratio. In addition, provision for computer data logging is desirable.

The measurement of low liquid flow rates has received some attention in the literature. Yang et al (1988) describe a 'transit time' flowmeter using periodic temperature fluctuations as tracers to measure liquid flow rates between 0.1 and several $ml.min^{-1}$. An electrolytic cell has been used as a doser, generating gas which displaces liquid from a closed vessel (Lyutfaliev and Ismailov, 1974). The transit time of soap bubbles has long been used to determine low gas flow rates (Shmulevich et al, 1973). Photo-electric determination of float position in variable area flowmeters has been used in flow control (Lutz, 1971).

A flowmeter combining the transit time principle with electronic event detection has been used to measure permeate flow rates in microfiltration (Heinemann et al, 1987). Air bubbles were introduced into a glass capillary by periodic relaxation of a solenoid pinching a silicon rubber tube connected to an air supply. Improvements in bubble size control and a reduction in mechanical complexity over the system of Heinemann et al (1987) are presented here.

MATERIALS and METHODS

The general arrangement of the flowmeter is shown in Figure 1. Permeate from a commercial hollow fibre ultrafiltration module is passed through a glass capillary tube fitted with three infra red sender- detectors (RS Components Ltd, stock No. 304-560). The mountings accept tubes of varying diameter and allow adjustment of tube position relative to the detectors.

Gas is generated with an electrolytic cell and is injected into the capillary tube just below the first detector. The electrolytic cell is constructed from glass with electrodes from platinum foil. The solution in the cell is water ionised with a small amount of H_2SO_4.

A gas bubble moves along the capillary past the second and third detectors. When a bubble fills the whole cross section of the tube, plug flow is approached

and the velocity of the bubble is proportional to the flow rate.

Figure 1

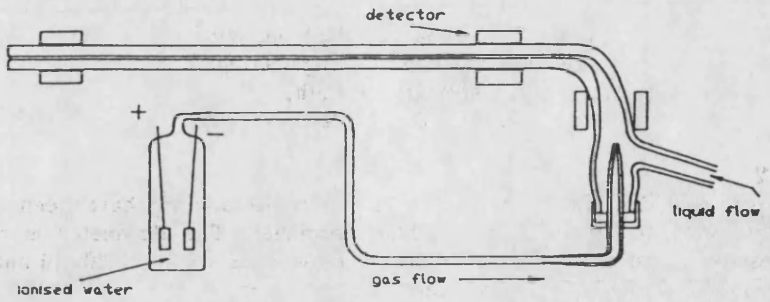

Bubbles are detected by the difference in permeability of the tube to infra red radiation when filled with gas or liquid. A signal is produced when the trailing edge of a bubble passes a detector.

Bubble production is controlled by the first detector. When a bubble separates from the injector nozzle and passes the first detector the signal produced is used to switch off the current to the cell. The time between separation and signal is dependent on the liquid velocity, but over the range of flow rates measured it is short enough to prevent premature separation of a second bubble.

The inverse of time taken for the bubble to pass between the second and third detectors is correlated with liquid flow rate. A maximum time is allowed between detection of the bubble by the first detector and turning on the electrolytic cell for the following bubble.

Figure 2. Bubble Flowmeter Control

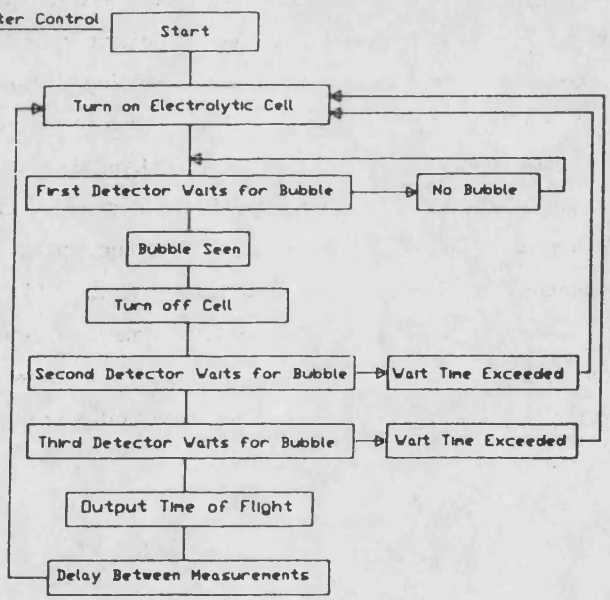

A flowchart of the bubble control logic is shown in Figure 2. The bubble control software is written as an Assembly-level procedure within a 'BASIC' program running on a BBC microcomputer. This allows the bubble control to run as a continuous background task. The bubble flowmeter is interfaced with the computer via the user port. A simplified listing of the 'BASIC' program (Figure 5) and a circuit diagram (Figure 4) are appended to this article. The bubble control procedure stores flowmeter output as time of flight (units of 0.01s) in a memory buffer. The BASIC program periodically checks this buffer for values which may then be averaged over a selected time period. Individual or averaged times of flight may be used to calculate flow rate ($ml.min^{-1}$). Values of flow rate may be

sent to a printer, stored on floppy disc and displayed on screen in 'chart recorder' form.

RESULTS and DISCUSSION

The flowmeter has been shown to operate reliably over the following flow ranges:

2.5mm diameter capillary: 1 to 50 $ml.min^{-1}$

1.0mm diameter capillary: 0.1 to 10 $ml.min^{-1}$

Larger or smaller capillary tubes could be substituted to extend the range of flows measured. It would be necessary to increase the diameter of the gas injection nozzle for larger tubes in order to produce bubbles which fill the whole cross section of the capillary.

Time delay between measurements (Figure 2) may be reduced to 1s without affecting the performance of the flowmeter. The frequency of measurements is dependent on flow rate, the time delay and the time taken from switching on current to the cell to bubble separation. Experimental data shows that for the 2.5mm capillary;

at 1 $ml.min^{-1}$, time of flight of the bubble is much greater than the delay between measurements and the bubble generation time. Measurement frequency is thus equal to the inverse of time of flight and is approximately 1 min^{-1}.

at 50 $ml.min^{-1}$, time delay between measurements and bubble generation time control the measurement frequency, which is approximately 7 min^{-1}.

At 1 $ml.min^{-1}$ the measurement frequency is sufficient for most membrane experiments except those concerned with the initial flux decline in the first seconds of operation.

A calibration for the 2.5mm capillary (Figure 3) is linear over the range shown and has been found to remain unchanged over a period of months. Linear regression was used to fit the data to a straight line relationship. The regression parameters were:

Standard error of Y estimate = 0..37

R^2 = 0.9993

Standard error of coefficient = 8×10^{-5}

Typical errors are: 5% at 1 $ml.min^{-1}$: 1% at 40 $ml.min^{-1}$. The straight line equation is incorporated into the BASIC logging program which allows direct output of flowrate in $ml.min^{-1}$. Data recorded on disc may be plotted using a spreadsheet package. The spreadsheet allows large amounts of data to quickly be manipulated, compared with other data, and plotted.

The electrolytic cell has proved to be reliable and simple to construct. Bubble size can be controlled down to a small value which reduces the possibility of bubble splitting (a significant problem with mechanical gas injection) which results in miscalculation of flowrate. Small bubbles also reduce errors caused by

volume addition to the measured stream.

Figure 3.

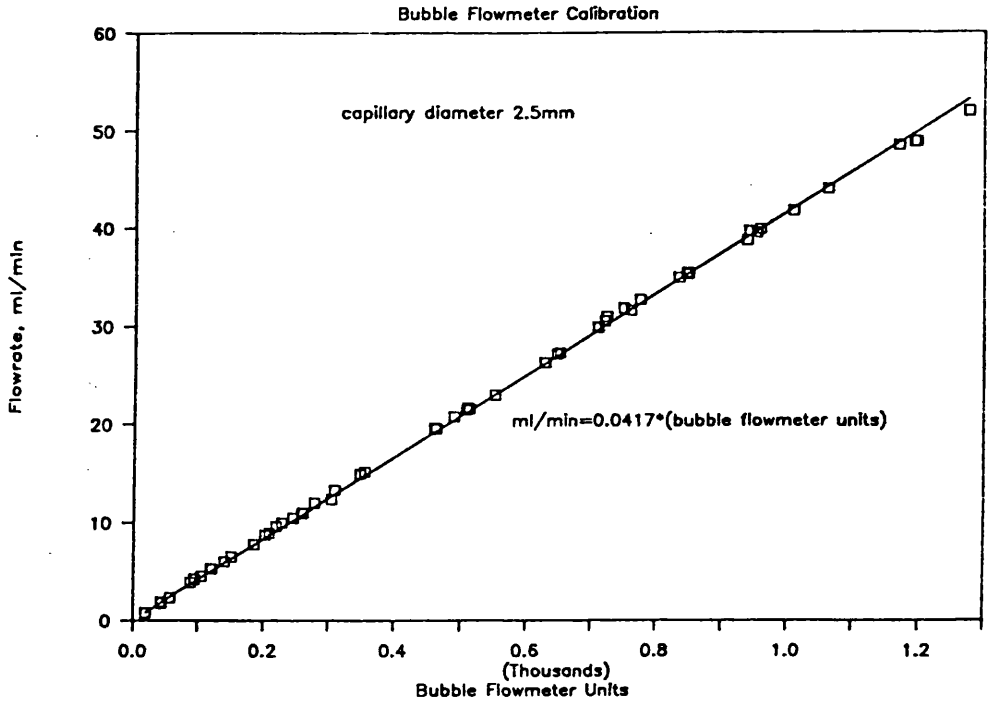

CONCLUSION

Reliable and accurate measurement of a wide range of ultrafiltration fluxes by transit time has been demonstrated. Continuous operation over a period of days is possible, with data displayed and recorded on paper and/or on disc. 'Post-mortem' manipulation, comparison and plotting of data using a spreadsheet is possible. The components used in the bubble flowmeter are inexpensive and widely available.

ACKNOWLEDGEMENT

N.S. is supported by SERC. The encouragement and advice of Dr. John Hubble is gratefully acknowledged.

REFERENCES

Heinemann,P.R., Howell,J.A., Bryant,R,A. (1987). Separations for Biotechnology, Verral,M.S. and Hudson,M.J. ed., Biochem. and Biotechnol., Ch 30, pp 397-399.

Lutz,K. (1971). DECHEMA Monographs, Oelflingen/Baden, Ger. 67(Tail 2), 611-627.

Lyutfaliev,K.A., Ismailov,I.M. (1974). Proekt. Pilotnykh Ustanovok Neftepererab. Neftekhim., Mater. Ostrasl. Semin., Grozn,A.Z. ed., Grozny, USSR: Neft. Nauchno-Issled. Inst., pp 148-151.

Shmulevich,E.A., Bol'shakov,D.A., Chekhov,E.E. (1973). Zh. Fiz. Khim., Yaroslavl, USSR. 47, 264-265.

Yang,C., Kummel,M., Soeberg,H. (1988). Rev. Sci. Instrum., Lyngby, Den. 59, 314-317.

Figure 4. Circuit Diagram

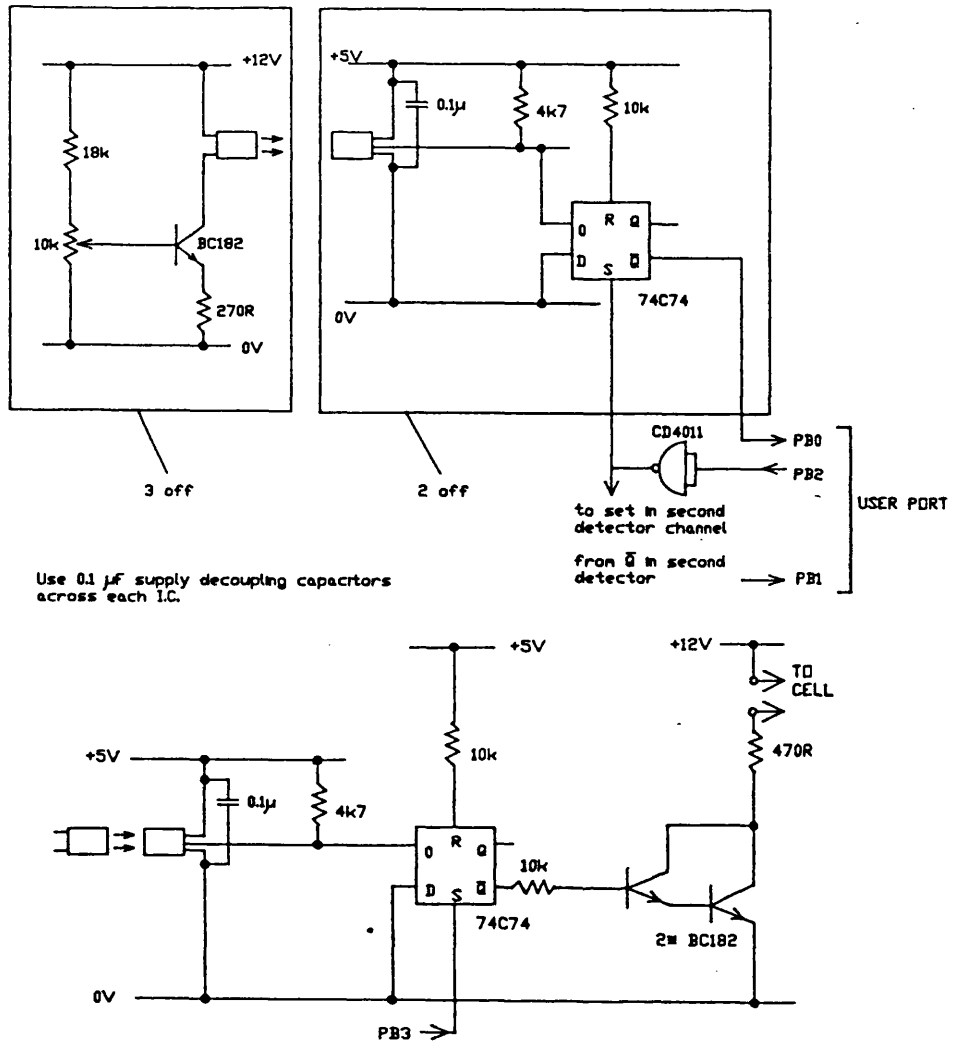

Figure 5. Program Listing

```
10 PROCassemble: CALL setup: CALL enable
20 REPEAT: A%=FNgetflow: IF A% <> 0 THEN PRINT 100000/A%*1 ELSE UNTIL FALSE
30 UNTIL FALSE
40 DEF FNgetflow: CALL readbuf1: time%=(!readtemp AND 65535): IF time%<>0
   THEN=(time%-(!reload3 AND 65535)) ELSE =0:ENDPROC
50 DEF PROCassemble: V=&FE60: IOB=V: IOA=V+1: DDRB=V+2: INFR=V+13: IER=V+14
60
70 vect=&204 : timebase=100 : startime=65535 : sysflags=&FE4D
80 DIM X% 1000: FOR N%=0 TO 3 STEP 3: P%=&70
90 [ OPT N%
100 .oldvect EQUW 0 \ old vector store - must be page 0
110 .reload0 EQUW 65400 \ delay between measurements
120 .reload1 EQUW 65500 \ pump on time
130 .reload2 EQUW 60000 \ first detector wait time
140 .reload3 EQUW 60000 \ second detector wait time
150 .countdown EQUW 0 \ timeout counter
160 .readtemp EQUW 0 \ value read from fifo - bubble time
170 .writetemp EQUW 0 \ temp store for datum to be written - redundant
180 .readptr EQUB 0 \ read pointer for fifo store
190 .writeptr EQUB 0 \ write pointer for fifo store
200 .readwriteflag EQUB 0 \ set to 0 if last operation was a read, 1 if write
210 .vector EQUW 0 \ points to required process - must be page 0
220 .iobtemp EQUB 0 \ temp store for user port
230 .baseptr EQUW base \ points to start of fifo memory
240 ]
250 P%=X%
260 [ OPT N%
270 .setup SEI: LDA #&8C: STA DDRB: LDA #&7F: STA INFR:STA IER \ clear all flags
280 LDA #(proc0 MOD 256): STA vector: LDA #(proc0 DIV 256): STA vector+1
290 JSR changevect: CLI: RTS
300
310 .intin  PHA: PHP: LDA sysflags: AND #&40: BEQ procout \ check rtc flag
320 LDA IOB: STA iobtemp: ORA #&4: STA IOB: AND #&FB: STA IOB \ pulse to reset ffs
330 JMP(vector)
340
350 .procout: PLP: PLA: JMP (oldvect)
360
370 .changevect SEI: LDA vect: STA oldvect: LDA vect+1: STA oldvect+1:
    LDA #(intin MOD 256): STA vect: LDA #(intin DIV 256): STA vect+1: CLI: RTS
380
390 .proc0 JMP procout
400 .proc1 LDA IOB: AND #&F7: STA IOB \ pulse to start gas
410 LDA reload1: STA countdown: LDA reload1+1: STA countdown+1
420 LDA #(proc2 MOD256): STA vector: LDA #(proc2 DIV256): STAvector+1: JMPprocout
430 .proc2 INC countdown: BNE donowt2: INC countdown+1: BNE donowt2
440 LDA IOB: ORA #&08: STA IOB \ end of pulse
450 LDA reload2: STA countdown: LDA reload2+1: STA countdown+1
460 LDA #(proc3 MOD 256): STA vector: LDA #(proc3 DIV  256): STA vector+1
470 .donowt2 JMP procout
480 .proc3 LDA #1: BIT iobtemp: BEQ timeout3 \ if bubble at first det..
490 LDA reload3: STA countdown: LDA reload3+1: STA countdown+1: LDA #(proc4 MOD 256):
    STA vector: LDA #(proc4 DIV  256):STA vector+1: JMP procout \ then wait at no.2
500 .timeout3 INC countdown: BNE donowt3: INC countdown+1: BNE donowt3
510 .copout3 LDA #(proc1 MOD 256): STA vector: LDA #(proc1 DIV 256): STA vector+1
520 .donowt3 JMP procout \..else if timeout then back to start else do nothing
530 .proc4 LDA #2: BIT iobtemp: BEQ timeout4 \ if bubble at no.2..
540 LDA countdown: STA writetemp: LDA countdown+1: STA writetemp+1
550 JSR writebuf \ ..then write t.o.f. to fifo buffer..
560 LDA #(proc5 MOD 256): STA vector: LDA #(proc5 DIV  256): STA vector+1: LDA reload0:
    STA countdown: LDA reload0+1: STA countdown+1: JMP procout \..and wait..
570 .timeout4 INC countdown: BNE donowt4: INC countdown+1: BNE donowt4
580 .copout4 LDA #(proc1 MOD 256): STA vector: LDA #(proc1 DIV 256): STA vector+1
590 .donowt4 JMP procout \..else wait for timeout. If timeout then restart.
600 .proc5 INC countdown: BNE donowt5: INC countdown+1: BNE donowt5:
    LDA #(proc1 MOD 256): STA vector: LDA #(proc1 DIV 256): STA vector+1
610 .donowt5 JMP procout \ still waiting between measurements
620 .proc6 JMP procout
630
640 .enable SEI: LDA #(proc1 MOD 256): STA vector: LDA #(proc1 DIV 256): STA vector+1:
    CLI: RTS \ start flow measurement
650
660 .disable SEI: LDA #(proc0 MOD 256): STA vector: LDA #(proc0 DIV 256):
    STA vector+1: LDA IOB: AND #&08: STA IOB: CLI: RTS \ stop flow measurement
670
680 .writebuf PHA: TYA: PHA: LDY writeptr: CPY readptr: BNE doit0
690 LDA readwriteflag: BEQ doit0: PLA: TAY: PLA: RTS \ no such luck!
700 .doit0 LDA writetemp: STA (baseptr),Y: INY: LDA writetemp + 1: STA (baseptr),Y
710 INY: LDA #1: STA readwriteflag: STY writeptr: PLA: TAY: PLA: RTS \ done
720
730 .readbuf1 SEI:PHA:TYA:PHA: LDY readptr: CPY writeptr: BNE doit1
740 LDA readwriteflag: BNE doit1: LDA #0: STA readtemp: STA readtemp+1
750 PLA: TAY: PLA: CLI: RTS \ zero if empty
760 .doit1 LDA (baseptr),Y: STA readtemp: INY: LDA (baseptr),Y: STA readtemp+1: INY
770 LDA #0: STA readwriteflag: STY readptr: PLA: TAY: PLA: CLI: RTS \ done
780 .base NOP \ beginning of fifo buffer
790 ]
800 NEXT
810 ENDPROC
```

Last Page of Chapter 2

CHAPTER 3

PROTEIN - MEMBRANE INTERACTIONS in a CONSTANT FLUX ULTRAFILTRATION APPARATUS

ABSTRACT

Adsorption of BSA onto polysulphone and regenerated cellulose membranes in the absence of a transmembrane flux has been investigated. Membranes used were Amicon hollow fibres (polysulphone) and Millipore 'Minitan' flat sheets (polysulphone and regenerated cellulose). Spectrophotometric determination of retentate protein concentration allowed membrane associated protein to be calculated by difference. The effects of concentration, shear, pH and ionic strength on the adsorption of BSA to the membranes have been determined. The kinetics and reversibility of BSA adsorption have also been investigated.

Adsorption increases with concentration even at high protein concentrations, which is a significant factor when considering the effect of concentration polarisation on membrane fouling. Adsorbed amounts measured on membranes are high compared with adsorption to non membrane polymers, probably due to a combination of multilayer and support side (permeate) adsorption. There is evidence for a dynamic exchange of protein between adsorbed and dissolved states, accompanied by protein denaturation. Therefore enzyme deactivation in the presence of a membrane in a reactor could be severe, due to loss of enzyme activity by denaturation.

The hydrophilic regenerated cellulose membrane was found to adsorb less protein than the hydrophobic polysulphone membranes, but only after several cycles of exposure to protein and cleaning. The technique used in this work has been shown to produce internally consistent results which are valuable for the comparison of different membranes and adsorption conditions. Better than order of magnitude estimates for adsorbed amounts can be made.

INTRODUCTION and LITERATURE SURVEY

General Introduction

Adsorption of proteins from solution to solid surfaces has been widely studied, although there has been relatively little work on systems involving ultrafiltration membranes. Typically, membranes have been shown to adsorb more than 1000 $mg.m^{-2}$ protein, whereas the maximum adsorption for non membrane surfaces is about 5 $mg.m^{-2}$ (Hanemaaijer et al, 1989). Maximum protein adsorption to non membrane surfaces often corresponds to a close-packed monolayer, although in some cases a stepped isotherm indicates the existence of more than one layer, or of changes in adsorbed protein structure (Fair and Jamieson, 1980).

A comprehensive monograph on protein adsorption at the solid-liquid interface (non membrane systems) has been published by Norde (1986). Saturation isotherms of finite initial slope are usually obtained in non membrane systems. Frequently the saturation amount is reached at low concentrations (around 1 $g.l^{-1}$)(Fair and Jamieson, 1980; Jonsson et al, 1982).

The saturation isotherms obtained in many cases have resulted in attempts to analyse the data in terms of the Langmuir theory of adsorption. However the Langmuir theory requires (Norde, 1986):

(a) Reversibility.
(b) No interaction between adsorbed molecules.
(c) No deformation of the molecules upon adsorption.
(d) Adsorption must take place on fixed sites.

Protein adsorption from solution does not usually satisfy these requirements and so it seems doubtful that the Langmuir theory has physical significance in this case.

Measurement of Adsorption

Several methods have been used to measure the amount of protein adsorbed onto a membrane:

(a) Solubilisation of protein using sodium dodecyl sulphate (SDS) followed by spectrophotometric determination of the solution

concentration has been widely used (Fane et al, 1983; Hanemaaijer, 1989; Lockley et al, 1988; Suki et al, 1984).

(b) Measurement of the reduction in concentration of a solution in contact with the membrane or other surface. This allows the adsorbed amount to be inferred. Solution concentration is usually measured by UV absorbance. For accuracy the surface area to volume ratio of the system should be high. (Hanemaaijer, 1989; Ingham et al, 1980; Turker and Hubble, 1987).

(c) Radiolabelling of protein molecules followed by measurement of the level of radioactivity of the membrane. (Aimar et al, 1985; Matthiasson, 1983; Nilsson, 1988). Aimar et al also used radioactive labelling of solutions to determine reduction in solution concentration and hence adsorbed amount.

(d) The Kjeldahl digestion method was applied to membranes with adsorbed protein by Gacesa et al (1983) and Patel and Reuter (1985).

(e) Quinn (1979) used electrolyte conductance to measure protein adsorption to a track-etched mica 'membrane'.

Measurements of protein adsorption to non membrane solids have been made by various types of spectroscopy and by electrochemical, optical and thermodynamic methods. These are described in more detail in a comprehensive review of protein adsorption at solid-liquid interfaces by Norde (1986).

Indirect measures of protein adsorption to membranes have been used by several workers:

(f) Change of solvent permeability of the membrane after exposure to protein solution (Choe et al, 1986; Dejmek and Nilsson, 1989; Nabetani et al, 1988; Quinn, 1979; Reihanian et al, 1983; Nystrom, 1989).

(g) Changes in the rejection of smaller molecules (Nabetani et al, 1988; Zeman, 1983).

Adsorbed Amount - Isotherms

Isotherms show the effect of protein concentration on adsorbed amount under otherwise constant conditions. Investigations

carried out to determine the effects of concentration, pH, ionic strength and shear on adsorbed protein levels have produced varying results. In particular, several different types of equilibrium isotherm have been obtained.

A common type of isotherm is the 'saturation' type which exhibits a rapid increase in adsorbed amount at low concentration. The adsorbed amount then approaches a constant value at higher concentrations (Dillman and Miller, 1973; Aimar et al, 1986; Suki et al, 1984; Turker and Hubble, 1987). Dillman and Miller (1973) obtained saturation above a concentration of 4 $g.l^{-1}$ BSA. The maximum adsorbed amount was 4 $mg.m^{-2}$ which is much lower than for other work. This could have been due to the type of membranes used ('cation exchange') or to incomplete recovery of adsorbed protein by the amido black procedure used for determination of the adsorbed amount. Aimar et al (1986) produced isotherms at concentrations up to 50 $g.l^{-1}$ BSA on IRIS 3038 membranes. At this concentration, saturation was not reached although the curves displayed downward concavity. The isotherms were modelled as Freundlich, i.e. exponential functions of a saturation concentration. Suki et al (1984) reported little change in adsorbed amount between bulk concentrations of 1 and 2 $g.l^{-1}$ in an ultrafiltration experiment. However this may have been due to concentration polarisation causing a high concentration at the membrane, masking the effect of bulk concentration. Turker and Hubble (1987) showed a saturation type isotherm up to a concentration of 15 $g.l^{-1}$ BSA on Amicon hollow fibres, although complete saturation was not reached at this concentration. The isotherms were modelled as Langmuir using a saturation adsorbed amount.

Other investigations of protein adsorption have produced isotherms which are not of the simple saturation type. The adsorbed amount may increase in steps with increasing protein concentration. In several cases the adsorbed amount does not approach a limiting or saturation value even at very high concentrations (Matthiasson, 1983; Matthiasson et al, 1989; Nilsson, 1988). Matthiasson

(1983) found that for adsorption of BSA to various membranes, the adsorbed amount seemed to approach saturation up to 12 $g.l^{-1}$. Beyond this, to the highest concentration of 45g per 100ml, there was a linear increase of adsorbed amount with concentration. Nilsson (1988) obtained stepped isotherms showing two plateaus up to a concentration of 40% w/w. In this case the isotherm seemed to show saturation above 30% w/w, and the bulk of protein adsorption occurred below an equilibrium concentration of 10% w/w.

It has generally been found that the adsorbed amount per unit nominal surface area is two to three orders of magnitude greater for membranes than for non membrane surfaces. Hanemaaijer et al (1989) compared the adsorption of whey proteins onto polysulphone and cellulose membranes with adsorption to model polysulphone and silica surfaces. The maximum adsorbed amount was 1700 $mg.m^{-2}$ on polysulphone membranes, c.f. 5.5 $mg.m^{-2}$ on the polysulphone model surface.

The large amount of protein adsorbed onto membranes has been explained by Hanemaaijer et al (1989) as due to internal adsorption in the pores and support structure of the membranes. They proposed that the amount of internal surface area of anisotropic membranes could be $\cong$ 400 m^2 per m^2 of nominal membrane area. If this area were available for adsorption it would explain the high adsorption capacity of membranes in comparison to non membrane surfaces. Very high adsorbed amounts at the isoelectric point were explained by multilayer adsorption, due to the tendency for protein molecules to associate at the isoelectric point. However, it seems unlikely that multilayer adsorption can account for *all* the additional adsorption capacity of membranes. This is because 100 to 1000 protein layers would be needed to provide the difference in capacity mentioned in the previous paragraph, and it seems unlikely that sufficient binding forces could be transmitted through so many layers to achieve attachment.

Matthiasson (1983) measured the amount of BSA adsorbed to the support side of membranes. Support side adsorption represented up

to 35% of the total adsorbed protein.

The effect of pH on protein adsorption has been investigated by many workers (Fane et al, 1983; Hanemaaijer et al, 1989; Aimar et al, 1986; Dillman and Miller, 1973; Matthiasson, 1983; Patel and Reuter, 1985; Suki et al, 1984). A variation in adsorbed amount with pH is usually reported, with a maximum at the isoelectric point. This is normally explained by the minimisation of repulsion forces between protein molecules at this pH. Fane et al (1983) also report that higher salt concentrations produced higher adsorbed amounts.

The effect of shear on protein adsorption has been investigated, although not in membrane systems. Chuang et al (1978) showed that the effect of increasing flow was to increase adsorption of human plasma proteins to cuprophane or PVC. Other work on the effect of shear has been summarised by Nilsson (1989).

In conclusion, the extent to which the adsorbed amount varies with concentration is dependent on the system considered. Adsorbed amount frequently does not approach a constant value as concentration increases. Very large amounts of protein are adsorbed onto membranes when compared to non membrane surfaces. This has been explained both in terms of adsorption within the pores and support structure of membranes, and multilayer adsorption. Maximum adsorption usually occurs at the isoeletric point.

Adsorption Kinetics

Usually the bulk of adsorption occurs quickly, followed by a slow approach to a constant value (Aimar et al, 1986; Dillman and Miller, 1973; Fane et al, 1983). The time taken for complete adsorption varies widely, as shown by the following results for the time taken to reach equilibrium:

(a) 5 hr at concentrations of less than 10 $g.l^{-1}$, longer at higher concentrations (Aimar et al, 1986).

(b) 4 hr at 2 $g.l^{-1}$ (Dillman and Miller, 1973).

(c) 30 min to more than 4 hr, depending on membrane material (Lockley et al, 1988).

(d) 10 min to 60 min at 2 $g.l^{-1}$, depending on membrane material (Matthiasson, 1983).

(e) 20 to 60 min, depending on salt concentration (Turker and Hubble, 1987).

Adsorption kinetics have been shown to depend on protein concentration (Aimar et al, 1986), becoming slower at higher concentrations. However Suki et al (1984) found slower kinetics at 1 $g.l^{-1}$ than at 20 $g.l^{-1}$.

Lockley et al (1988) showed that adsorption kinetics varied according to the membrane used; adsorption was complete within half an hour on a cellulose acetate membrane, 3 hr on a PVDF membrane and was still increasing after 4 hr on a polysulphone membrane.

Reversibility

There seems to have been relatively little work done on the reversibility of adsorption to membranes, although reversibility in non membrane systems has been widely considered. From non membrane work, the more recent conclusions seem to be that adsorption is reversible upon dilution, but the process is so slow as to appear irreversible. Desorption can be assisted by changes in pH and ionic strength.

Dillman and Miller (1973) reported two types of adsorption to membranes, one of which is 'easily reversible', the other irreversible. The two amounts of protein were determined by successive applications of amido black dyeing followed by NaOH removal and concentration measurement by UV absorbance. Washing the membranes with buffer for 10 min did not remove a significant amount of protein.

It is often assumed that in membrane and non membrane systems, adsorbed protein can be completely redissolved using a surface

active agent, for example SDS (Suki et al, 1984). This has been used as a method for determining the adsorbed amount of protein.

Norde (1986) discussed the reversibility of protein adsorption at solid-liquid interfaces, and made the following general observations:

(a) There is little or no desorption on dilution with the same solvent.

(b) Additional desorption may occur by changing conditions such as ionic strength, pH, temperature.

(c) Exchange of protein between the adsorbed and dissolved states takes place.

(d) Adsorbed proteins can be displaced by different proteins.

(e) Protein molecules undergoing structural changes during adsorption may not revert to their original state on desorption.

The thermodynamics of protein adsorption has been used to explain some of the above phenomena. Adsorbed protein molecules may be attached by many segments, so the molar free energy of adsorption can be large. Changes in molecular structure on adsorption also contribute to the molar free energy. Desorption requires this free energy to be overcome, so the desorption process is slow, and over the time scale of most experiments, the rate of desorption is often undetectable.

Dynamic exchange of protein between dissolved and adsorbed states has been demonstrated (Brash and Samak, 1978). The extent of exchange was shown to depend on the shear at the interface in some cases, suggesting that collisions between molecules are important in the exchange process. Only part of the adsorbed protein was exchangeable, even over several days.

The results of Beissinger and Leonard (1980), on the kinetics of adsorption and desorption of gamma-globulin from quartz, seem to show that complete desorption would never occur.

Modelling of Protein Adsorption

Relatively little work has been published on modelling of protein adsorption onto solid surfaces from solution. The wide variety of results obtained in protein-membrane systems suggests that predictive models for adsorption isotherms may not be feasible.

Where saturation isotherms have been obtained, results have been interpreted in terms of Langmuir adsorption (Dillman and Miller, 1973; Turker and Hubble, 1987). Norde (1986) suggests that protein adsorption to solids is not consistent with the Langmuir assumptions, but Turker and Hubble (1987) obtained an adequate fit to their data with a Langmuir type model. Aimar et al (1986) fitted their data with a 'Freundlich' model which is an exponential function of a saturation adsorbed amount. They also modelled adsorption kinetics as an exponential function.

In non membrane systems, Norde (1986) in his monograph mentions little work on the modelling of equilibrium adsorbed amount (isotherms). An exception is the work of Fair and Jamieson (1980) who divide their stepped isotherm into three regions:

(a) At low concentrations, molecules adsorb in a random, independent manner.

(b) At intermediate concentrations, a protein layer of unordered, glassy structure is formed.

(c) At high concentrations, a two dimensional protein crystal is formed at the solid surface.

Modelling of adsorption kinetics has received more attention. Kinetics have been modelled as (Norde, 1986):

(a) A diffusion controlled process with instantaneous, irreversible reaction at the surface.

(b) A second order irreversible reaction at the surface.

(c) A second order Langmuir (reversible) reaction at the surface.

Combinations of the above mechanisms have been used to explain

observed adsorption kinetics. Other mechanisms considered have been:

(d) Reversible second order adsorption with a desorption rate that decreases with the time for which the molecule is adsorbed. This allows for the fact that desorption is often slow and/or incomplete.

(e) Two adsorbed states, possessing different rates of desorption. Transition from one adsorbed state to the other occurs at the surface.

Norde (1986) concluded that each of the models is suspect in some way, and that the main problem is related to poor understanding of the mechanism of desorption.

A dynamic model of protein adsorption was presented by Lundstrom (1985). It is based on the assumption that protein molecules may undergo conformational changes after adsorption. The model was able to fit data for adsorption kinetics obtained by Jonsson et al (1982).

A comprehensive model for protein adsorption should be based on a thorough understanding of all the mechanisms involved. A valid model would thus be able to describe both the kinetics and equilibrium behaviour of protein-membrane systems. The requirements for a model of adsorption are likely to include:

(a) Adsorbed amount depends on bulk protein concentration, also on shear at the solution-membrane interface.

(b) Equilibrium isotherms are not of the saturation type, and may show multiple plateaus over several decades of concentration.

(c) Desorption does occur, but probably very slowly.

(d) Rate of desorption may depend on the degree of surface coverage.

(e) Exchange of protein molecules between the adsorbed and dissolved states may well occur.

It is difficult to imagine a model scheme where adsorption reaches

equilibrium at a given concentration, but where the reverse reaction (desorption) takes place extremely slowly. An analogue of a simple enzyme catalysed reaction has been considered, where protein molecules are reversibly adsorbed onto the membrane and subsequently undergo a conformational change to an irreversibly adsorbed state. This approach has not been successful.

Evidence of adsorption to the spongy support region of membranes will be presented later in this chapter. In view of this, a model should perhaps take into account transport of protein molecules through the separating skin of an anisotropic membrane and subsequent adsorption to the support region.

Effect of Adsorption on Solvent Flux

A considerable amount of work has been done on the effect of protein adsorption on membrane permeability. In the absence of polarised macrosolutes, the permeability of a membrane may be calculated from the flux of buffer at a known transmembrane pressure. For example, Dejmek and Nilsson (1989) showed that after rinsing, adsorbed protein represented 30% of the total membrane resistance to buffer flux.

Experiments usually involve exposing the membrane to protein solution statically or with stirring/tangential flow. There has been a transmembrane flux in some work. The presence of a flux implies that concentration polarisation will have occurred, introducing some doubt as to the concentration at the interface.

The flux reduction or adsorption resistance has been related to the adsorbed amount (usually expressed in terms of mass of protein per unit nominal membrane area). Aimar et al (1986) show a log-log relation between adsorption resistance and adsorbed amount. Matthiasson (1983) investigated the effect of adsorbed amount on the 'relative resistance' (RR):

$$RR = \frac{\text{series resistance of adsorbed layer}}{\text{clean membrane resistance}}$$

The effect varied depending on the membrane used. Nilsson (1989) also measured the effect of adsorbed amount on the relative resistance. The relative resistance increased rapidly up to an adsorbed amount of ≅ 100 mg protein. m^{-2}, after which there was a more gradual, linear increase with adsorbed amount up to the maximum of 1200 $mg.m^{-2}$.

Changes in pH can affect the amount of protein adsorbed at a given concentration. However pH change can have a greater effect on membrane permeability than the change in adsorbed amount would suggest (Suki et al, 1984). This is due to the changes in the net charge and size of the protein molecule with pH, or to changes in membrane structure.

Ionic strength of the solution has been shown to affect adsorption. The presence of salt has been found to increase adsorption in some cases (Fane et al, 1983). More commonly, salt has been found to reduce adsorption (Dillman and Miller, 1973). The increase in membrane resistance due to adsorbed protein may be reduced by the presence of salt (Aimar et al, 1986; Nystrom, 1989), although it is not clear whether this is due to reduction in adsorbed amount or to changes in the nature of the adsorbed molecules.

Some data on the effect of protein adsorption on permeability has been presented in terms of 'flux reduction' (at constant pressure). Membranes are usually rinsed after exposure to protein solutions and the flux (measured after rinsing) is compared to the flux previously obtained with the clean or new membrane. Various mathematical functions of the clean and fouled membrane fluxes have been used (Nilsson, 1988; Matthiasson, 1983; Reihanian et al, 1983; Hanemaaijer et al, 1989; Nystrom, 1989). Matthiasson (1983) considered the 'relative flux reduction' (RFR):

$$RFR = 1 - \frac{\text{flux after adsorption}}{\text{flux before adsorption}}$$

The variation of RFR with increasing equilibrium protein

concentration showed more than one plateau in some cases. Even at very high concentrations (50g per 100ml) with some membranes the RFR did not approach a limiting value. Nilsson (1988) also considered RFR as a function of protein concentration. The results showed multiple plateaus up to the maximum concentration of around 25% w/w. Nystrom (1989) plotted RFR as a function of computed wall concentration in ultrafiltration. Reihanian et al (1983) plotted the permeability ratio (permeability after adsorption / permeability before adsorption). The permeability ratio was shown to change slowly with concentration above 2 $g.l^{-1}$. Similar results are reported by Hanemaaijer et al (1989).

Surface treatments have been shown to alter the effect of exposure to protein on the permeability of membranes. Nystrom (1989) showed that the RFR due to fouling was reduced when membranes were pretreated with the polyelectrolyte polyethyleneimine. Hanemaaijer et al (1989) investigated hydrophilic polymer coatings on a polysulphone membrane, which were shown to reduce the effect of exposure to protein in some cases.

The increased membrane resistance due to protein adsorption has often been represented in terms of a series resistance, i.e. a layer on top of the membrane whose resistance is added to that of the clean membrane. The adsorption resistance has been related to the protein concentration to which the membrane is exposed. Several workers report a fairly rapid increase in resistance at lower concentrations, followed by a slower increase or a plateau at higher concentrations (Aimar et al, 1986; Fane et al, 1983; Nabetani et al, 1988).

Aimar et al (1986) fitted the adsorption resistance as an exponential function of the concentration to which the membrane had been exposed. Nabetani et al (1988) rinsed and then sponged the membrane to obtain two values of series resistance, which they attributed to protein adsorbed (1) to the membrane surface and (2) in the pores.

It has been proposed (Dejmek and Nilsson, 1989; Nilsson, 1988) that reduction in permeability after protein adsorption is caused by changes in pore size due to adsorption within the pores. According to this proposal, the drop in permeability should not be represented as a series resistance but as a reduction in an average pore size determined for a clean membrane. Quinn (1979) used hydraulic permeability measurements to infer the thickness of a protein layer adsorbed within a pore in a track etched mica membrane. The pore size reduction approach was shown to be statistically more significant than a series resistance (Dejmek and Nilsson, 1989).

In conclusion, adsorption of proteins to membranes has been shown to have a considerable effect on the membrane permeability. This effect has been quantified both in terms of the protein concentration to which the clean membrane has been exposed and the amount of protein attached to the membrane. Loss of permeability has been explained as a protein layer in series with the membrane, or as a reduction in pore size due to internal adsorption. Recently, the emphasis in the literature has been on the latter approach. The effect of protein concentration (or adsorbed amount) on membrane permeability is highly dependent on the protein(s) and membranes used and the pH and ionic environment.

Effect of Adsorption on Pore Size and Retention Properties

Several investigators have interpreted the decrease in membrane permeability after protein adsorption in terms of pore narrowing caused by adsorption in the pores. Clearly if this is so, the retention properties of the membrane should also be altered.

Rejection is usually found to increase after protein adsorption (Ingham et al, 1980; Nabetani et al, 1988). The effect of protein adsorption on rejection is influenced by ionic strength. Ingham et al (1980) found that the increase in rejection of lysozyme in the presence of albumin could be reversed by adding salt. Cleaning of a membrane after protein adsorption may only partially reduce the rejection back to the new membrane value

(Nabetani et al, 1988).

The effect of protein adsorption on rejection has been modelled in terms of a reduction in a characteristic pore size of the membrane, due to adsorption onto the walls of the pore (Hanemaaijer et al, 1989; Zeman, 1983). The characteristic pore size of new and fouled membranes has been determined by measuring the rejection of low molecular weight saccharides (Hanemaaijer et al, 1989). Zeman (1983) modified the steric rejection theory (Ferry, 1936) to describe the effect of macromolecular adsorption on rejection. Again, a pore size reduction model was used. The model was able to predict qualitatively the shape of the rejection curve describing rejection as a function of the ratio of molecular radius to pore radius.

MATERIALS and METHODS

The constant flux ultrafiltration apparatus used in this study of protein adsorption to membranes was largely the same as that described in Chapter 2 (Fig 1). However, the crossflow (recycle) pump used for this work was a diaphragm metering pump with two heads operating 180° out of phase, giving a maximum crossflow of ≅ 600 ml.min^{-1} at a frequency of 200 min^{-1}. The membranes used in this work were Amicon H1P10-8 polysulphone hollow fibres and Millipore 'Minitan' flat plates in polysulphone (PTGC OMP) and regenerated cellulose (PLGC OMP). All the membranes were of 10,000 nominal molecular weight cutoff. The protein used was bovine serum albumin (BSA)(Sigma A7906).

Fig 1. Constant Flux Ultrafiltration Apparatus.

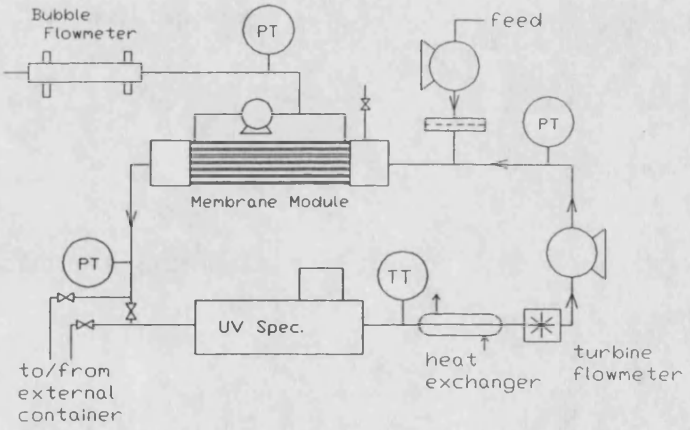

For adsorption experiments the recycle loop was opened to include a stirred beaker. Successive additions of small amounts of solution of a known concentration were made to the beaker. The solution added was typically at 50 to 60 g.l^{-1} giving a final bulk concentration of about 25 g.l^{-1}. The bulk concentration was allowed to reach equilibrium after each addition of protein. Adsorption isotherms were constructed by calculating the mass of protein on the membrane by mass balance, at each equilibrium step. The results are expressed in terms of mass (g) of BSA adsorbed per unit membrane area (m^2), to allow comparison between different modules. The membrane areas used were based on:

(a) Manufacturers information on dimensions and number of fibres (Amicon hollow fibre membranes).

(b) Measurement of membrane plates and separators (Millipore 'Minitan' membranes).

Concentration polarisation effects were eliminated by closing the permeate line to prevent a flux through the membrane. Buffer was circulated in the permeate region to minimise any diffusional gradients.

Membrane Cleaning

The membrane cleaning regime initially used in this work was based on the use of a detergent / proteolytic enzyme solution ('Tergazyme'). The Tergazyme solution (at a concentration of 4 $g.l^{-1}$) was circulated round the retentate side of the membrane at a crossflow rate of 600 $ml.min^{-1}$ at 20 °C for 3 hr. The permeate line remained clamped during this period. After cleaning the system was thoroughly rinsed with distilled water followed by buffer.

A NaOH backflush cleaning regime was used for the bulk of the work, details of which are presented in Chapter 2.

RESULTS and DISCUSSION

Accuracy of Concentration Measurement

The spectrophotometric method used in this work to determine adsorbed amounts is convenient, but highly sensitive to the ratio of the membrane area to the system volume. The accuracy problem is illustrated by some figures typical of the highest concentrations, where errors are largest:

If 6 g protein is dissolved in 220 ml system volume with 1275 cm^2 exposed membrane area, a bulk protein concentration of about 26.4 $g.l^{-1}$ will exist in equilibrium with the adsorbed protein. Accuracy of concentration measurement is assisted by the logging equipment, which allows a definition of 1 part in 1000 of the spectrophotometer full scale deflection. At 26.4 $g.l^{-1}$ this corresponds to an accuracy of about $\pm$ 0.1% (Fig 2). The resulting error in adsorbed amount is about $\pm$ 3%. Drift of the zero reference could contribute an additional 2 or 3 parts in 1000 of the absorbance scale during an experiment, so that a 10% error in adsorbed amount is likely. Quite smooth isotherms have been obtained, however, with reasonable agreement between successive experiments. Control experiments have been performed and are discussed later.

Fig 2. Spectrophotometer Calibration

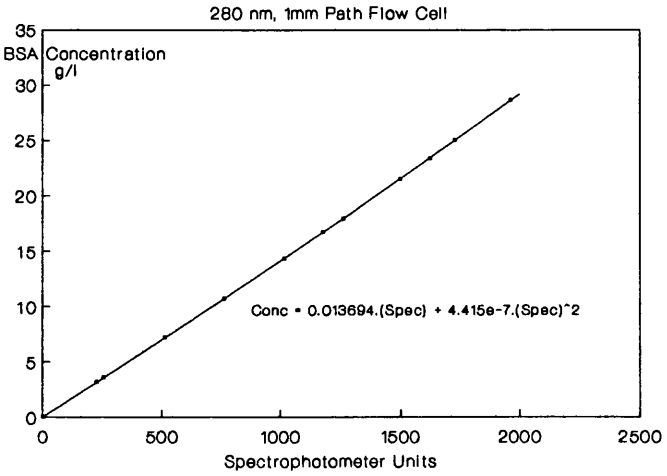

Membrane Cleaning

Three protein adsorption isotherms (Fig 3) were obtained with the Amicon H1P10-8 polysulphone membrane. The tergazyme cleaning regime was used after the first and second isotherms. The results show that the adsorption capacity was reduced greatly between the second and third experiments. It was concluded that the tergazyme regime was not capable of cleaning the membrane well enough to give reproducible adsorption results.

Fig 3. Effect of Cleaning Method

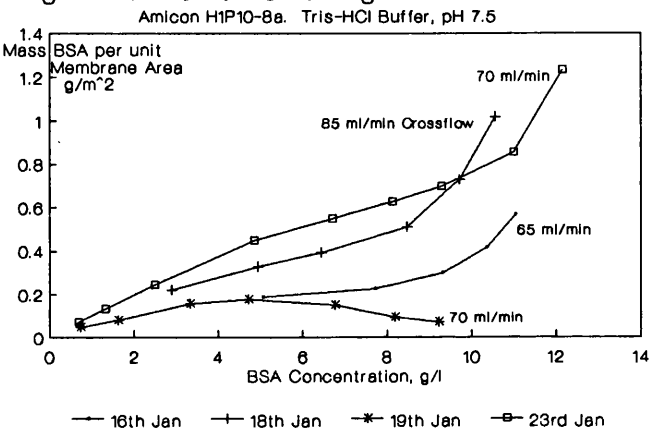

After the third experiment shown in Fig 3, the NaOH cleaning procedure recommended by the manufacturers was adopted (Turker and Hubble, 1987; Chapter 2 of this thesis). Isotherms obtained after implementing this procedure were found to give reproducible results, suggesting that all (or nearly all) the adsorbed protein was removed from the membrane.

In the case of the Millipore 'Minitan' regenerated cellulose membrane (using the NaOH backflush cleaning method), the first four isotherms obtained were fairly consistent, and an example of these is the upper curve on Fig 4. After these isotherms, a run at a lower pH (4.8 c.f. 7.5 for the rest of the isotherms) was carried out. Subsequent isotherms obtained at the original condition of pH 7.5 showed that the adsorption capacity of the membrane had dropped almost to zero (see later section on control

experiments, Fig 9)(lower curves, Fig 4).

Fig 4. Drop in Adsorption Capacity of Cellulose Membrane

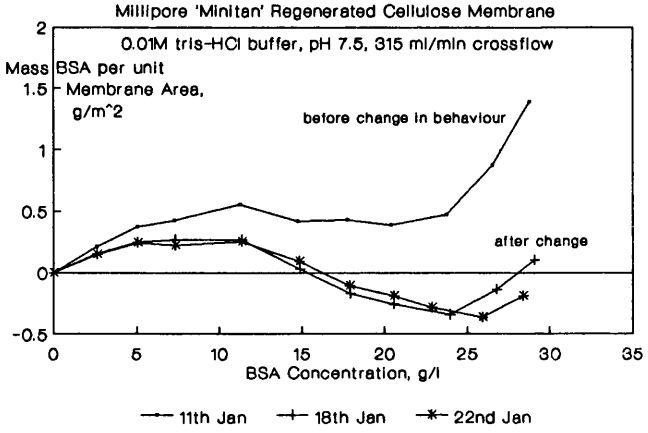

Two possible explanations for this behaviour exist: one is that protein became attached to the membrane in such a way that it could not be removed by NaOH cleaning, even after extended soaking in NaOH for 48hr after one experiment. Such irreversibly bound protein may have resulted in a drop in the capacity for further adsorption. Alternatively, the change in pH from 7.5 to 4.8 (or repeated cleaning with NaOH, with its associated pH change) could have caused an irreversible change to the membrane, altering its adsorption characteristics.

These results demonstrate a difference between the Millipore regenerated cellulose membrane and the Amicon polysulphone membrane. The 'low protein binding' characteristic attributed to the regenerated cellulose membrane by the manufacturer (probably due to the relative hydrophilicity of the membrane) may refer to that obtained after a period of use and cleaning. This work indicates that after this period, the adsorption capacity of the regenerated cellulose membrane is very low.

Effect of Method of BSA Addition on Adsorption

A comparison has been made between the adsorbed amount after gradual increase of BSA concentration and after a single addition

of concentrated BSA with the Amicon polysulphone hollow fibre membrane (Fig 5). The results in Fig 5 were all obtained under the same solution conditions and crossflow rate. The single addition result is in close agreement with the isotherm obtained by stepwise addition of protein. Jonsson et al (1982) suggested that in the case of a gradual increase in concentration, the adsorbed amount would be lower than that for a single addition. They attributed this to spreading of the adsorbed protein layer at low concentration, decreasing the number of sites available for subsequent adsorption. However in these experiments, any difference observed is within the day-to-day variation of results obtained.

Fig 5. Effect of Method of Protein Addition

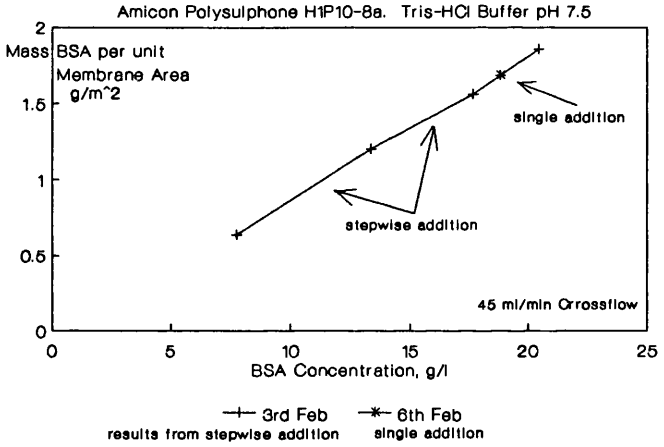

Adsorption Capacity of a New Membrane

A new Amicon H1P10-8 polysulphone hollow fibre cartridge was used to obtain an adsorption isotherm. New membranes are supplied packed in glycerol for protection against drying effects. Before the adsorption experiment was carried out, the new membrane was rinsed at high crossflow rate (600 $ml.min^{-1}$) with several changes of distilled water, the permeate being discarded. The isotherm obtained may be compared with the following one produced on the same membrane after cleaning once with NaOH (Fig 6). The results show that the adsorption capacity of the new membrane was lower than that of the same membrane after cleaning. This may be due to

residual glycerol on the membrane rendering the surface hydrophilic and thus reducing adsorption capacity (Norde, 1986). Alternatively, the NaOH could modify the surface charge or structure of the membrane resulting in greater adsorption.

Fig 6. New Membrane Behaviour

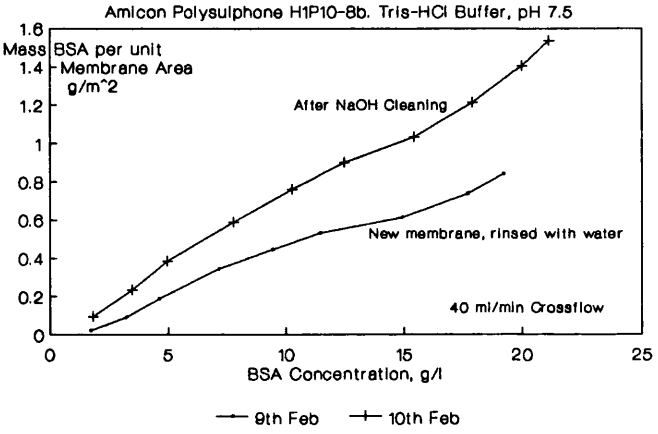

Effect of Different Batches of BSA

On comparing isotherms on the Amicon membrane produced with different batches of BSA from the same supplier under otherwise similar conditions, it was apparent that significantly different results were obtained (Fig 7). The difference between the two batches was greater than those caused by day-to-day variations in results. Changing the batch of BSA seemed to affect both the adsorbed amount (at a given concentration) and the position of the upturn in the isotherm. Possible reasons for the differences are:

(a) Presence of impurities which affected the interaction of the protein with the membrane (for example lipids).

(b) Differences in protein structure due to age, method of purification, etc.

(c) Changes in water content of the BSA. (BSA was added by weight).

Fig 7. Effect of BSA Batch Variations

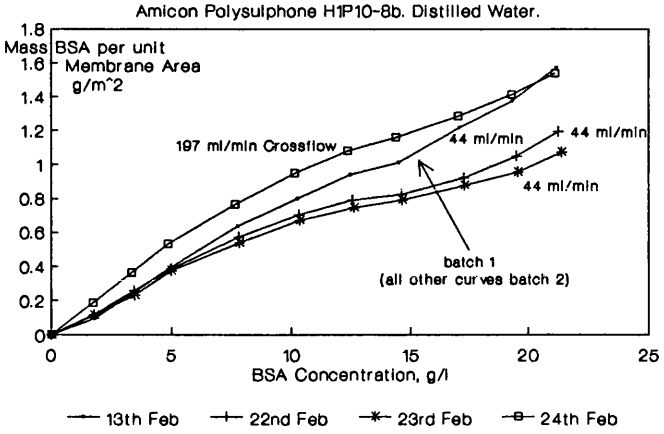

Validation of the Adsorption Measurements

The UV absorbance of the BSA solution was found to rise with time, in the presence as well as in the absence of a membrane (Fig 8), resulting in higher calculated protein concentrations. The increase in UV absorbance could have been due to protein polymerisation or agglomeration in the presence of the solid surfaces in the system or the UV radiation. Such an absorbance rise would result in an underestimate of approximately 0.7 $g.m^{-2}$ at the end of a typical isotherm experiment, c.f. an adsorbed amount of $\cong$ 1.5 or 2 $g.m^{-2}$ calculated from this work. It would also account partly for the negative 'adsorbed amount' indicated at higher concentrations by control isotherms where there was no membrane present or where adsorbed amounts were low (Fig 9), as the higher concentrations occur at the end of an experiment.

Adsorption behaviour of the system with no membrane present was tested. The Minitan membrane unit was replaced by a length of tubing to give approximately the same system volume. An equilibrium 'adsorption isotherm' was obtained in exactly the same way as before (Fig 9) and is expressed in terms of the total adsorbed amount, after correction for a slightly different system volume. The results show that:

(a) The regenerated cellulose membrane was adsorbing little

or no protein in later experiments, as concluded earlier.

(b) Artifacts of the system result in non-zero adsorbed amounts in the absence of a membrane.

Fig 8. Time Dependent Rise In UV Absorbance

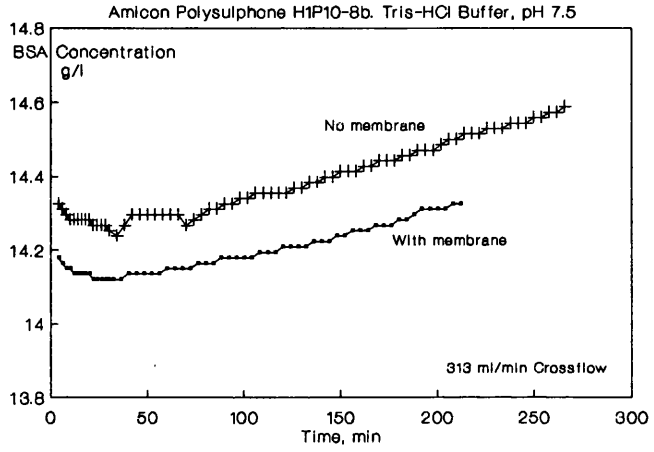

Fig 9. Control Isotherms - With and Without Membrane

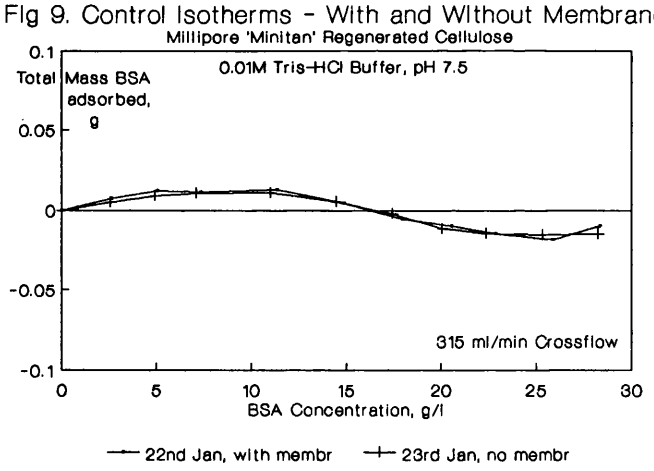

Positive 'adsorbed amounts' obtained without a membrane could indicate adsorption to the walls of the system. However the system wall area at approximately 650 cm^2 is of the same order as the membrane area available for adsorption (508 cm^2). For the positive 'adsorbed amount' indicated by the control experiment, protein loading would have to be of the same order as that obtained on membranes. Work by others has shown that maximum

adsorption to non-membrane polymers is only 5 $mg.m^{-2}$ (Hanemaaijer et al, 1989), which would not account for the observed results. Negative 'adsorbed amounts' could be a result of protein denaturation caused by shear, UV radiation or interaction with the surfaces in the system, resulting in increased UV absorbance.

Nature of Isotherms Obtained

Isotherms describing adsorption to the retentate side of both polysulphone and regenerated cellulose membranes showed that the adsorbed amount did not approach a constant value up to the maximum equilibrium protein concentration of ≅ 26 $g.l^{-1}$ used. For Amicon polysulphone membranes, a slight point of inflexion was observed in the concentration range 10 to 15 $g.l^{-1}$ (Fig 6), whilst the Millipore 'Minitan' regenerated cellulose membrane exhibited a more marked plateau (Fig 10). In the light of the long term absorbance rise measured in the system, the high concentration regions of the isotherms may in fact represent higher adsorbed amounts than those indicated, so that the upturns in adsorbed amount at higher protein concentrations may be more severe than those shown.

Fig 10. Isotherms on Regenerated Cellulose Membrane

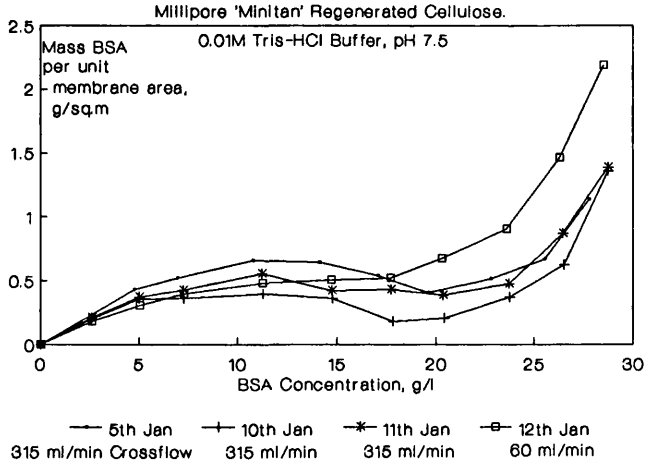

Other workers have obtained similar results showing adsorbed amounts increasing steeply with concentration, even at high concentrations (Matthiasson, 1983; Nilsson, 1988). The existence

of a point of inflexion or plateau in the isotherm may indicate a transition between two types of adsorption, for example between two packing densities in the adsorbed layer or between monolayer and multilayer adsorption.

Effect of Crossflow Rate on Adsorption

Five experiments at different crossflow rates were performed, all using the same Amicon polysulphone hollow fibre membrane and the same solution conditions (Fig 11). The first three experiments at 44, 85 and 200 ml.min^{-1} crossflow rate showed that there was an increase in adsorption with increasing crossflow rate. The last two experiments at 18 ml/min crossflow rate were not consistent with this. It was felt that daily variations in the behaviour of the protein-membrane system (which have been observed) could account for this. Other experiments confirmed the effect of increasing crossflow rate on adsorption.

Fig 11. Effect of Crossflow Velocity on Adsorption

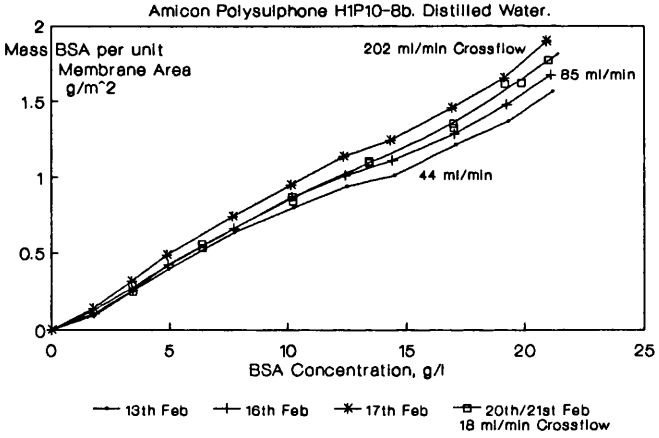

The effect of increasing crossflow rate upon adsorption has been investigated by Chuang et al (1978) for albumin adsorption to non membrane polymer surfaces. They also reported increasing adsorption with increasing crossflow rate.

The effect of increased shear on adsorption has been explained in terms of improved mass transfer, leading to faster adsorption

which reduces the time available for the spreading of protein layers over the surface (Nilsson, 1989). Layer spreading has been linked with reduction in total adsorption (Jonsson et al, 1982). The tendency of shear to remove protein molecules from the surface has been discussed, although the free energy of protein adsorption is probably too large for shear removal to be observed.

Experiments performed at very low crossflow rates with the hollow fibre membranes were found, in some cases, to result in much decreased adsorption (Fig 12). The shape of the isotherms was also different from the shape obtained at higher crossflow rates. These results seem to support the theory of layer spreading, under conditions of low mass transfer, resulting in lower adsorbed amounts.

Fig 12. Adsorption at Low Crossflow

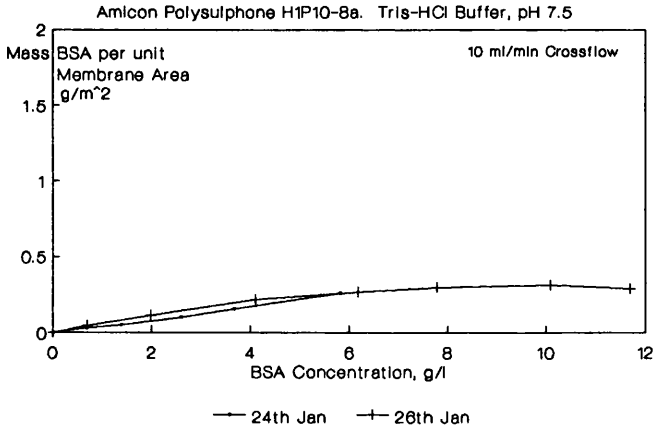

Work with the Millipore 'Minitan' regenerated cellulose membrane indicated an increase in adsorption with *decreasing* crossflow (at least at high protein concentrations)(Fig 10). The effect of shear on the removal of bound protein may have been greater with the regenerated cellulose membrane, overshadowing any kinetic layer spreading phenomenon.

There are unfortunately no results available for the effect of crossflow on adsorption to *polysulphone* Millipore 'Minitan'

membranes, for comparison with regenerated cellulose. It is difficult to comment further on the effect of crossflow on adsorption to regenerated cellulose membranes, as subsequent experiments gave much lower adsorbed amounts, possibly due to incomplete removal of protein by cleaning (discussed earlier).

Effect of Ionic Strength

The effect of ionic strength of the buffer on protein adsorption was investigated (Fig 13). Isotherms obtained using distilled water (pH approx 5) and 0.01M Tris-HCl buffer (pH 7.5) were found to be little different. However with 0.1M Tris-HCl buffer (pH 7.5) there was significantly less adsorption at the higher crossflow rate. Higher ionic strength seemed to 'salt in' the BSA to solution, resulting in less adsorption. These results agree with the findings of most others (Dillman and Miller, 1973), although salt has also been shown to increase adsorption (Fane et al, 1983). The effect on adsorption of changing salt concentration may depend on the pH of the solution relative to the isoelectric point of the protein.

Fig 13. The Effect of Ionic Strength on Adsorption

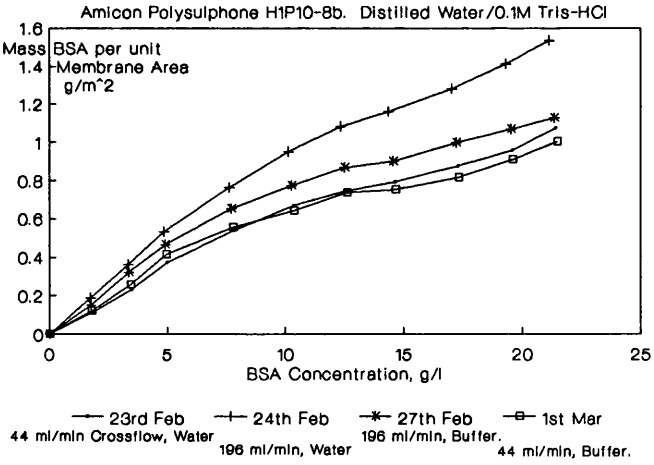

Effect of pH

The effect of pH on adsorption was studied. Buffers of varying pH but a constant concentration of 0.01M were used:

Tris-HCl pH 7.5

Sodium Acetate-Acetic Acid pH 4.8

Glycine-HCl pH 2.5

Glycine-NaOH pH 10.0

Adsorption isotherms were determined using each of the above buffers, the system having previously been equilibrated with the appropriate buffer. All other conditions were maintained constant for this series of experiments.

Examination of the isotherms (Fig 14) shows that, at least at higher concentrations, adsorption was greatest at the isoelectric point (pH 4.8 for BSA). Increasing the pH above the isoelectric point gave less adsorption. Decreasing the pH to 2.5 gave greater adsorption at the lower bulk protein concentrations, but there is a maximum in the isotherm, and at higher concentrations the adsorbed amount was much lower at pH 2.5 than at the isoelectric point. The behaviour of the system at pH 2.5 is difficult to explain, but it seems likely that conformational changes in the protein molecules occurred at such a low pH. It is possible that conformational changes in the adsorbed protein layer affect the adsorbed amount, causing the maxima and minima in the pH 2.5 isotherm. Alternatively, changes in the structure of the protein (similar to those observed over relatively long periods of time at pH 7.5) may have affected the absorbance of the BSA, rendering concentration measurement inaccurate.

Fig 14. The Effect of pH on Adsorption

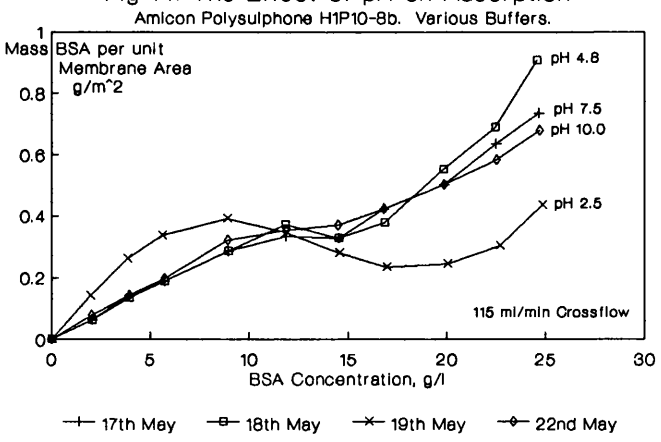

The results agree with the conclusions of several workers who report greatest adsorption at the isoelectric point. In this work the effect of pH is less marked than previously reported (Fane et al, 1983).

Support Side Adsorption

Comparison of adsorption to the retentate (thin skin) and permeate (porous support) sides of the membrane provides an insight into the influences of support side adsorption.

Experiments were performed using a Millipore 'Minitan' membrane module, chosen because crossflow conditions and exposed membrane areas could be determined for both the retentate and permeate chambers. The adsorption behaviour of the membranes could be compared by reversing the roles of the retentate and permeate ports of the module.

Experiments were performed under similar conditions to those using hollow fibre membranes: Protein solution was recirculated across the membrane whilst the flow chamber on the opposite side of the membrane was closed off but filled with circulating buffer.

Adsorption to the permeate side of the polysulphone Millipore 'Minitan' membrane was considerably greater than to the retentate, and seemed almost linear with concentration (Fig 15). Adsorption to the retentate side showed similar characteristics to isotherms obtained on Amicon H1P10-8 polysulphone hollow fibre membranes, but the adsorbed amount was greater on the Millipore membrane by a factor of 1.5 to 2.

Fig 15. Comparison of Adsorption to Retentate and Permeate

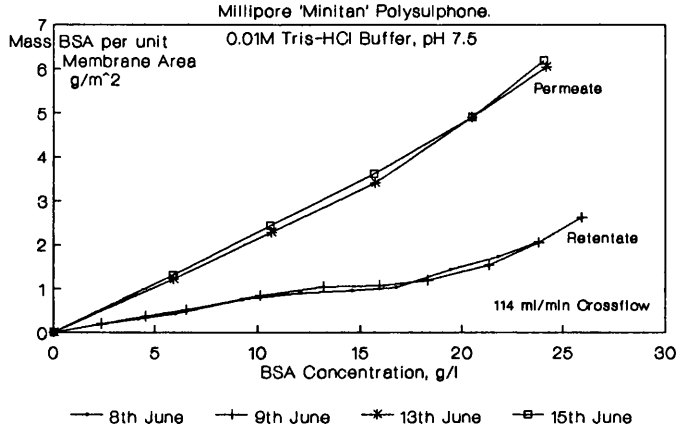

Assuming that the nature of adsorption to all parts of the membrane was similar, the results show that protein was able to migrate to some extent through the membrane skin from the retentate side to the permeate side. If this were not the case then far greater adsorption would be expected from the permeate side, due to its greater area. This argument relies on the assumption that anisotropic membranes consist of a very thin skin which is relatively flat and has small holes which facilitate separation (retentate side) and a relatively thick, spongy support region with much larger holes (permeate side). Therefore the area for adsorption provided by the support region is much greater than the nominal membrane area.

Permeate side adsorption was a factor of 2.5 to 3 times greater than retentate adsorption, suggesting that the membrane skin presented a time-independent restriction to the migration of protein into the porous support region.

The proposal that the high adsorption capacity of membranes is provided by migration of protein into the spongy support region would have to be confirmed by electron microscopy to visualise protein adsorption.

Transport through the membrane skin (which theoretically rejects the protein) could be by conformational changes in the protein structure, allowing it to pass through the pores. Alternatively, the pore size distribution present in membranes could allow unmodified protein molecules to pass through the larger pores. Diffusive and/or convective transport could then provide access to the rest of the support region. During adsorption experiments, no protein was detected in the liquid in the permeate region. However when a flux was applied, protein was detected in the permeate, but the concentration was too low to be accurately measured by UV absorbance.

Reversibility upon Dilution

Adsorption reversibility on dilution was investigated with:

Amicon H1P10-8 hollow fibre (polysulphone).

Retentate side of Millipore 'Minitan' flat sheet (polysulphone).

Retentate side of Millipore 'Minitan' flat sheet (regenerated cellulose).

Permeate side of Millipore 'Minitan' flat sheet (polysulphone).

Adsorption isotherms were obtained, as in previous experiments, by stepwise addition of concentrated BSA solution. Desorption isotherms were then obtained by removing a measured volume of the equilibrium bulk solution and replacing it with buffer. The system was allowed to reach equilibrium between each step. The results for polysulphone membranes are shown in Fig 16, where the curves starting from the origin show adsorption isotherms obtained in the usual way and the curves in the direction of decreasing concentration show dilution (desorption). Results for the regenerated cellulose membrane are shown in Fig 17.

Fig 16. Reversibility upon Dilution

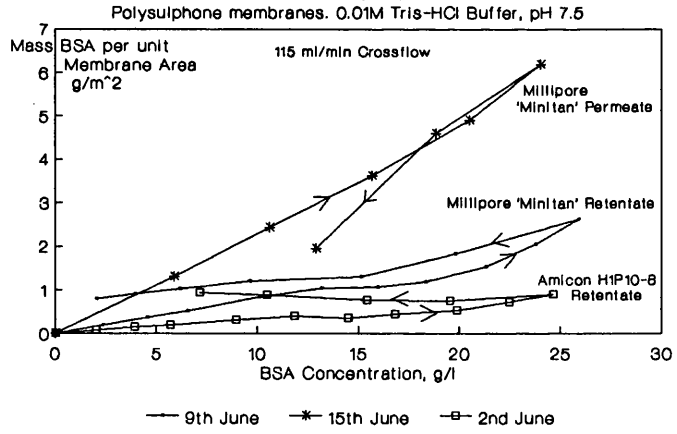

In desorption experiments, the time dependent UV absorbance rise of the BSA (Fig 8) must be considered. However, it has been shown that the A_{280} rise in a system without a membrane was equivalent to a rate of change of concentration of about 0.0014 $g.l^{-1}.min^{-1}$. The lowest steady rate of change of concentration in a desorption experiment was about 0.0026 $g.l^{-1}.min^{-1}$ (see section on kinetics, later in this Chapter). Therefore desorption from the membrane

(and/or change in the UV absorbance of the protein by interaction with the membrane) does take place, but the rate and amount is difficult to determine accurately.

Fig 17. Reversibility With Regenerated Cellulose Membrane

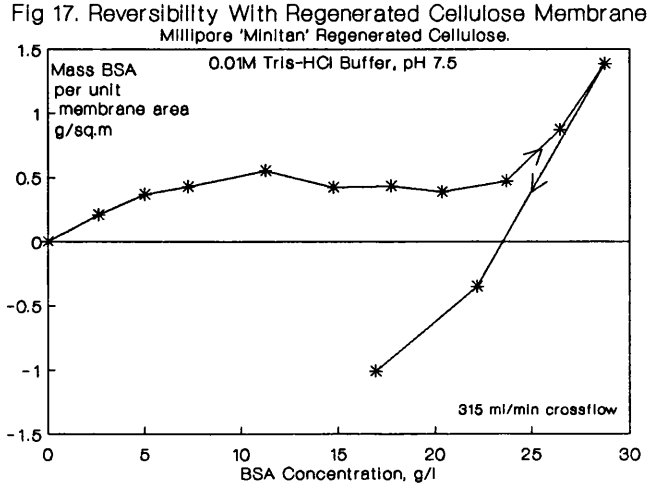

Dilution with the Amicon membrane produced little or no desorption over the time scale of the experiment (1 to 2 hr). In many cases an increase in adsorbed amount was observed on dilution. Structural changes in the adsorbed protein layer on dilution of the bulk solution may have allowed greater adsorption.

The retentate side of the polysulphone Millipore 'Minitan' exhibited some desorption on dilution, and the permeate side of the same membrane showed considerable reversibility. In some cases, further dilution resulted in negative adsorbed amounts, as shown by the results for the regenerated cellulose membrane (Fig 17). This is obviously unrealistic, but might be explained by structural modification of proteins upon desorption leading to a greater UV absorbance. The presence of the Amicon polysulphone membrane had little effect on the long term UV absorbance rise measured in the system (Fig 8), but it is possible that the presence of the Millipore membranes (polysulphone and regenerated cellulose) did produce an absorbance rise.

These results demonstrate that membranes of the same material and nominal molecular weight cutoff do not necessarily behave in the same way (Amicon polysulphone c.f. Millipore polysulphone). These

two membranes have quite different adsorption capacities and reversibility/denaturation characteristics.

If protein denaturation did not account for all the measured concentration rise upon dilution of the system, then the Millipore membranes showed some desorption upon dilution, contradicting conclusions in the literature that desorption is often so slow as to be unnoticeable. Some multilayer adsorption may have occurred under these conditions, so that the weaker binding forces in layers of protein more distant from the membrane could have resulted in measurable desorption. The evidence of desorption presented here is not conclusive, due to the possibility of increases in the UV absorbance of the protein.

Kinetics

The kinetics of adsorption and desorption of BSA with Millipore 'Minitan' and Amicon H1P10-8 polysulphone membranes have been investigated (Figs 18 to 23). Adsorption to the retentate sides of the membranes reached equilibrium within approximately 15 min (Figs 18-20). Kinetic data was obtained by continuous measurement of the concentration of the retentate stream being circulated across the membrane. Very long term experiments were impractical due to a gradual rise in UV absorbance of the BSA solution (Fig 8), as discussed earlier.

Adsorption to the permeate side of the Millipore 'Minitan' polysulphone membrane was much slower than to the retentate side (Fig 21). At low concentration, equilibrium was not attained after 4 hr. After further additions of protein to the same system, equilibrium was essentially reached after 40 min.

Adsorption kinetics have been modelled in terms of diffusion-controlled transport to the solid-liquid interface (Norde, 1986). The diffusion controlled approach is supported by these results, since the adsorption capacity from the permeate side of the membrane is greater (Fig 15), and it seems reasonable to suppose that some of the additional capacity available is not easily

reached by the protein molecules.

Desorption kinetics for the retentate and permeate sides of the Millipore 'Minitan' polysulphone membrane were investigated (Figs 22,23). Desorption from the permeate side was shown to attain a constant rate; equilibrium was not reached after 3 hr. Similar results were observed for the retentate side up to 80 min. Desorption from Amicon membranes was not observed over the time scale of the experiments. These results may support the theory that desorption does take place in liquid-solid protein adsorption, although the rate of desorption seems to be highly dependent on the membrane used. However, a rise in the UV absorbance of the protein upon desorption from the membrane might imply greater desorption than was actually the case. Different observed degrees of adsorption may be due to differences in structural modification (and thus changes in the UV absorbance) of the protein by the different membrane surfaces investigated.

Fig 18. Kinetics of Adsorption

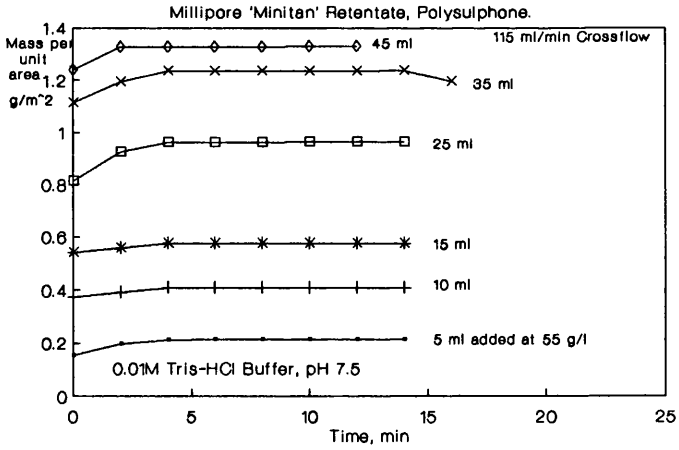

Fig 19. Kinetics of Adsorption

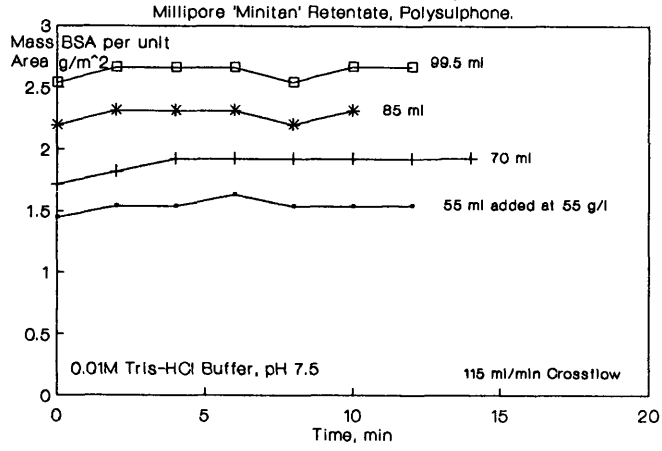

Fig 20. Kinetics of Adsorption

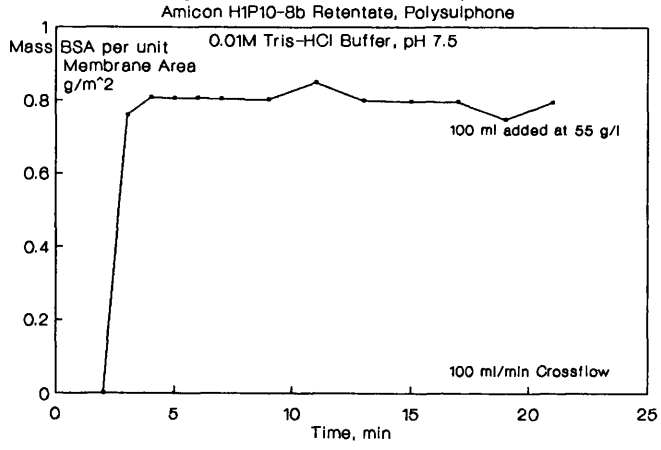

Fig 21. Kinetics of Adsorption

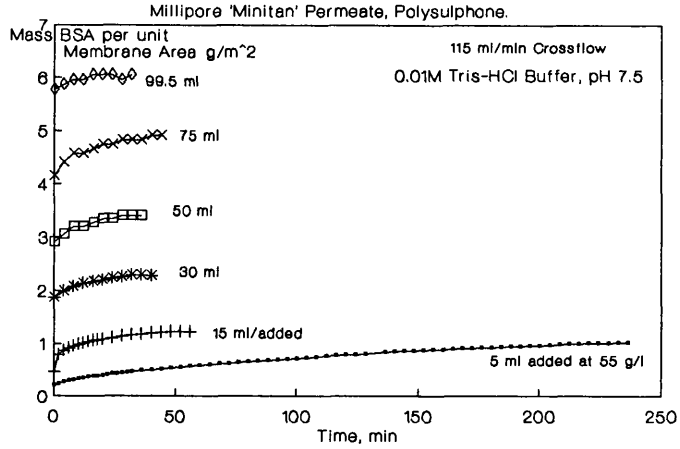

Fig 22. Kinetics of Desorption

Millipore 'Minitan' Retentate, Polysulphone.

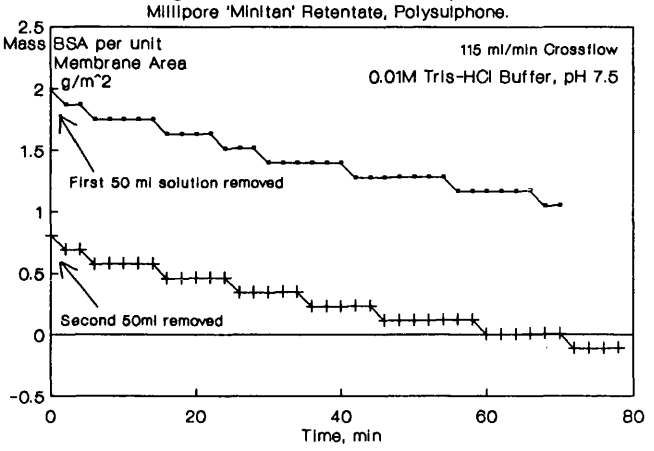

Fig 23. Kinetics of Desorption

Millipore 'Minitan' Permeate, Polysulphone.

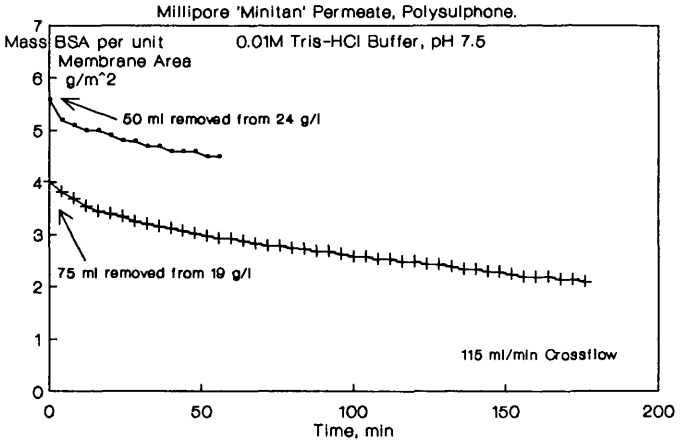

SUMMARY and CONCLUSIONS

In order to obtain repeatable results it is necessary to backflush the membrane with 0.1M NaOH after each experiment. Even so, long term changes in behaviour have been observed. In particular, work with regenerated cellulose membranes showed initially similar adsorbed amounts to those obtained in the bulk of the work with polysulphone membranes. After some use, however, the adsorption capacity of the regenerated cellulose membrane decreased considerably, possibly due to the presence of tightly bound protein occupying the adsorption sites, or to a change in the membrane structure. The choice of membrane material is clearly an important factor in determining the long term as well as short term adsorption behaviour.

Adsorbed amounts resulting from single large additions of protein compared closely with isotherms obtained from stepwise increases in concentration. This indicates that the concentration history in a single experiment did not affect the adsorbed amount, provided that the concentration never exceeded the final equilibrium value. However the work on the effect of crossflow on adsorption provided some evidence supporting the proposal of Jonsson et al (1982) that slower protein addition should lead to decreased adsorption due to the time available for spreading of protein over the membrane surface.

New polysulphone membranes were found to have a lower adsorption capacity before cleaning with NaOH, even though they were thoroughly rinsed to remove the glycerol preserving solution. Polysulphone membranes are hydrophobic and thus have a relatively high adsorption capacity, and it seems that the presence of residual glycerol may have reduced the hydrophobicity of the membrane before it was cleaned with NaOH. This demonstrates the possibility of treating membranes in order to reduce adsorption (fouling).

Adsorption was found to be sensitive to the source of protein, two

different batches of BSA from the same supplier giving considerably different results. This illustrates the importance of the solute in determining protein-membrane interactions, and the difficulty of applying a general model to protein adsorption to membranes.

The validity of the technique used in this work was examined by performing an experiment in the absence of a membrane. The results indicated that there may be some adsorption to the non membrane surfaces of the system. In addition, a long term rise in UV absorbance of the protein (even in the absence of a membrane) means that the accuracy of adsorption measurements decreases with time. However, the technique used here has been shown to give internally consistent results and is therefore valuable for the comparison of different membranes and adsorption conditions. Better than order of magnitude estimates of adsorbed amounts can be made.

Equilibrium adsorption isotherms obtained are not of the saturation type. In nearly all cases the isotherms had a decreasing gradient up to an equilibrium protein concentration of 8 to 15 $g.l^{-1}$, above which the gradient increased again up to the maximum concentration of 20 to 26 $g.l^{-1}$. The form of the isotherms was in keeping with some published work, although others have obtained saturation isotherms.

The amount of protein adsorbed to membranes measured in this (and other) work is far greater than the amount adsorbed to non membrane polymers (1500 $mg.m^{-2}$ as compared to 5 $mg.m^{-2}$) (Hanemaaijer et al, 1989). The large adsorption capacity is probably provided partly by multilayer adsorption and partly by migration and adsorption within the support structure of the membrane. The point of inflexion on the adsorption isotherms suggests a transition between adsorbed states or formation of additional adsorbed layers. Adsorption within the support structure of membranes could perhaps be visualised by electron microscopy techniques.

From investigations of the effect of crossflow, pH and ionic strength, it has been concluded that:

(a) Increasing shear considerably increases the adsorbed amount on polysulphone membranes, in agreement with previous work (Chuang et al, 1978). However the work with regenerated cellulose membranes indicated (inconclusively) that the opposite effect may occur with this material. It is possible that the effect of rate of adsorption on the adsorbed amount (Jonsson et al, 1982) is important in determining the effect of crossflow, due to different mass transfer conditions between the bulk solution and the membrane.

(b) Adsorption increased towards the isoelectric point of BSA, although the effect was only apparent at higher concentrations (greater than 20 $g.l^{-1}$). Decreasing the pH to 2.5 with a polysulphone membrane resulted in an apparent maximum and minimum in the isotherm, but this may well have been due to changes in the structure and thus the UV absorbance of the BSA at this low pH. The first experiment at pH 4.8 with the regenerated cellulose membrane (after several experiments at pH 7.5) resulted in a substantial decrease in the adsorption capacity of the membrane. The adsorption capacity was not recovered after cleaning, and it is not clear whether the change in behaviour was due to the change in pH or to the aging of the membrane.

(c) Increasing salt concentration reduced adsorption to polysulphone membranes, in accordance with some, but not all, published work.

Adsorption within the support structure of the membranes requires migration of protein molecules through the separating skin of the anisotropic membranes. In this work, evidence for support side adsorption has been provided by comparing the adsorption capacities of the retentate and permeate sides of a polysulphone membrane. Adsorption to the permeate (open support) side was about three times greater than than adsorption to the retentate (separating skin) side of membranes, whereas the available area on the permeate side is about 400 times greater (Hanemaaijer et al,

1989). It seems, therefore, that migration of protein from the retentate through to the support structure of the membrane does occur, since otherwise the permeate side adsorption should be about two orders of magnitude greater than retentate adsorption.

Desorption seemed to occur, but at different rates depending on the membrane surface: no desorption from Amicon polysulphone hollow fibre membranes was observed, whereas desorption from Millipore 'Minitan' polysulphone and regenerated cellulose membranes did not reach equilibrium after 3 hr. As negative 'adsorbed amounts' were calculated during desorption in some cases, it is likely that denaturation of protein upon desorption resulted in increased UV absorbance, thus distorting the results. Exchange of protein between adsorbed and dissolved states was demonstrated by Brash and Samak (1978), and if this is accompanied by protein denaturation, a gradual denaturation of all the protein present could occur. This might be an important factor affecting the performance of enzyme membrane reactors, as denaturation of enzymes usually results in loss of activity.

Adsorption to the retentate sides of polysulphone Amicon hollow fibre and Millipore 'Minitan' flat sheet membranes was essentially complete within 15 min, although a very slow increase in adsorbed amount may occur after this. In contrast, adsorption to the permeate side of the polysulphone Millipore membrane was not complete after 4 hr, probably demonstrating increased diffusional resistance present due to the difficulty of access to some of the additional surface area available from the support side of the membrane.

REFERENCES

Aimar, P.; Baklouti, S.; Sanchez, V.
"Membrane solute interactions: Influence on pure solvent transfer during ultrafiltration."
J. Membr. Sci., 29 (1986) 207-224.

Aimar, P.; Lafaille, J.P.; Sanchez, V.
"Influence of adsorption on protein ultrafiltration using organic/inorganic membranes."
Proc. 2nd Int. Conf. Foul. Clean. Food. Process. Lund., (1985).

Beissinger, R.L.; Leonard, E.F.
"Immunoglobulin sorption and desorption rates on quartz: Evidence for multiple sorbed states."
J. Am. Soc. Artif. Int. Organs, 3 (1980) 160-175.

Brash, J.L.; Samak, Q.M.
"Dynamics of interactions between human albumin and polyethylene surface."
J. Colloid Interface Sci., 65 (1978) 495-504.

(1) Choe, T.B.; Masse, P.; Verdier, A.; Clifton, M.J.
"Membrane fouling in the ultrafiltration of polyelectrolyte solutions: Polyacrylic acid and bovine serum albumin."
J. Membr. Sci., 26 (1986) 17-30.

Chuang, H.Y.K.; King, W.F.; Mason, R.G.
"Interaction of plasma proteins with artificial surfaces: Protein adsorption isotherms."
J. Lab. Clin. Med., 92 (1978) 483-496.

(2) Dejmek, P.; Nilsson, J.L.
"Flux based measures of adsorption to ultrafiltration membranes."
J. Membr. Sci., 40 (1989) 189-197.

Dillman, W.J.; Miller, I.F.
"On the adsorption of serum proteins on polymer membrane surfaces."
J. Colloid. Interface Sci., 44 (1973) 221-241.

Fair, B.D.; Jamieson, A.M.
"Studies of protein adsorption on polystyrene latex surfaces."
J. Colloid Interface Sci., 77 (1980) 525-534.

Fane, A.G.; Fell, C.J.D.; Suki, A.
"The effect of pH and ionic environment on the ultrafiltration of protein solutions with retentive membranes."
J. Membr. Sci., 16 (1983) 195-210.

Ferry, J.D.
"Statistical evaluation of sieve constants in ultrafiltration".
J. Gen. Physiol., 20 (1936) 95-104.

Gacesa, P.; Eisenthal, R.; England, R.
"Immobilization of urease within a thin channel ultrafiltration cell."
Enzyme. Microb. Technol., 5 (1983) 191-195.

Hanemaaijer, J.H.
"Fouling of ultrafiltration membranes. The role of protein adsorption and salt precipitation."
Proceedings of a Workshop on Membranes, Univ. Twente, Netherlands (1989).

Hanemaaijer, J.H.; Robbertsen, T.; Boomgaard, T.; Gunnink, J.W.
(3) "Fouling on ultrafiltration membranes. The role of protein adsorption and salt precipitation."
J. Membr. Sci., 40 (1989) 199-217.

Ingham, K.C.; Busby, T.F.; Sahlestrom, Y.; Castino, F.
(4) "Separation of macromolecules by ultrafiltration: Influence of protein adsorption, protein-protein interactions, and concentration polarization".
Ultrafiltration Membranes and Applications, ed Cooper,A.R. (1980).

Jonsson, U.; Ivarsson, B.; Lundstrom, I.; Berghem, L.
"Adsorption behaviour of fibronectin on well-characterised silicon surfaces."
J. Colloid Interface Sci., 90 (1982) 148-163.

Lockley, A.K.; White, W.J.P.; Hall, G.M.
"A method of assessing protein adsorption onto ultrafiltration membranes."
Int. J. Food Sci. Technol., 23 (1988) 11-15.

Lundstrom, I.
"Models of protein adsorption on solid surfaces."
Prog. Colloid Polymer Sci., 70 (1985) 76-82.

Matthiasson, E.
"The role of macromolecular adsorption in fouling of ultrafiltration membranes."
J. Membr. Sci., 16 (1983) 23-26.

Matthiasson, E.; Hallstrom, B.; Sivik, B.
"Adsorption phenomena in fouling of UF membranes."
Engineering Sciences in the Food Industry ed McKenna, B.M. (1989).

Nabetani, H.; Nakajima, M.; Watanabe, A.; Nakao, S.; Kimura, S.
(5) "Change of permeate flux and solute rejection by ovalbumin adsorption on ultrafiltration membranes."
Membrane, 13 (1988) 51-57.

Nilsson, J.L.
"Fouling of ultrafiltration membranes by a dissolved whey permeate concentrate and some whey proteins."
J. Membr. Sci., 36 (1988) 147-160.

Nilsson, J.L.
"A study of ultrafiltration membrane fouling."
PhD Thesis, Division of Food Engineering, Lund University, (1989).

Norde, W.
"Adsorption of proteins from solution at the solid-liquid interface."
Adv. Colloid and Interface Sci., 25 (1986) 267-340.

Nystrom, M.
(6) "Fouling of unmodified and modified polysulphone ultrafiltration membranes by ovalbumin."
J. Membr. Sci., 44 (1989) 183-196.

Patel, R.S.; Reuter, H.
"Deposit formation on a hollow fiber ultrafiltration membrane during concentration of skim milk."
Milchwissenschaft, 40 (1985) 592-595.

Quinn, J.A.
"Thickness and density of protein films adsorbed in track-etched membranes."
Natl. Sci. Found. Res. Appl. Natl. Needs (Rep) (1979) 503-510.

Reihanian, H.; Robertson, C.R.; Michaels, A.S.
(7) "Mechanism of polarisation and fouling of ultrafiltration membranes by proteins."
J. Membr. Sci., 16 (1983) 237-258.

Suki, A.; Fane, A.G.; Fell, C.J.D.
(8) "Flux decline in protein ultrafiltration."
J. Membr. Sci., 21 (1984) 269-283.

Turker, M.; Hubble, J.
"Membrane fouling in a constant flux ultrafiltration cell."
J. Membr. Sci., 34 (1987) 267-281.

Zeman, L.J.
"Adsorption effects in rejection of macromolecules by ultrafiltration membranes."
J. Membr. Sci., 15 (1983) 213-230.

Last Page of Chapter 3

CHAPTER 4

CONCENTRATION POLARISATION in a CONSTANT FLUX ULTRAFILTRATION APPARATUS: PREDICTION of BULK PROTEIN CONCENTRATIONS USING a LUMPED PARAMETER MODEL

ABSTRACT

Changes in the bulk protein concentration due to polarisation have been measured in a constant flux hollow fibre ultrafiltration apparatus operating with a fixed mass of protein under conditions of total protein rejection. A simple, lumped parameter model capable of analytical solution has been developed to describe these concentration changes. The model is capable of a reasonable description of concentration polarisation over a range of crossflows and fluxes, especially when crossflows are non pulsating, and is based on a limited number of parameters which can be estimated from empirical expressions. Optimal values for the model parameters in the system suggest that the boundary layer is thinner under pulsating crossflows. The amount of protein adsorbed to the membrane was found to increase after polarisation towards a little used membrane, but not after polarisation towards a well used membrane. The resistance of the rinsed membrane after polarisation was found to be strongly dependent on the flux which had been applied, even when there was no evidence of increased protein adsorption.

NOMENCLATURE

C	Protein concentration	$g.l^{-1}$
d	Diameter of hollow fibres	m
D	Protein diffusivity	m^2s^{-1}
J	Flux through membrane	$m.s^{-1}$
k	Mass transfer coefficient	$m.s^{-1}$
K	Constant in laminar flow mass transfer correlation	-
L	Length of hollow fibres	m
n	Exponent in laminar flow mass transfer correlation	-
N	Number of hollow fibres in cartridge	-
Q	Volumetric flowrate	m^3s^{-1}
r	Radius of hollow fibres	m
R	Relative membrane resistance	-
Re	Reynolds number $\left[\frac{\rho\ d\ u}{\mu}\right]$	-
Sc	Schmidt number $\left[\frac{\mu}{\rho\ D}\right]$	-
Sh	Sherwood number $\left[\frac{k\ d}{D}\right] = \left[\frac{d}{\delta}\right]$ when $k = \frac{D}{\delta}$	-
u	Average axial velocity in fibres	$m.s^{-1}$
V	Total volume of recycle loop	m^3
y	Distance perpendicular to membrane	m
β	Dimensionless group $\left[\frac{J\ y}{D}\right]$	-
δ	Thickness of boundary layer	m
μ	Viscosity of solution	$kg.m.s^{-1}$
ρ	Density of solution	$kg.m^{-3}$

Sub- and Superscripts:

b	'Bulk' region in fibres
bl	Boundary layer region in fibres
F	Region of the recycle loop between feed and entrance of hollow fibres
l	Feed into recycle loop
m	Average over the concentration boundary layer
o	Before polarisation

R Region of the recycle loop between exit of hollow fibres and feed

w At the solution-membrane interface

INTRODUCTION

Under any realistic operating conditions, some degree of concentration polarisation during ultrafiltration is inevitable. Concentration polarisation means that the macromolecule distribution within an ultrafiltration unit changes and hence dictates the concentration to which the membrane is exposed. Concentration polarisation therefore affects fouling and hence the membrane resistance.

Concentration polarisation will affect the performance of an enzyme membrane reactor both by causing non uniform distribution of enzyme (and possibly substrate and product) and by affecting membrane resistance and/or solute rejection. Ideally, quantification and prediction of concentration polarisation is needed in order to model the performance of an enzyme membrane reactor.

Given that fouling has been shown to be a time dependent phenomenon, a practical complication in constant pressure ultrafiltration is that transmembrane flux will vary with time and so concentration polarisation will be time dependent.

To take account of polarisation and fouling effects rigorously, a complete mathematical description of an enzyme membrane reactor is required. Such a description involves solution of the convection-diffusion, momentum and reaction rate equations for the membrane configuration used. Expressions relating protein concentration at the membrane surface to permeability, rejection and possibly adsorption are also needed. Solution of such problems is computationally intensive and the values of some of the parameters (such as those describing the relationships between membrane resistance, wall concentration and time) may be difficult or impossible to determine. In many cases assumptions (such as constant membrane resistance and solute rejection) have to be made which reduce the reliability of distributed parameter models. As an alternative, a simple lumped parameter approach using easily

obtainable parameters could offer acceptable solutions to some problems, together with significant computational savings.

Although concentration polarisation in unstirred ultrafiltration has been measured using an optical technique (Vilker et al, 1981), direct measurement of concentration polarisation in crossflow ultrafiltration is likely to be extremely difficult, and at present it seems that polarisation must be inferred by other means.

Models of concentration polarisation in crossflow filtration have been based on various sets of assumptions. One class of model requires solution of the convection-diffusion equations for the geometry concerned, together with functions describing the velocity field (Bhattacharyya et al, 1990; Fell et al, 1990; Kleinstreuer and Belfort, 1984; Kleinstreuer and Paller, 1983; Carter and Hasting, 1980; Shah, 1971; Merson and Ginette, 1970). The assumption of constant membrane resistance is usually made. Alternatively, models have been based on an assumed relationship between polarisation layer thickness and wall concentration gradient, using an osmotic pressure model for permeation rate (Leung and Probstein, 1979; Clifton et al, 1984; Aimar et al, 1989).

It is possible to develop a simplified model of some of the effects of concentration polarisation, by considering the polarisation layer as a region of uniform concentration equal to an average of the real concentration profile. Such a model can also be used to estimate the protein concentration at the solution-membrane interface (wall). If the wall concentration under polarisation conditions is known, information can be obtained on protein adsorption to membranes at higher concentrations than may be attained in zero flux experiments (Gill et al, 1988). Wall concentration can also be correlated with membrane resistance (Kimura and Nakao, 1980) and may be of use in explanation of rejection behaviour.

The lumped parameter approach used here was based on that proposed by Hong et al (1981), who developed an analytical expression giving the mass of protein in the polarised layer of a stirred ultrafiltration cell used as an enzyme reactor. The expression derived by Hong et al (1981) has been adapted to describe polarisation effects in a crossflow ultrafiltration system. The ability of this lumped parameter model to describe changes in the measured bulk protein concentration in the constant flux hollow fibre ultrafiltration apparatus has been evaluated.

The advantages of using constant flux systems to give conditions of constant concentration polarisation have been discussed. However, a potential problem is that many positive displacement pumps capable of delivering a constant flowrate against varying pressures will give pulsatile flows. The effect of pulsatile flow in ultrafiltration systems has been studied (particularly in conjunction with baffles) by other workers (Finnigan and Howell, 1989), and has been shown to significantly increase fluxes, suggesting that concentration polarisation is reduced. Whilst a quantitative investigation of the effects of pulsating flow was beyond the scope of this work, it is clearly an aspect which must be considered when the utility of a model is assessed, and so two types of recycle pump giving smooth and pulsatile flows have been employed in this work.

MATERIALS and METHODS

The constant flux ultrafiltration apparatus used in this concentration polarisation study was largely the same as that described in Chapter 2. An Amicon H1P10-20 polysulphone hollow fibre membrane was used for all the polarisation work. The use of a constant flux system eliminated the effect of time dependent changes in the degree of concentration polarisation due to changes in membrane resistance. Under the conditions used, the concentration of protein in the permeate remained very low. The permeate was recycled to a feed vessel of small volume, ensuring that the mass of protein in the recycle loop remained constant.

Two types of recycle pump were employed in this work to investigate the effects of pulsatile flow on concentration polarisation. These were a diaphragm metering pump with two heads operating 180° out of phase giving a frequency of 200 strokes.min^{-1}, and a small, essentially pulse free gear pump. The amplitude of the diaphragm pump stroke was adjusted to give the desired crossflow rate, with maximum amplitude corresponding to about 600 ml.min^{-1}.

Protein used was BSA (Sigma A7906) in an 0.01 M Tris-HCl buffer at pH 7.5. Concentrated solution containing a total mass of 1g BSA was injected into the recycle loop through a septum. Whilst the protein was being injected, the recycle loop was opened to allow displaced liquid ($\cong$ 15 ml) to escape. The permeate tube was clamped to prevent a transmembrane flux at this stage. After protein addition the recycle pump was turned on and the protein concentration in the recycle loop allowed to reach equilibrium. The equilibrium adsorbed amount at zero flux was determined by mass balance, from the known system volume.

Changes in the measured bulk protein concentration with flux were determined by opening the permeate tube and setting the desired flowrate on the feed pump. Several different feed flowrates were evaluated in a single run. The recycle concentration was allowed

to approach a constant value at each feed flow.

MODEL DEVELOPMENT

Hong et al (1981) derived an expression relating the steady state bulk protein concentration in stirred batch ultrafiltration to the initial, pre-polarised concentration. Their expression is based on integration of the concentration profile in the boundary layer close to the membrane, to obtain the total amount of protein in the boundary layer:

Fig 1. Schematic of Concentration Polarisation

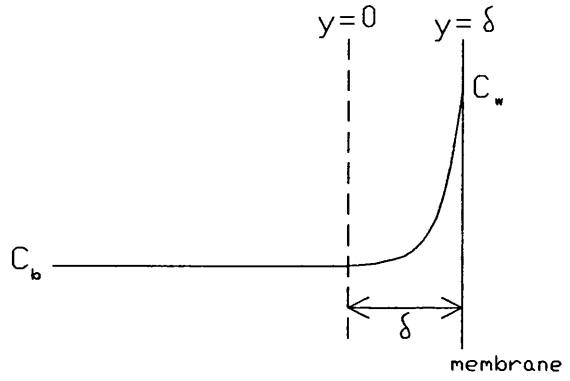

The convection-diffusion equation in one dimension for the boundary layer is (Fig 1):

$$J\,C = D\,\frac{dC}{dy} \quad ...(1)$$

Integrating equation (1) over the boundary layer yields:

$$C_y = C_b\, e^{\left[\frac{J\,y}{D}\right]} \quad ...(2)$$

The average protein concentration in the boundary layer is obtained by integrating equation (2):

$$C_m = C_b \int_0^{\delta} e^{\left[\frac{J\,y}{D}\right]}\, dy$$

$$C_m = \frac{C_b}{\beta}\left[e^{\beta} - 1\right] \quad ...(3) \qquad \text{where } \beta = \frac{J\,\delta}{D}$$

The distribution of protein in the recycle loop must be considered in order to determine the significance of concentration measurements made during polarisation. The rig is shown schematically as a single hollow fibre, with the recycle loop divided into regions (Fig 2). A mass balance over the regions of the system before and after application of a feed flow is:

$$V C_b^0 = V_b C_b + V_{bl} C_m + V_R C_R + V_F C_F \quad ...(4)$$

A steady state mass balance over the outlet of the hollow fibre cartridge gives:

$$Q_b C_b + Q_{bl} C_m = Q_R C_R \quad ...(5)$$

Steady state flow and mass balances over the feed junction give:

$$Q_R + Q_1 = Q_F \quad ...(6)$$

$$Q_R C_R = Q_F C_F \quad ...(7)$$

Fig 2. Regions of the Constant Flux Rig

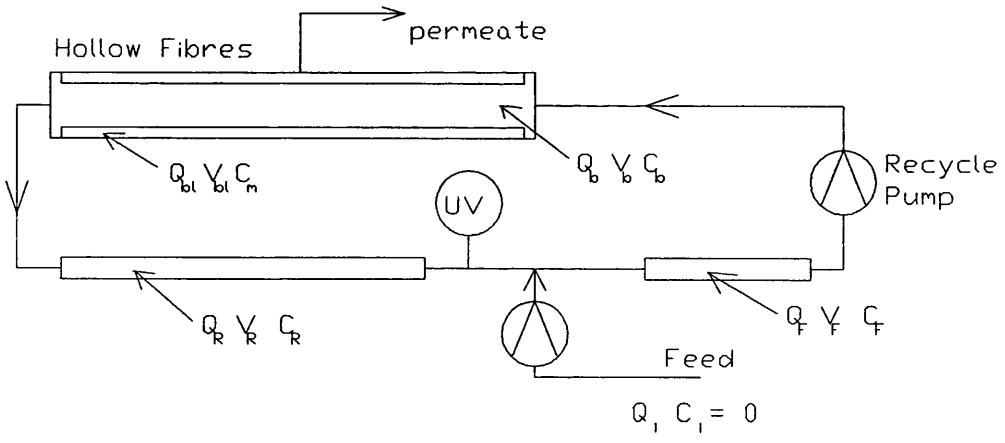

In order to calculate the total axial volumetric flowrate in the boundary layers it is necessary to assume a form for the axial velocity profile in the hollow fibre. Under the conditions applying in this study, the use of a linear approximation to the axial velocity profile in the boundary layer (based on a velocity at the inner edge of the boundary layer calculated from the standard parabolic profile) resulted in a maximum boundary layer axial flow difference of about 10% when compared to a parabolic

profile. Both the linear and parabolic profiles are approximations to the real situation where radial permeation disturbs the axial velocity profile close to the wall. The simpler linear profile has been used for this work:

$$Q_{bl} = N \pi \delta \left[2 r - \delta \right] u \frac{\delta}{r} \left[2 - \frac{\delta}{r} \right] \quad \ldots(8)$$

From equations (3) to (7) the following can be derived:

$$C_R = \frac{V C_b^0}{V_b \frac{C_b}{C_R} + V_{bl} \frac{C_m}{C_R} + V_R + \frac{V_F Q_R}{Q_R + Q_i}} \quad \ldots(9)$$

$$\frac{C_b}{C_R} = \frac{Q_R}{Q_b + \frac{Q_{bl}}{\beta} \left[e^{\beta} - 1 \right]} \quad \ldots(10)$$

$$\frac{C_m}{C_R} = \frac{Q_R}{Q_{bl} + \frac{\beta Q_b}{e^{\beta} - 1}} \quad \ldots(11)$$

The boundary thickness, δ, can be estimated from the widely used laminar flow mass transfer correlation (the Leveque equation):

$$Sh = K \left[Re\ Sc \frac{d}{L} \right]^n$$

Which leads to:

$$\delta = \frac{1}{K} \left[\frac{D\ d\ L}{u} \right]^n \quad \ldots(12)$$

The volumes of the regions of the recycle loop were measured directly, as were the crossflow and feed velocities Q_R and Q_i. Dimensions of the hollow fibres were determined from manufacturers' data. In comparing the model with experimental results, the usual values for protein diffusivity and the constants in equation 12 were considered (Table 1), although a parameter estimation approach was adopted here. Equations (8) to (10), (12) were used to predict the measured concentration, C_R, under known conditions of flux, crossflow and initial equilibrium bulk concentration. They were also used to calculate the average boundary layer concentration, C_m, and (using equation 2) the

concentration at the solution-membrane interface, C_w.

Table 1. Model Parameters from Literature

Parameters for Model Fitting		Usual Values
D	Protein Diffusivity	from $7.0\times10^{-11}m^2.s^{-1}$ at 0.1% w/w to $4.7\times10^{-11}m^2.s^{-1}$ at 40% w/w (Gill et al, 1988)
K	Constant in the Leveque equation	1.62
n	Exponent in the Leveque equation	$\frac{1}{3}$

Experimental data was used to determine the best fit parameters for the model, with literature values (Table 1) as starting points. The parameters available for manipulation were the constants K and n in the Leveque equation (12) and the protein diffusivity, D. Data obtained with the diaphragm and gear recycle pumps was considered separately, due to the obvious difference in behaviour of the system with the two pumps.

Optimum values of the three parameters were obtained by evaluating the sum of squares of the differences between the experimental and model results for the whole range of fluxes and crossflows. A simplex parameter search routine confirmed the best estimates for the three parameters.

RESULTS and DISCUSSION

General Discussion

The effect of flux upon the measured concentration in the recycle was determined for a range of conditions. The results are expressed as measured concentrations in the recycle loop ($g.l^{-1}$) rather than calculated values of membrane associated protein ($g.m^{-2}$), as such a calculation would be complicated by the need to take into account the distribution of protein in the recycle loop.

The initial measured concentration in each experiment corresponds to the equilibrium liquid concentration after protein adsorption to the membrane, but before any transmembrane flux is applied. The results then demonstrate the effect of flux on the measured BSA concentration. Fig 3 is an example of raw experimental data using a membrane with little prior exposure to protein. The order of the experimental points shows that application of a flux causes concentration polarisation of protein towards the membrane, resulting in a decrease in protein concentration in the bulk and a corresponding increase in protein concentration at the membrane surface. Results at a range of crossflows are summarised for the diaphragm pump (Fig 4) and for the gear pump (Fig 5).

Fig 3. Polarisation Experiment Showing Order of Measurements

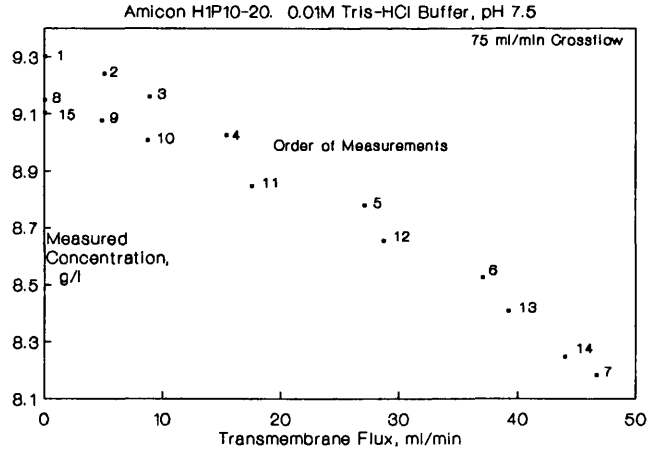

Earlier work has shown that adsorption increases with concentration even at very high concentrations (Matthiasson et al, 1989). This is supported by work using the constant flux ultrafiltration apparatus to measure the amount of adsorbed protein in the absence of transmembrane flux at concentrations of up to 25 $g.l^{-1}$ (Chapter 3). It seems reasonable to suppose that the increase in surface concentration due to polarisation should cause an increase in the adsorbed amount. Fig 3 confirms this, with lower equilibrium (or zero flux) concentrations after polarisation. However some subsequent experiments produced results for the first (pre flux) concentrations which were lower than those shown in Fig 3. After application of a flux, the zero flux concentration returned to its normal level. It is difficult to explain this phenomenon, except by the possibility that a component present in the protein may have caused unusually high adsorption, before being washed out of the system when flux was applied.

The effect of polarisation on protein adsorption to the membrane became less marked as the membrane was exposed to protein and cleaned many times. It seems probable that the number of sites available for adsorption decreased, perhaps due to incomplete removal of protein during cleaning.

Fig 4. Data for Polarisation with Diaphragm Pump

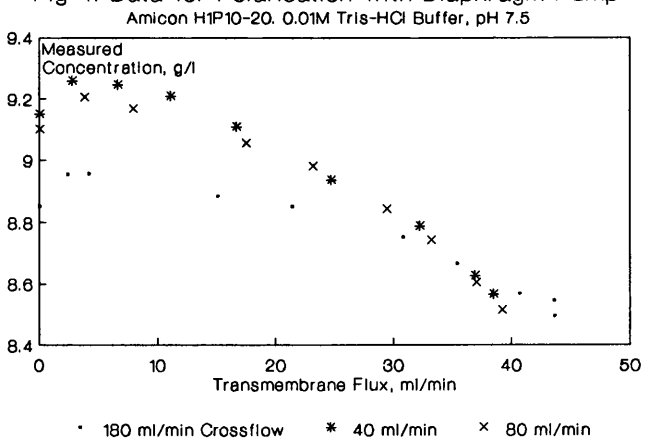

Fig 5. Data for Polarisation with Gear Pump

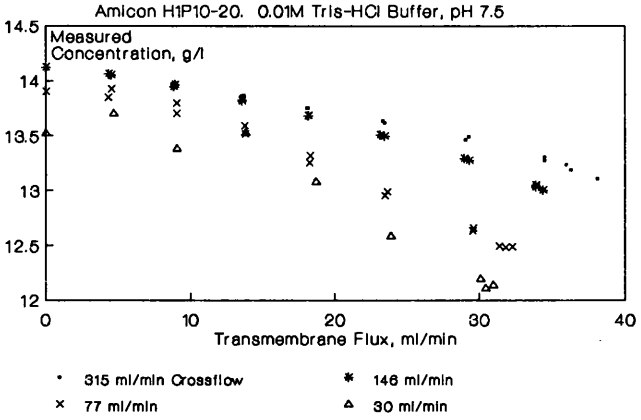

Maxima in the Measured Concentration

It was initially expected that the measured protein concentration would decrease with increasing flux, as more of the protein became polarised towards the membrane. However most of the experiments carried out with the diaphragm recycle pump showed an initial increase of concentration with flux, followed by a concentration decrease at higher fluxes (Fig 4). Considerable investigation into the maximum in the measured concentration was undertaken, to determine the effects of different membranes (including the smaller fibre Amicon H1P10-8), different recycle and feed pumps (peristaltic and gear recycle pumps, feed from a pressurised vessel) and the removal of components in the recycle loop (pressure transducers, temperature probe, turbine flowmeter). The above changes were unable to eliminate the maximum in the measured concentration, so it seems to be a real characteristic of the system.

It was found that some expansion of the system occurred on increasing pressure, due to the elasticity of the membrane material and small air pockets in the recycle tubing. The expansion was measured as a function of flux for the different regions of the system (Table 2). The linear functions approximating the expansion of the different regions of the system

were incorporated into the model, which combines quantification of the amount of protein in the polarised boundary layer with a mass balance of the system. The model predicted the maximum in the measured concentration curve (Fig 6), but the predicted maxima were less pronounced than the experimental ones. Use of varying system volume was not a requirement for maxima to be predicted by the model.

Table 2. Measured Results for System Volume Increase

volumes in ml. J in $ml.min^{-1}$	Diaphgram Pump System	Gear Pump System
fibre volume, $V_{b1} + V_b$	7.9 + 0.043 J	7.9 + 0.043 J
feed volume, V_F	10.0 + 0.021 J	8.0 + 0.021 J
return volume, V_R	85.0 + 0.093 J	47.5 + 0.093 J

Experiments with the gear recycle pump did not show a maximum in the concentration curve, except at the lowest recycle rate of 30 $ml.min^{-1}$ (Fig 5). The model was better able to describe the gear pump results than those obtained with the diaphragm pump (Figs 6, 7). The pulsatile recycle flow from the diaphragm pump may have caused the system to behave differently, possibly by affecting both the protein distribution in the recycle tubing and the degree of polarisation. Pulsatile flows have been shown to improve fluxes in crossflow filtration, presumably by decreasing concentration polarisation (Finnigan and Howell, 1989).

Fig 6. Model vs. Experimental Results for Diaphgram Pump

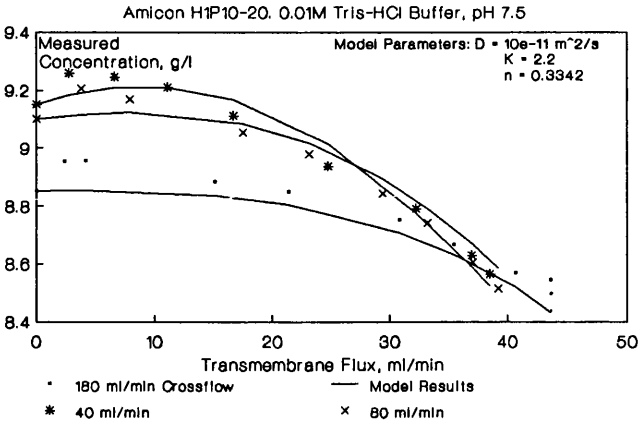

Fig 7. Model vs. Experimental Results for Gear Pump

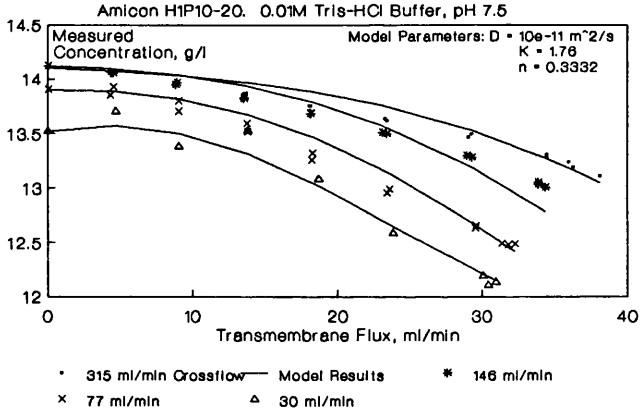

Effect of Crossflow

Data obtained at a range of recycle flows for both diaphragm and gear pumps shows the effect of crossflow on the measured protein concentration (Figs 4, 5). In general, lower crossflow rates resulted in greater polarisation and hence a lower measured protein concentration. This is consistent with the basic theory for the effect of crossflow on the thickness of the concentration boundary layer.

Some departure from the expected effect of crossflow occurred with the diaphragm pump at lower fluxes and crossflow rates (Fig 4). The maximum in the concentration curve is more pronounced at lower crossflows, and can result in a lower crossflow giving a higher concentration at the same flux. The model was able to describe this by considering the effect of feed flowrate on the protein concentration in the different regions of the recycle loop.

Modelling

Results obtained with the diaphragm pump were relatively poorly described by the model (Fig 6). The largest discrepancies occurred at low fluxes where the maximum in the measured concentration was much greater than that predicted by the model.

The model was better able to describe data obtained with the gear recycle pump (Fig 7). The range of crossflows considered was greater in the case of the gear pump experiments (30 to 315 $ml.min^{-1}$, c.f. 40 to 180 $ml.min^{-1}$ with the diaphragm pump).

Optimised parameters (those giving the minimum sum of squared errors) for the gear and diaphragm pump systems are shown in Table 3. The best value for protein diffusivity, D, for both systems was 10×10^{-11} m^2s^{-1}, whereas literature values for BSA vary from 7.0×10^{-11} m^2s^{-1} at 0.1% w/w to 4.7×10^{-11} m^2s^{-1} at 40% w/w (Gill et al, 1988). The diffusivity giving the best model fit is greater than that usually measured. The best value for the exponent, n, in equation (12) is similar for the two different recycle pumps and is very close to the value of $^1/_3$ which is conventionally implied when the equation is used. The best value for the multiplier, K, in equation (12) is greater for the diaphragm system, suggesting that the concentration boundary layer was thinner under pulsatile flow conditions.

Table 3. Model Parameters Giving Minimum Sum of Squared Errors

	Protein Diffusivity D, m^2s^{-1}	Constants in Leveque Equation	
		K	n
Gear	$10e^{-11}$	1.76	0.3332
Diaphgram	$10e^{-11}$	2.20	0.3342

Boundary Layer and Wall Concentrations

The values of the average boundary layer concentration, (C_m), and the wall concentration, (C_w), calculated by the model are shown in Fig 8. The predictions shown are for the lowest and highest crossflows in the gear pump system. The volumes and flowrates in the fibre boundary layer and bulk regions are shown for information in Table 4. Given that the maximum obtainable degree of polarisation was not great (due to the pressure limitations of hollow fibres), the values of C_m and C_w seem appropriate.

Fig 8. Calculated Wall and Average Boundary Layer Concs.

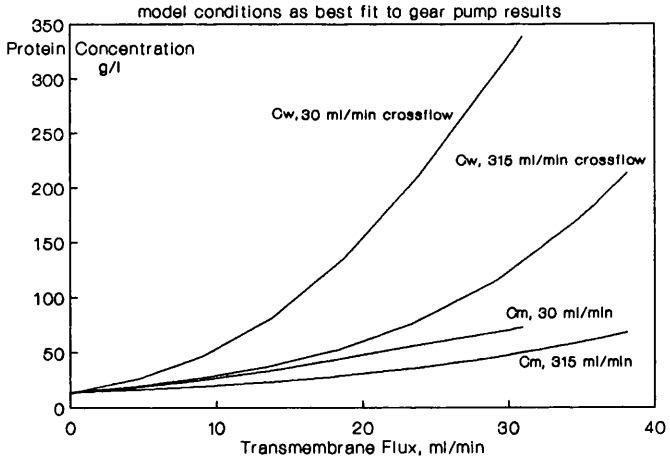

The amount of additional adsorption after polarisation implied by Fig 3 is about 2.5 $g.m^{-2}$, which represents a significant increase over the total of ≅ 1.5 $g.m^{-2}$ obtained at a concentration of ≅ 25 $g.l^{-1}$ during adsorption experiments (Chapter 3). This supports work showing that protein adsorption increases with concentration even at the high concentrations occurring during polarisation

(Matthiasson et al, 1989). It may be possible to determine protein adsorption at high concentrations by using polarisation conditions combined with lumped parameter modelling to estimate wall concentrations (such as those shown in Fig 8) . However this approach would be susceptible to the changes in adsorption behaviour discussed earlier.

Table 4. Calculated Volumes and Axial Flowrates for the Boundary Layer and Bulk Regions of the Fibres

Flux	Crossflow	Q_{bl}	Q_b	V_{bl}	V_b
ml.min^{-1}	ml.min^{-1}	ml.min^{-1}		ml.	
4	315	12.2	303	1.6	6.5
37	315	11.8	303	1.9	7.7
5	30	4.7	25.3	3.2	4.9
31	30	3.8	36.2	3.3	5.9

Effect of Polarisation on Membrane Resistance

A series of experiments was undertaken to determine the effect of flux on the membrane resistance. The recycle loop was charged with a fixed protein load and a single flux only was applied, after which the equilibrium concentration at zero flux was re-measured (example experimental data, Fig 9). The same flux was then reapplied to determine whether time dependent effects were significant. The results are summarised in Table 5, and show that there is a time dependent rise in measured protein concentration. This rise is superimposed on any decrease in concentration due to additional adsorption caused by polarisation. A similar rise in measured concentration was observed during the work on protein adsorption (Chapter 3), and has been attributed to a time dependent change in the absorbance of the protein solution..

Fig 9. Example Data for Single Flux Polarisation Experiment

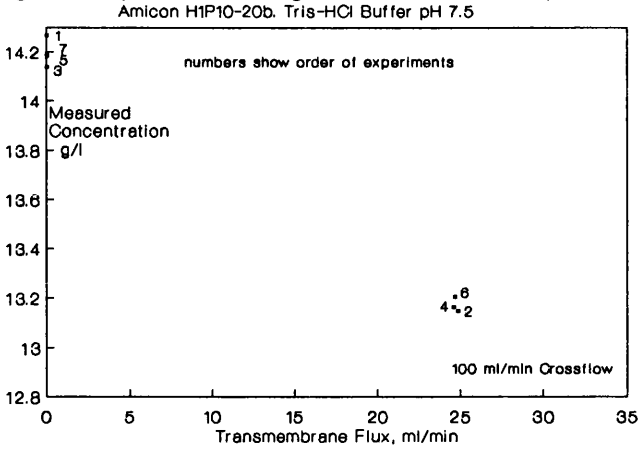

Table 5. Summary of Results for Single Flux Polarisation Experiments

Flux $ml.min^{-1}$	Successive Measured Concentrations, $g.l^{-1}$								
	Zero Flux	Appl Flux	Zero Flux	Appl Flux	Zero Flux	Appl Flux	Zero Flux	Appl Flux	Zero Flux
4.7	13.67	13.74	13.74	13.80	13.82	13.88	13.87	13.91	13.92
15.3	14.08	13.74	14.05	13.73	14.05				
24.7	14.27	13.15	14.13	13.16	14.18	13.20	14.19		
28.0	14.17	13.12	14.13	13.12	14.13	13.13	14.16		
31.8	14.10	12.96	14.08	12.96	14.12	12.96	14.15		
33.5	14.06	12.85	14.13	12.95	14.17	12.97	14.21		

The membrane had been used and cleaned many times before commencing this set of experiments, therefore observed increases in adsorption following polarisation were small. The resistance of the cleaned membrane was determined before each experiment. After each polarisation run was completed, the protein solution was flushed out of the system with distilled water and the membrane resistance measured with buffer. The clean membrane resistance could then be compared with the resistance after polarisation at a single flux. Comparison was based on the relative resistance, R:

$$R = \left[\frac{\text{Membrane Resistance after Polarisation}}{\text{Cleaned Membrane Resistance before Polarisation}} \right] - 1$$

The cleaning regime may not have completely restored the membrane permeability after each experiment, but use of the relative resistance reduced the effect of long term fouling on the results.

The effect of applied flux on the relative resistance was measured for a range of fluxes (Fig 10). Although the higher fluxes did not cause appreciably greater adsorption for this membrane, there was a significant effect on the membrane resistance. The effect of higher fluxes might be to increase the incidence of pore blocking, which could significantly affect the membrane resistance without involving a measureable amount of protein.

Fig 10. Effect of Flux on Rinsed Membrane Resistance

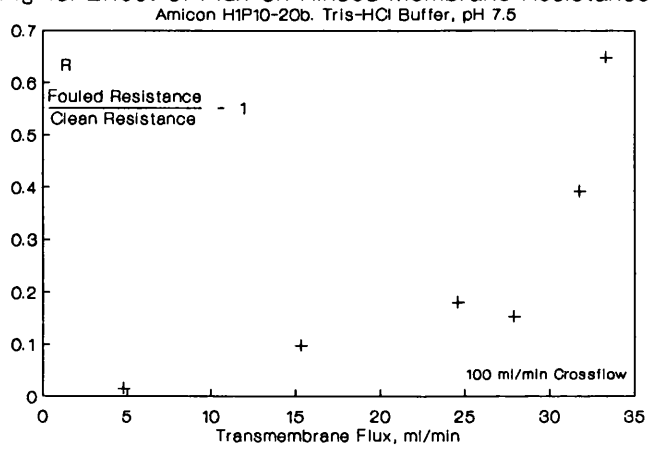

The relationship between transmembrane flux and pressure drop in the polarisation experiments was measured (Figs 11, 12). Pressure rose more rapidly at the lower recycle rate, showing the effect of increased polarisation, but a limiting flux was not reached. Using the simple model presented here, it may be possible to correlate the membrane resistance observed during ultrafiltration with the protein concentration at the solution-membrane interface. Results (not presented) showed that the flux vs. pressure relationship in the absence of polarised protein was linear for this membrane and pressure range.

Fig 11. Flux vs. Pressure in Polarisation Experiments

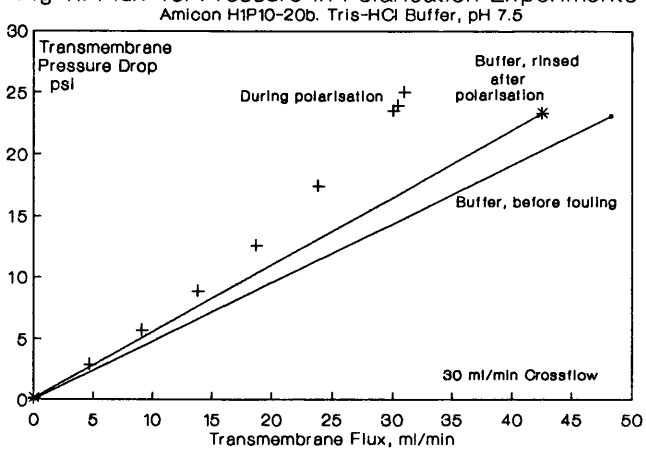

Fig 12. Flux vs. Pressure in Polarisation Experiments

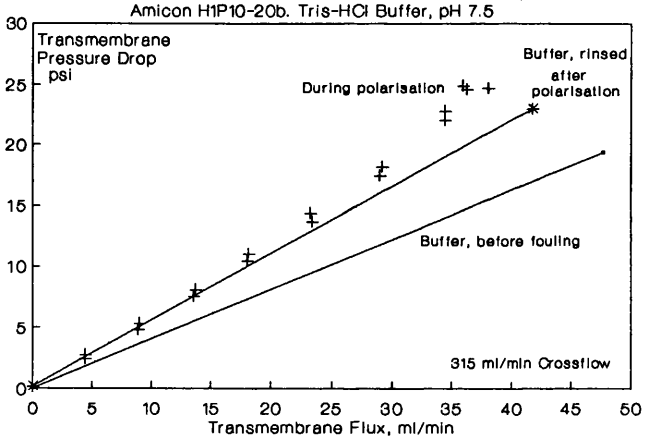

CONCLUSIONS

The lumped parameter model for concentration polarisation proposed here is simple, and can be solved without the use of complex numerical techniques. It was capable of a reasonable description of polarisation over a range of crossflows and fluxes, especially where crossflows were non pulsating. The model could be used to calculate the value of protein concentration at the solution-membrane interface, possibly leading to a consideration of the effect of polarisation on adsorption, membrane resistance and solute rejection.

The diffusivity giving the best fit for the model was greater than the value normally used for BSA. It was not possible to determine whether this was due to improper description of the system by the model, or to differences in the behaviour of the protein under polarisation conditions. The model parameters giving the best fit to experimental data suggested that the polarised boundary layer was thinner under pulsatile flow conditions.

The model presented here is based on the assumption that the boundary layer is of constant thickness, as described by the laminar flow mass transfer correlation. This is a major simplification of the true situation, because models of concentration polarisation have shown that the polarised boundary layer develops from the channel entrance (Clifton et al, 1984). The assumptions have, however, lead to a model which can conveniently be used to provide a reasonable estimate of the bulk protein concentration, which is an important factor in determining the performance of a soluble enzyme membrane reactor. The description of bulk protein concentration by the model has been verified, but the validity of the predictions of protein concentrations in the polarised protein layer and at the membrane surface is less certain. The equations presented here allow these values to be calculated (Fig 8) and the results are consistent with those usually reported. However in reality both the concentration profile and the boundary layer thickness vary with

fibre length, so the values calculated using this simplified model must be regarded only as indications of the average values. Experimental verification of boundary layer concentration predictions remains a major technical problem.

Polarisation was shown to cause an increase in membrane resistance measured after rinsing the membrane. The degree of increase in membrane resistance was strongly dependent on flux and hence polarisation, although polarisation was shown to cause little additional adsorption to a membrane which had been used and cleaned many times.

REFERENCES

Aimar, P.; Howell, J.A.; Turner, M.
"Effects of concentration boundary layer development on the flux limitations in ultrafiltration".
Chem. Eng. Res. Des., 67 (1989) 255-261.

Bhattacharyya, D.; Back, S.L.; Kermode, R.I.; Roco, M.
"Prediction of concentration polarisation and flux behaviour in reverse osmosis by numerical analysis".
J. Membr. Sci., 48 (1990) 231-262.

Carter, J.W.; Hasting, A.P.M.
"The reduction of concentration polarisation by the use of impermeable or fully permeable membrane sections".
IChemE North Western Branch Papers, 4 (1980) 6.1-6.19.

Clifton, M.J.; Abidine, N.; Aptel, P.; Sanchez, V.
"Growth of the polarization layer in ultrafiltration with hollow fibre membranes".
J. Membr. Sci., 21 (1984) 233-246.

Fell, C.J.D.; Kim, K.J.; Chen, V.; Wiley, D.E.; Fane, A.G.
"Factors determining flux and rejection of ultrafiltration membranes".
Chem. Eng. Process., 27 (1990) 165-173.

Finnigan, S.M.; Howell, J.A.
"The effect of pulsatile flow on ultrafiltration fluxes in a baffled tubular membrane system".
Chem. Eng. Res. Des., 67 (1989) 278-282.

Gill, W.N.; Wiley, D.E.; Fell, C.J.D.; Fane, A.G.
"Effect of viscosity on concentration polarisation in ultrafiltration".
AIChE J., 34 (1988) 1563-1567.

Hong, J.; Tsao, G.T.; Wankat, P.C.
"Membrane reactor for enzymatic hydrolysis of cellobiose".
Biotechnol. Bioeng., 23 (1981) 1501-1516.

Kimura, S.; Nakao, S.
Kenkyu Hokoku - Asahi Garasu Kogyu Gijutsu Shoreikai, 37 (1980) 211-226.

Kleinstreuer, C.; Belfort, G.
"Mathematical modeling of fluid flow and solute distribution in pressure driven membrane modules".
Synthetic Membrane Processes - Fundamentals and Water Applications. Ed Belfort, G. Academic, Orlando (1984).

Kleinstreuer, C.; Paller, M.S.
"Laminar dilute suspension flows in plate and frame ultrafiltration units".
AIChE J., 29 (1983) 529-533.

Leung, W-F.; Probstein, R.F.
"Low polarization in laminar ultrafiltration of macromolecular solutions".
Ind. Eng. Chem. Fundam., 18 (1979) 274-278.

Matthiasson, E.; Hallstrom, B.; Sivik, B.
"Adsorption phenomena in fouling of UF membranes".
Engineering Sciences in the Food Industry, Ed McKenna,B.M. (1989).

Merson, R.L.; Ginette, L.F.
"Improved processing of foods by reverse osmosis".
Applied Polymer Symp., 13 (1970) 309-322.

Shah, Y.T.
"Mass transport in reverse osmosis in case of variable diffusivity".
Int. J. Heat Mass Transfer, 14 (1971) 921-930.

Vilker, V.L.; Colton, C.K.; Smith, K.A.
"Concentration polarisation in protein ultrafiltration".
AIChE J., 27 (1981) 632-645.

Last Page of Chapter 4

CHAPTER 5

The EFFECT of MEMBRANE FOULING and CLEANING on REJECTION of a LOW MOLECULAR WEIGHT TRACER in ULTRAFILTRATION

ABSTRACT

Rejection of a low molecular weight chemical tracer (adenosine 5′ monophosphate, molecular weight 347.2) by an Amicon polysulphone hollow fibre membrane (nominal molecular weight cutoff 10,000) was measured using a spectrophotometric method in a constant flux ultrafiltration apparatus. Fouling, produced by prior exposure of the membrane to a protein solution under zero flux conditions, followed by rinsing, was found to increase tracer rejection. Cleaning of the membrane after exposure to protein did not restore the initial rejection characteristics, although membrane permeability did not decrease substantially. The increase in rejection was reversed by prolonged soaking of the membrane in buffer. Polarised protein had little effect on tracer rejection, when compared to the membrane with adsorbed protein only, except at the highest fluxes compatible with the pressure rating of the membrane.

INTRODUCTION

Solute rejection by ultrafiltration membranes is a complex phenomenon, which often cannot be adequately described by the nominal molecular weight cutoff (nmwco) data supplied by manufacturers. Frequently, molecules larger than the nmwco are not completely rejected (Jandel et al, 1980), whilst molecules much smaller than the nmwco are partially rejected (Hanemaaijer et al, 1989; Nakao and Kimura, 1981). The rejection of smaller solutes in ultrafiltration may be important in a number of circumstances, for instance:

(a) Enzyme membrane reactors which require relatively small product molecules to pass through the membrane whilst the macromolecular enzyme must be retained (Cheryan and Deeslie, 1983; Jandel et al, 1980).

(b) Ultrafiltration of blood for the removal of urea, as proposed by Calderaro et al (1980).

(c) Separation of small product molecules from treated or untreated fermenter broths.

(d) Ultrafiltration of fruit juices, where the retention of flavour compounds is important.

Measurement of the rejection of a range of smaller molecules of various sizes has been used as a means of membrane characterisation. HPLC has frequently been used to measure the rejection of mixtures of molecules (for example Jonsson and Christensen, 1984). Photometric (Jandel et al, 1980), refractive index and chemical (Dorson et al, 1975) techniques have also been used.

Nobrega et al (1989) studied the molecular weight distribution of the feed and permeate during ultrafiltration of a mixture of dextrans under various operating conditions. The partial rejections obtained for the different molecular weight fractions gave information on the membrane characteristics. It was possible to detect changes in the membrane characteristics due to

ultrafiltration of a protein solution. Zeman (1983) and Hanemaaijer et al (1989) used solute rejection data and the Ferry (1936) equation to quantify pore size reduction after adsorption of macromolecules. Nakao and Kimura (1981) used the Spiegler and Kedem (1966) equation to fit rejection data for molecules ranging in size from glycerine (MW 92) to PEG #4000 (MW 3000). Data was corrected for concentration polarisation, allowing a solute permeability and reflection coefficient to be calculated, from which the membrane structure was assessed. Jonsson and Christensen (1984) used equations relating the solute/pore radius ratio to the distribution coefficient for rejection of polymers. They then estimated the average pore radius and the pore size distribution for cellulose acetate membranes.

The effect of solute concentration at the membrane surface on rejection has been investigated theoretically by Wendt et al (1981). They used the Speigler and Kedem (1966) equation to model the factors affecting rejection coefficients. They concluded that for real membrane characteristics, the effect of solute concentration on rejection should be relatively small. The effect of concentration polarisation of saccharides during rejection tests was assumed negligible by Hanemaaijer et al (1988) due to the high diffusivity and relatively low rejection of the molecules tested. However, Nakao and Kimura (1981) corrected their results for the effects of concentration polarisation, presumably because some of the larger molecules in their study were subject to significant polarisation.

Exposure of membranes to proteins (resulting in protein adsorption) has been shown to result in a reduction in pore size, quantifiable by an increase in rejection of smaller solutes (Hanemaaijer et al, 1989; Zeman, 1983). Dorson et al (1975) found that protein adsorption occurring during ultrafiltration caused increased rejection even after rinsing of the membrane. The rejection increase was affected by ultrafiltration pressure, which suggests that increased protein polarisation may have caused

greater adsorption or pore blockage and hence affected the rejection of smaller solutes. Ingham et al (1980) diafiltered solutions containing PEG #4000 and albumin. The increase in rejection of PEG was attributed to adsorbed, rather than polarised protein. Calderaro et al (1980) measured the rejection of a range of radiolabelled molecules by haemofilters in the presence and absence of human plasma. They concluded that the degree of concentration polarisation of protein significantly affected rejection. The effect of polarised protein on the rejection of small solutes is therefore uncertain.

Rejection of molecules such as dextrans has been modelled according to hard sphere theory (Zeman and Wales, 1981). However, deviation from the hard sphere theory can occur due to membrane pore size distribution (Jonsson, 1986) or to solute-membrane interactions, resulting in a reduction of the effective pore size (Long et al, 1981).

In conclusion, small solutes can be rejected significantly by membranes of relatively high nmwco. Adsorption of macromolecules to membranes increases the rejection of small molecules, even if bulk protein is rinsed out before the rejection of small molecules is measured. There is conflicting evidence concerning the effect of polarised protein layers, which in themselves may or may not contribute significantly to rejection of small solutes. However the increased adsorption associated with concentration polarisation does appear to cause an increase in the rejection of smaller solutes.

The rejection of small solutes under conditions of adsorbed and polarised protein is important in any process requiring passage of the small molecules at the same time as retention of macromolecules. The behaviour of cleaned membranes is more significant than that of new ones in such systems, as membranes are likely to be cleaned and re-used many times. If the degree of protein polarisation is found to significantly affect rejection of

small solutes, this could influence the feasibility and operating regime of a membrane separation process.

Here, an investigation into the rejection of a low molecular weight tracer molecule (5'adenosine monophosphate (5'AMP), MW 347.2) by an Amicon polysulphone hollow fibre membrane of nmwco 10,000 was undertaken. The tracer 5'AMP was selected for rejection studies as it satisfies the requirements of low molecular weight, high UV absorbance at a different wavelength from BSA and reasonable cost for the large volumes of solution required. The effects of adsorbed and polarised protein on the tracer rejection were measured for a range of operating conditions, and the effect of membrane cleaning on long term rejection characteristics was assessed.

MATERIALS and METHODS

Gel Permeation Chromatography

Measurement of the rejection of small molecules by an ultrafiltration membrane in the presence of protein required that interactions between the tracer molecule and the protein were slight. Significant interaction between the tracer molecule and the protein might have caused formation of protein-tracer complexes resulting in non typical protein-membrane interactions and incorrect determination of tracer rejection.

An investigation into the interaction between protein (BSA, Sigma A7906) and possible tracer molecules was therefore undertaken using gel permeation chromatography (Fig 1). The gel (Sephadex G25) was contained in an Omnifit column (6.6mm id, 87mm high). Valves, tubing, connectors and a pressurised buffer feed system were all obtained from Omnifit. A UV monitor (Altex model 152) operating at 254nm and connected to a chart recorder indicated column outlet concentrations. Buffer flowed through the column at about 0.1 ml.min^{-1} at a pressure drop of 1.5 psig. The volume of the injection loop was 0.22 ml.

Fig 1. Gel Permeation Apparatus

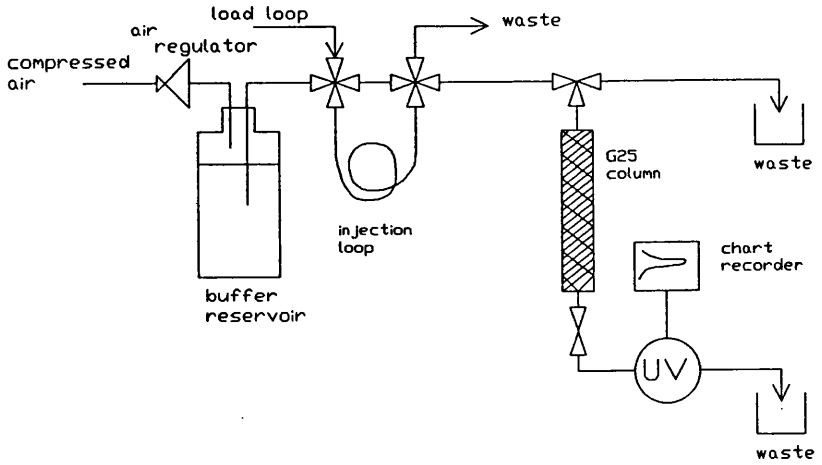

The column operated in a 'desalting' mode and provided complete separation of non interacting proteins (excluded from the resin) and tracers (freely permeable in the resin) over the molecular weight ranges studied. Peaks produced by the UV monitor on passing solutions of protein, tracer and mixtures of the two through the column were recorded and compared. Differences between the areas of peaks obtained for single solutes (tracer or protein) and the corresponding areas for the same solutes in a mixture indicated an interaction between the solutes.

Tracer Rejection Experiments

The constant flux ultrafiltration apparatus used in this rejection study was largely the same as that described in Chapter 2. The membrane used was an Amicon H1P10-20 polysulphone hollow fibre cartridge of nominal 10,000 molecular weight cutoff. The tracer selected for rejection studies was adenosine 5' monophosphate (5'AMP) (Sigma A2252) which has a molecular weight of 347.2 $g.mol^{-1}$. 5'AMP absorbs UV light strongly at 254nm (molar extinction coefficient $\cong 1.5 \times 10^4$ $litre.mol^{-1}.cm^{-1}$ at 260nm), allowing its concentration in the retentate and permeate to be determined by absorbance measurement. It was necessary to measure permeate solution absorbance in order to determine observed rejections of tracer, and for this purpose a second spectrophotometer (Shimadzu UV-120-02) operating at 254nm with a 10mm path length flow cell was incorporated into the permeate line.

Rejection coefficients for the cleaned membrane in the absence of protein were determined by measuring the concentrations of tracer in the retentate and permeate when steady state had been reached. The observed rejection coefficient is given by:

$$R_{obs} = 1 - \frac{\text{Tracer Concentration in Permeate}}{\text{Tracer Concentration in Retentate}}$$

The effect of flux on the rejection of 5'AMP was determined by altering the feed pump setting. The system was allowed to reach steady state at each feed flowrate.

Measurement of Tracer Rejection after Protein Adsorption

Rejection of 5'AMP was also determined for a membrane which had been exposed to protein (BSA). The recycle loop was opened to include a stirred beaker, to which a concentrated protein solution containing a known mass of BSA was added. The permeate tube was closed at this stage to prevent a transmembrane flux. Bulk protein concentration in the recycle was determined by UV absorbance at 280nm. At equilibrium, the mass of BSA associated with the membrane could be determined, given that the volume of the system was known (Chapter 3). The protein solution was then rinsed out with distilled water followed by buffer, the recycle loop was closed and the permeate tube opened, and tracer solution was fed into the system. Recycle and permeate solution absorbances were monitored at 254nm, allowing the rejection of 5'AMP to be evaluated at a range of fluxes. Some desorption of BSA into the bulk solution may have occurred, however the absorbance of BSA at 254nm is relatively low (Fig 2). Therefore at the concentrations of 5'AMP used in this work, any desorbed protein would have had a negligible effect on the total absorbance measured.

Fig 2. Schematic Absorbance Spectra of BSA and 5'AMP

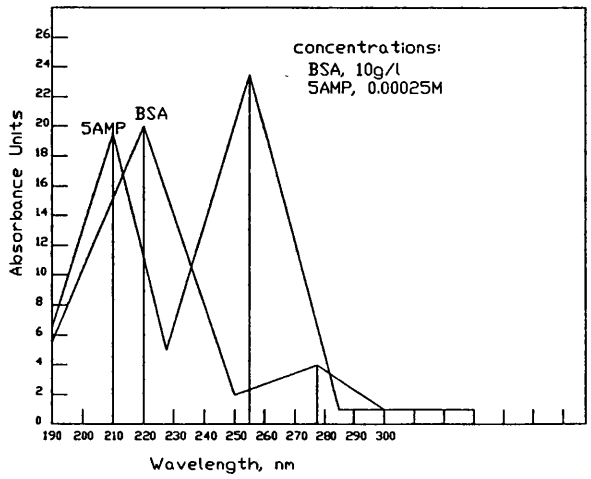

Measurement of Tracer Rejection with Protein Polarisation

Investigation of the rejection of 5'AMP with simultaneous concentration polarisation of protein required measurement of both BSA and 5'AMP concentrations in the same solution. This was achieved by measurement of the recycle solution absorbance at both 254 and 280nm. As the spectrophotometer zero could not be adjusted during experiments, the zero readings for buffer at the two wavelengths were noted before and after each experiment, and the readings obtained during experiments were corrected for zero difference and zero drift. The contribution of BSA and 5'AMP to absorbance at 254 and 280nm was found to require a correction factor in addition to the standard expressions for the absorbance of two compounds at two wavelengths:

$$A_{280} = E_{280}^{BSA} C_{BSA} + E_{280}^{AMP} C_{AMP} - F_{280} C_{BSA} C_{AMP} \quad \ldots(1)$$

$$A_{254} = E_{254}^{BSA} C_{BSA} + E_{254}^{AMP} C_{AMP} - F_{254} C_{BSA} C_{AMP} \quad \ldots(2)$$

Where: A_b = Corrected spectrophotometer output at wavelength b.

C_{BSA} = Concentration of BSA, $g.l^{-1}$.

C_{AMP} = Concentration of 5'AMP, $mol.l^{-1}$.

E_b^a = Constant for component a at wavelength b.

F_b = Correction constant for wavelength b.

Table 1. Spectrophotometer Calibration Constants for BSA / 5'AMP Mixtures

	E^{BSA}	E^{AMP}	F
254nm	32.62	1.354×10^6	4800
280nm	69.72	3.454×10^5	700

The constants fitting the calibration data obtained from mixtures of BSA and 5'AMP are summarised in Table 1 (Fig 3). The need for a correction factor indicates that some interaction between BSA and 5'AMP occurred. However, given the results of gel permeation experiments (see Results and Discussion) it is unlikely that this

would significantly affect the measured rejection of 5'AMP.

Fig 3. Spectrophotometer Calibration for BSA / 5AMP Mixtures

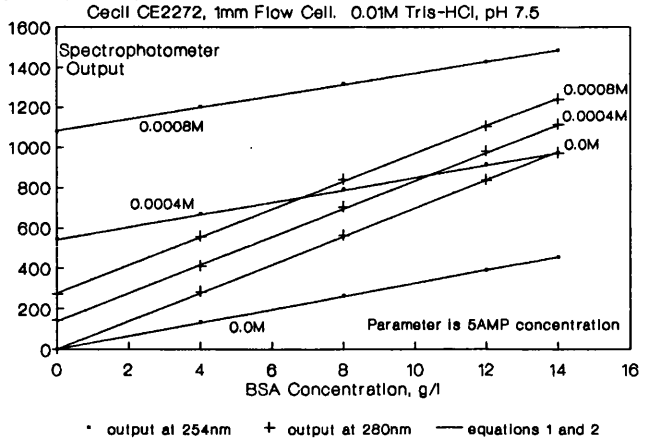

After determining the rejection of tracer by the clean membrane at a single flux, the feed pump was switched off and a small volume of concentrated protein solution containing a known mass of BSA was injected into the recycle loop via a septum. Liquid was displaced through the membrane during this operation. The feed pump was then switched on at a low setting and the recycle and permeate absorbances allowed to reach equilibrium. Recycle spectrophotometer readings at 254 and 280nm were taken, from which the concentrations of BSA and 5'AMP were calculated by iterative solution of equations 1 and 2 using the constants in Table 1. Rejection, polarisation and pressure drop data at constant crossflow rate and protein loading was obtained for a range of fluxes in each experiment.

Membrane Cleaning

Membrane cleaning was carried out according to the procedure described in Chapter 2.

RESULTS and DISCUSSION

Interaction Between BSA and Tracer Molecules

In order to verify that the tracer (5'AMP) did not interact significantly with the protein (BSA), a solution of BSA and 5'AMP at concentrations of 5 $g.l^{-1}$ and 0.0002M respectively in 0.01M tris-HCl buffer, pH 7.5 was injected into the gel permeation column. The two peaks obtained were quite closely reproduced on injecting separate solutions at the same concentrations (Fig 4), indicating that interactions between BSA and 5'AMP were limited.

Fig 4. Gel Permeation Testing of the Interaction Between BSA and 5AMP in 0.01M Tris-HCl pH 7.5

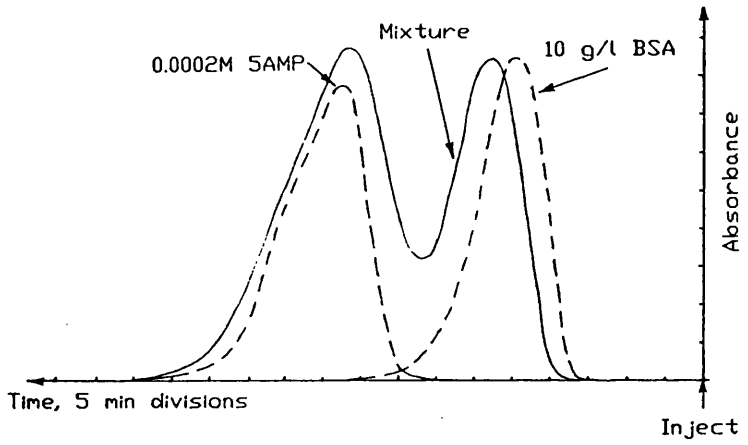

Rejection of Tracer by the Clean Membrane

Experiments were carried out to determine the effect of flux on the rejection of tracer at different crossflow (recycle) rates (Fig 5, Table 2). Crossflow had no noticeable effect on the rejection vs flux curves, suggesting that concentration polarisation of tracer under these conditions hardly influenced rejection. This confirms the observations of Hanemaaijer et al (1988), who also found that crossflow had a negligible effect on the rejection a mixture of low molecular weight polysaccharides.

Fig 5. Tracer Rejection by Clean Membrane

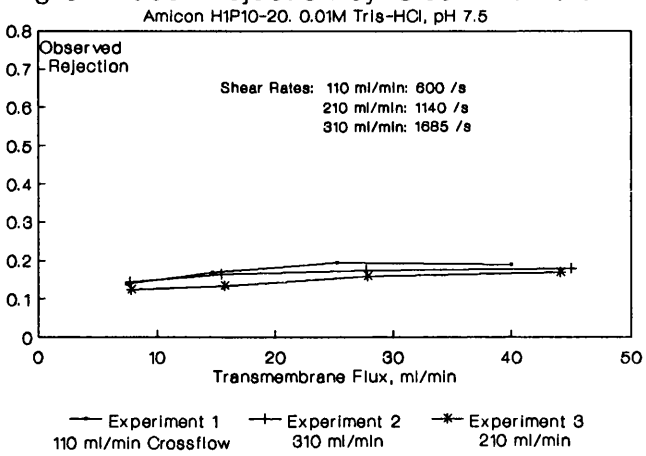

Table 2. Summary of Tracer Rejection Experiments with a Clean Membrane

Expt N°	Flux ml.min^{-1}	Reject.	Membr. Perm. ml.min^{-1}psi^{-1}	Cross-flow rate ml.min^{-1}	Tracer Concn. mol.l^{-1}	Cleaning Method Before Expt.
1	7.40 14.7 25.2 40.0	0.140 0.170 0.194 0.190	2.40 2.38 2.34 2.27	110	0.001	Backflush
2	7.70 15.5 27.7 45.0	0.145 0.165 0.174 0.180	2.41 2.43 2.40 2.25	310	0.001	Not Cleaned
3	7.80 15.7 27.8 44.1	0.125 0.135 0.160 0.170	2.44 2.42 2.40 2.20	210	0.001	Not Cleaned

Observed rejection of tracer increased slightly with flux up to a permeate flowrate of about 20 ml.min^{-1}, beyond which there was little effect of flux on rejection. It seems that additional pore blockage by tracer molecules at higher fluxes did not occur.

Rejection of Tracer by a Membrane After Exposure to Protein

Membranes were allowed to adsorb BSA under zero flux conditions, after which they were rinsed and the rejection vs. flux characteristics for tracer were determined. Adsorbed protein remaining attached to the membrane after rinsing with distilled water was found to affect the rejection characteristics (Fig 6, Table 3). Observed rejection was increased by the presence of adsorbed protein, but the shape of the rejection vs. flux relationship was little different from that for a clean membrane. These results agree with those of Ingham et al (1980) and Dorson et al (1975) who found that adsorbed protein increased rejection. The effect of the adsorbed protein has been explained in terms of reduction in pore size (Hanemaaijer et al, 1989; Zeman, 1983).

Fig 6. Effect of Adsorbed Protein on Rejection

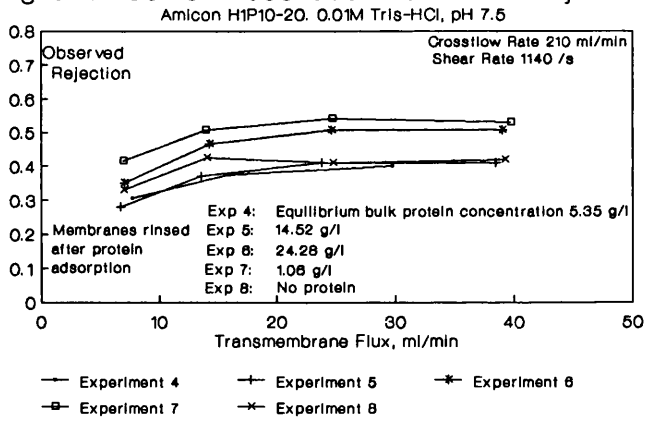

Work on the adsorption of proteins to membranes has shown that the adsorbed amount increases with protein concentration, even at very high protein concentrations (Matthiasson et al, 1989). The equilibrium concentration for protein adsorption might therefore be expected to affect the adsorbed amount and hence the rejection of tracer in these experiments. Adsorbed protein layers formed by ultrafiltration under conditions of increased concentration polarisation have been shown to exhibit increased rejection of

small solutes (Dorson et al, 1975). In this work, rejection was found to increase with equilibrium adsorption concentrations of 5, 15 and 24 $g.l^{-1}$ BSA, but did not decrease when a lower concentration of 1 $g.l^{-1}$ was used (Fig 6, Table 3). The membrane was cleaned by backflushing with NaOH after each experiment, but rejection did not return to the values obtained before the series of adsorption experiments. It appears that irreversible fouling of the membrane took place which considerably affected rejection. It is therefore difficult to draw firm conclusions on the effect of the extent of protein adsorption on the rejection characteristics of the membrane.

It was considered possible that cleaning by backflushing with NaOH resulted in blockage of pores by protein which had migrated into the structure of the membrane during fouling. A modified cleaning procedure was therefore adopted, consisting of the usual backflush followed by ultrafiltration (forward flushing) of about 2l of 0.1M NaOH at high crossflow, in order to remove any protein that had been forced backwards into the pores. This cleaning procedure did not result in any reduction of the observed rejection when compared with the previous backflush - only method (Table 3, Fig 7).

The 'irreversible' fouling demonstrated by these experiments also reduced the effect (on rejection) of subsequent exposure to protein (Table 3, Fig 7). Such fouling seems to result from 'permanent' occupation of active sites on and in the membrane structure, reducing the potential for subsequent protein-membrane interactions and hence their effect on membrane characteristics.

Table 3. Tracer Rejection Experiments after Protein Adsorption and Rinsing

Expt N°	Flux ml. min^{-1}	Reject.	Membr. Pbty. ml. min^{-1} psi^{-1}	Protein Concn. / Ads. Amt. $g.l^{-1}$ / $g.m^{2}$	Tracer Concn. $mol.l^{-1}$	Cleaning Method Before Expt.
4	7.70 16.0 29.7	0.305 0.375 0.401	2.41 2.36 2.40	5.35 / 0.66	0.0004	Not cleaned as no protein in previous expt.
5	6.75 13.6 23.8 38.5	0.280 0.370 0.410 0.410	2.70 2.62 2.62 2.56	14.42 / 1.64	0.0004	Backflush with NaOH
6	7.05 14.3 24.6 39.0	0.350 0.465 0.507 0.506	2.14 2.10 2.04 1.97	24.28 / 3.79	0.0004	Backflush with NaOH
7	6.96 14.0 24.7 39.7	0.415 0.507 0.540 0.530	2.43 2.36 2.35 2.31	1.06 / 0.15	0.0004	Backflush with NaOH
8	7.00 14.1 24.7 39.3	0.330 0.425 0.410 0.420	2.52 2.47 2.46 2.37	No protein	0.0004	Backflush with NaOH
9	6.90 14.6 25.4 41.4	0.330 0.430 0.470 0.455	2.52 2.52 2.46 2.45	No protein	0.0004	Backflush + Forward flush with NaOH
10	5.65 12.4 21.2 34.0	0.332 0.440 0.480 0.480	2.35 2.48 2.45 2.43	5.31 / 0.76	0.0004	Backflush + Forward flush with NaOH
11	5.40 11.3 19.8 32.7	0.072 0.098 0.122 0.128	2.97 2.96 2.89 2.83	5.32 / 0.72	0.0002	Backflush + Forward flush with NaOH

continued overleaf...

Table 3. continued:

12	5.75 12.2 20.4	0.072 0.100 0.210	2.67 2.71 2.60	5.35 / 0.66	0.0002	Backflush + Forward flush with NaOH
13	6.10 12.6 20.0 32.8	0.440 0.540 0.584 0.588	2.43 2.47 2.38 2.34	≈ 5	0.0002	Backflush + Forward flush with NaOH

Fig 7. Effect of Back- and Forward-Flush Cleaning

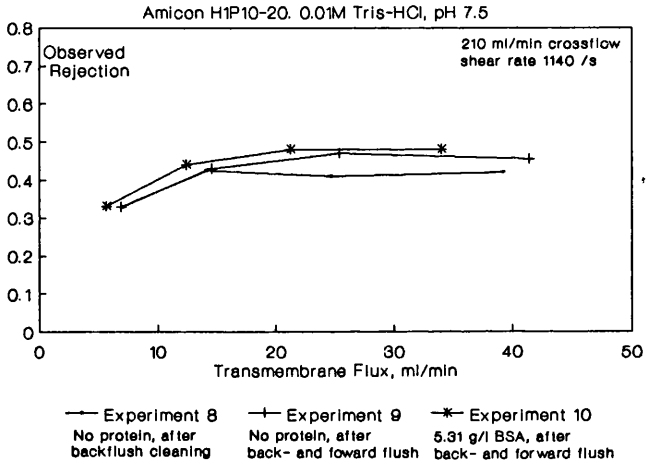

Subsequent work indicated that these 'irreversible' fouling effects may be reversible over a long period of time. The membrane, after back and forward flush cleaning, was left in buffer for a period of four weeks. A series of experiments were then performed, exposing the membrane to BSA at a concentration of 5 $g.l^{-1}$, followed by rinsing and rejection measurement (Table 3)(Fig 8). The observed rejection of tracer had dropped considerably over the period of 'resting' the membrane, but began to rise rapidly again even though the membrane was cleaned by back and forward flushing after each experiment. These results support findings that desorption of 'irreversibly' bound protein may take place over a long period of time (Norde, 1986). Deliberate 'resting' of membranes in order to restore their ability to pass

smaller molecules is likely to be ineffective, due to the rapid rise of rejection on exposure to protein. Investigation into prefouling by materials which occupy the active sites for adsorption, but which have less effect on rejection, may provide a partial solution to the problem.

Fig 8. Rejection by the 'Rested' Membrane

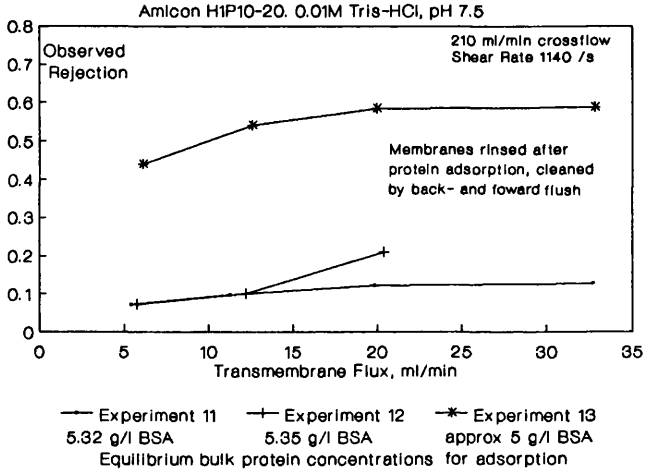

Effect of Protein Concentration on Permeability and Adsorbed Amount

Membrane permeability was measured during all tracer rejection experiments using the cleaned membrane (Table 2) and the membrane after exposure to protein under zero flux conditions (Table 3). The experiments performed after 'resting' the membrane for four weeks showed a decrease in permeability from one experiment to the next, accompanied by a rise in tracer rejection. It appears that the cleaning procedure was unable to prevent a buildup of membrane associated protein which affected both rejection and, to some extent, flux.

The amount of protein associated with the membrane under equilibrium adsorption conditions was calculated. This 'adsorbed amount' did not correlate well with tracer rejection (Table 3), although there was evidence that higher adsorbed amounts resulted in lower membrane permeabilities. Indirect evidence for a

correlation between adsorbed amount and rejection has been presented by others (Dorson et al, 1975). Whilst the amount of membrane associated protein measured at equilibrium during adsorption was not necessarily equal to the amount remaining after rinsing, protein adsorption is usually regarded as irreversible or slowly reversible (Norde, 1986). It seems likely that a substantial proportion of the membrane associated protein remained in place during rinsing.

Rejection of Tracer by a Membrane with Polarised Protein

The effect of a polarised protein layer on the observed rejection of tracer was studied. Different levels of protein polarisation were achieved by carrying out experiments at different crossflow rates and protein loadings. Each experiment consisted of measuring the tracer rejection of the clean membrane at a permeate flowrate of about 23 $ml.min^{-1}$, followed by addition of a known mass of protein to the recycle loop and determination of the observed rejection at a range of fluxes (Table 4).

Fig 9. Effect of Polarised Protein on Tracer Rejection

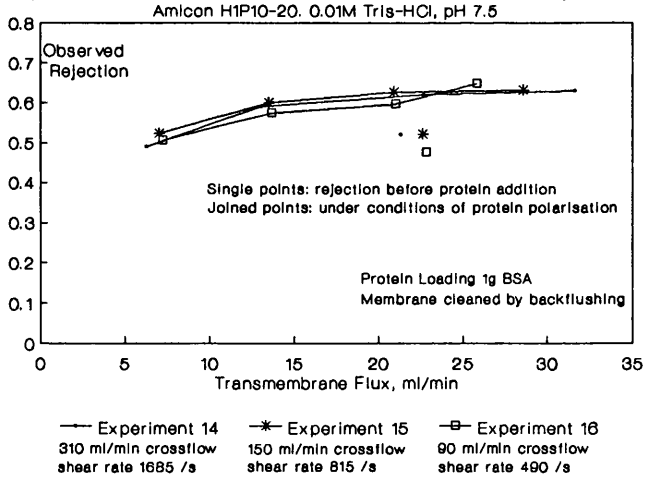

Table 4. Summary of Rejection Experiments in the Presence of Polarised Protein

Tracer concentration: 0.0002 $mol.l^{-1}$

Backflush cleaning with NaOH before each experiment.

Expt N°	Flux $ml.min^{-1}$	Rejection	Crossflow Rate $ml.min^{-1}$	Protein Mass g
14	21.3	0.52	310	No protein
	6.25	0.49		1.0
	13.0	0.59		
	22.6	0.62		
	31.7	0.63		
15	22.6	0.52	150	No protein
	7.00	0.52		1.0
	13.5	0.60		
	20.9	0.63		
	28.6	0.63		
16	22.8	0.48	90	No protein
	7.20	0.51		1.0
	13.6	0.58		
	21.0	0.60		
	25.8	0.65		
17	23.1	0.59	90	No protein
	7.30	0.46		0.2
	13.8	0.53		
	21.3	0.54		
	29.8	0.58		
18	23.4	0.63	310	No protein
	7.40	0.52		0.2
	14.2	0.60		
	21.6	0.62		
	30.3	0.62		

Experiments were performed at a fixed protein loading of 1g, and a range of crossflow rates. The presence of polarised protein increased the rejection of tracer when compared with the cleaned membrane (Fig 9), in agreement with the work of others (Calderaro

et al, 1980; Ingham et al, 1980). At the higher crossflow rates the shape and position of the rejection vs. flux curves is little different to those obtained with adsorbed protein only. At the lowest crossflow rate, however, there is an indication of an increase in observed rejection at high flux, where protein polarisation is greatest. This might signal an incipient change in the behaviour of the polarised protein close to the membrane.

Experiments using a lower protein loading of 0.2g indicated that at this concentration, tracer rejection in the presence of polarised protein was the same or less than with a cleaned membrane (Fig 10). In this case, lower levels of protein adsorption due to the lower bulk protein concentration are likely to have reduced the effect of fouling on rejection. Lower bulk protein concentration may have reduced the incidence of pore blocking which would lead to smaller increases in rejection. Time dependent changes in rejection due to 'irreversible' fouling (not removed by cleaning) may have resulted in the reduced effect of the presence of protein during the experiments with 0.2g protein loading.

Fig 10. Effect of Polarised Protein on Tracer Rejection

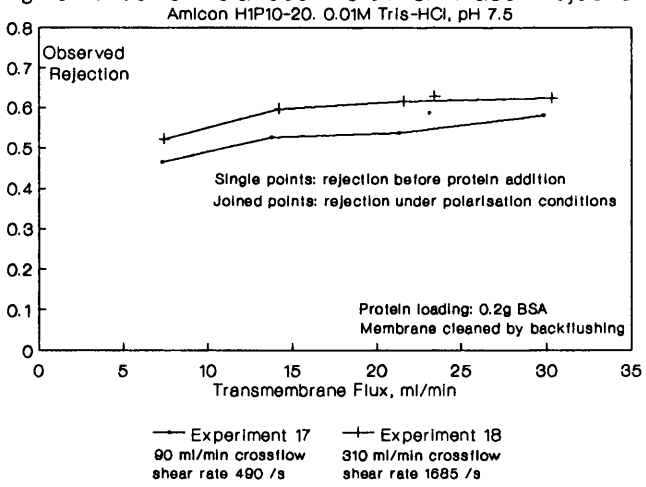

CONCLUSIONS

The rejection of a low molecular weight tracer (5'AMP, MW 347.2) by an Amicon polysulphone hollow fibre membrane of nmwco 10,000 was measured under the following conditions:

(a) The cleaned membrane.

(b) The membrane fouled by zero flux protein adsorption.

(c) The membrane under conditions of protein polarisation.

Rejection of the tracer by the cleaned membrane was about 0.15, whilst rejection in the presence of polarised protein was as high as 0.65. This level of rejection of a small molecule would be significant in an enzyme membrane reactor, if the reactor relied on low molecular weight products passing through the membrane.

Repeated exposure of the membrane to protein caused an increase in observed rejection, even though the membrane was cleaned after each exposure by back and forward flushing with 0.1M NaOH, demonstrating that 'irreversible' fouling took place. The amount of protein adsorbed to the membrane did not strongly affect rejection, therefore it seems that rejection was determined by small amounts of tightly bound protein and not by the bulk of the adsorbed protein. Evidence for slow desorption of this tightly bound material was provided by a significant drop in rejection of tracer after soaking ('resting') the cleaned membrane in buffer for four weeks.

Polarised protein was found to have little effect on rejection, except under conditions of low crossflow rate and high flux where protein polarisation was greatest. It was not possible to investigate the effect of severely polarised protein on tracer rejection due to the pressure rating of the membrane module.

REFERENCES

Calderaro, V.; Memoli, B.; Andreucci, V.E.; Drioli, E.; Albanese, 0.
"Influence of concentration polarisation in post-dilutional hemofiltration of human plasma".
Artif. Organs, 4 (1980) 317-321.

Cheryan, M.; Deeslie, W.D.
"Soy protein hydrolysis in membrane reactors".
J. Am. Oil Chem. Soc., 60 (1983) 1112-1115.

Dorson, W.J.; Cotter, D.J.; Pizziconi, V.B.
"Ultrafiltration of protein molecules through deposited protein layers".
Trans. Amer. Soc. Artif. Int. Organs., 21 (1975) 132-137.

Ferry, J.D.
"Statistical evaluation of sieve constants in ultrafiltration".
J. Gen. Physiol., 20 (1936) 95-104.

Hanemaaijer, J.H.; Robbertsen, T.; van den Boomgaard, T.; Olieman, C.; Both ,P.; Schmidt, D.G.
"Characterization of clean and fouled ultrafiltration membranes".
Desalination, 68 (1988) 93-108.

Hanemaaijer, J.H.; Robbertsen, T.; van den Boomgaard, T.; Gunnink, J.W.
"Fouling of ultrafiltration membranes. The role of protein adsorption and salt precipitation".
J. Membr. Sci., 40 (1989) 199-217.

Ingham, K.C.; Busby, T.F.; Sahlestrom, Y.; Castino, F.
"Separation of macromolecules by ultrafiltration: influence of protein adsorption, protein-protein interactions, and concentration polarisation".
Ultrafiltration membranes and applications, ed Cooper, A.R. (1980) 141-158.

Jandel, L.; Schulte, B.; Bückmann, A.F.; Wandrey, C.
"Quantitative description of the rejection of polymeric catalysts by ultrafiltration membranes"
J. Membr. Sci., 7 (1980) 185-201.

Jonsson, G.
"Transport phenomena in ultrafiltration: Membrane selectivity and boundary layer phenomena".
Pure Appl. Chem., 58(12) (1986) 1647-1656.

Jonsson, G.; Christensen, P.M.
"Separation characteristics of ultrafiltration membranes".
Membranes and membrane processes, ed. Drioli, E.; Nakagaki, M. (1984) 179-190.

Long, T.D.; Jacobs, D.L.; Anderson, J.L.
"Configurational effects on membrane rejection".
J. Membr. Sci., 9 (1981) 13-27.

Matthiasson, E.; Hallstrom, B.; Sivik, B.
"Adsorption phenomena in fouling of ultrafiltration membranes".
Engineering sciences in the food industry, ed McKenna, B.M. (1989).

Nakao, S-I.; Kimura, S.
"Analysis of solutes rejection in ultrafiltration".
J. Chem. Eng. Japan, 14 (1981) 32-37.

Nobrega, R.; de Balmann, H.; Aimar, P.; Sanchez, V.
"Transfer of dextran through ultrafiltration membranes: a study of rejection data analysed by gel permeation chromatography".
J. Membr. Sci., 45 (1989) 17-36.

Norde, W.
"Adsorption of proteins from solution at the solid-liquid interface".
Adv. Colloid Interface Sci., 25 (1986) 267-340.

Spiegler, K.S.; Kedem, O.
Desalination, 1 (1966) 311.

Wendt, R.P.; Mason, E.A.; Bresler, E.H.
"Effect of heteroporosity on membrane rejection coefficients".
J. Membr. Sci., 8 (1981) 69-90.

Zeman, L.J.
"Adsorption effects in rejection of macromolecules by ultrafiltration membranes".
J. Membr. Sci., 15 (1983) 213-230.

Zeman, L.; Wales, M.
"Steric rejection of polymeric solutes by membranes with uniform pore size distribution".
Sepn. Sci. Technol., 16 (1981) 275-290.

Last Page of Chapter 5

CHAPTER 6

UREA HYDROLYSIS in a CONSTANT FLUX ENZYME MEMBRANE REACTOR: EXPERIMENTAL and CSTR - KINETIC MODELLING

ABSTRACT

Enzyme stability and kinetics were studied for hydrolysis of urea by urease in a constant flux membrane reactor. The constant flux ultrafiltration apparatus was based around an Amicon hollow fibre membrane cartridge. The concentration of the reaction product (ammonium ions) was measured with an ion sensitive electrode.

Rapid loss of activity occurred during reactor operation which could not be prevented by a sulphydryl protecting agent. The deactivation effect seemed to be largely due to enzyme adsorption and dynamic exchange between adsorbed and dissolved states, resulting in enzyme denaturation. Deactivation seemed to be reduced by the presence of inert protein, as would be expected in these circumstances. Rapid activity decline led to the development of a short term technique for kinetic experiments in which a fresh charge of enzyme was used to determine reactor performance at each of a range of operating conditions.

A parameter estimation approach was used to evaluate different kinetic models, and a simple CSTR enzyme kinetics model with constant rejections of substrate and product was able to describe the experimental results adequately. Product inhibition was significant under the conditions used, but the mechanism could not be determined with confidence without further experimental data. Enzyme polarisation did not appear to influence performance under the conditions used. However, significant substrate and product rejections were indicated even though the molecular weight cutoff of the membrane was much greater than the molecular weights of the substrate and product molecules.

The results from the model together with studies of rejection of small solutes in a non reacting system (Chapter 5) showed that substrate and product rejection are potentially significant factors affecting the performance of a membrane reactor.

NOMENCLATURE

c	Solute concentration	$M.L^{-3}$
E	Squared error	-
k	Parameter adjustment factor	-
K_d	Decay constant in enzyme deactivation	$\log(M(product).L^{-3}).T^{-1}$
K_m	Michealis constant	$M(substrate).L^{-3}$
K_i	Subst. inhibition constant	$M(substrate).L^{-3}$
K_p	Product inhibition constant	$M(product).L^{-3}$
Q	Volumetric flowrate	$L^3.T^{-1}$
r	Volumetric reaction rate	$M.L^{-3}.T^{-1}$
R	Rejection coefficient	-
S_E	Sum of squared errors	-
v	Volume of membrane reactor	L^3
V_m	Reaction velocity constant	$M(substrate).M(enzyme)^{-1}.T^{-1}$

Subscripts		Superscripts	
b	reactor region	e	enzyme
f	feed stream	p	product
p	product stream	s	substrate

INTRODUCTION

Numerous studies of enzyme membrane reactors have been made, mostly with the purpose of evaluating the feasibility of the membrane reactor for a particular reaction system. The purpose of this work was to investigate some of the general operational factors affecting the performance of a convective flux, enzyme-in-solution membrane reactor.

Rejection of enzyme, substrate and product by the membrane are important factors affecting membrane reactor performance. Substrate rejection in a tubular membrane reactor with membrane attached enzyme has been modelled (Luchini and Pozzi, 1986) but does not seem to have been considered with regard to an enzyme-in-solution reactor. The nominal molecular weight cutoff (nmwco) of the membrane is usually chosen to ensure essentially complete rejection of enzyme, to avoid a reduction in performance due to enzyme loss. When fouled with protein, a membrane of nmwco 10,000 has shown significant rejection of a small tracer molecule (MW 347.2)(Chapter 5). In a membrane reactor, substrate and product rejection will change the reaction conditions and hence the reactor performance, especially if inhibition by either or both these species occurs.

Protein polarisation may also affect performance, causing spatial variations in enzyme concentration leading to changes in reaction rate (Hong et al, 1981). Interactions between enzyme and membrane are also likely to affect performance. Rapid enzyme deactivation occurred when polysulphone hollow fibres were used in a membrane reactor (Kohlwey and Cheryan, 1981), but could be reduced by pretreatment of the membrane with BSA. Work on the interaction of protein with polysulphone hollow fibre membranes (Chapter 3) confirmed that considerable adsorption takes place, and supported evidence (Brash and Samak, 1978) that dynamic exchange takes place between adsorbed and dissolved states. Denaturation upon adsorption and/or desorption could therefore result in significant

enzyme deactivation.

A full mathematical description of the effects of solute rejection and polarisation in a membrane reactor entails solution of the convection-diffusion equations for enzyme, substrate and product in the hollow fibres, together with equations for reaction in the other regions of the system. Such models have been developed and solved for 'once through' tubular membrane reactors (Katoh et al, 1978; Shah and Remmen, 1971) but they are computationally intensive and require knowledge of many parameters, for example solute diffusivities, rejection coefficients and permeating fluid flow models.

Most models of enzyme membrane reactors have been based on simple continuous stirred tank reactor (CSTR) or plug flow reactor (PFR) models, combined with kinetic expressions (Alfani et al, 1990; Boudrant and Cheftel, 1976; Bowski et al, 1972; Bresollier et al, 1988; Cheryan and Deeslie, 1983; Frennesson et al, 1985; Ryu et al, 1972). Similar models have also been applied to more complex multienzyme systems with coenzyme regeneration (Bossow and Wandrey, 1987; Miyawaki et al, 1982). These models have not taken into account possible partial rejection of substrate and/or product, and have not always provided exact descriptions of experimental data (Cheryan and Deeslie, 1983). Problems have been reported in extrapolating kinetic data obtained elsewhere to membrane reactors (Wandrey et al, 1979). One cause of these problems could have been lack of attention to solute rejection.

The approach adopted here was to treat the constant flux ultrafiltration apparatus used throughout this work as a CSTR, an assumption validated by residence time distribution studies in similar systems (Gacesa et al, 1983; Turker, 1985). Some of the parameters were 'lumped' together by the use of the CSTR assumption, and those remaining were the system volume, solute rejections and kinetic parameters. Consideration of permeating fluid velocity profiles in the hollow fibres was avoided by this

approach. It was possible to optimise the values of the kinetic and rejection parameters (from starting estimates) by minimising the difference between an experimental data set and the corresponding model predictions. This allowed different kinetic models to be evaluated for the system in question.

The reacting system chosen for this work was urea hydrolysis by urease, because the product (ammonium ion) concentration could be continuously measured with an ion selective electrode:

$$(NH_2)_2CO + 3H_2O \longrightarrow CO_2 + 2NH_4OH$$

Continuous measurement of product concentration allowed reactor performance to be monitored and logged by microcomputer.

Urease is a highly specific and active enzyme (Reithel, 1971). Liberation of ammonium ions meant that a control system was required to maintain the desired pH in the reactor. Urease is inhibited by product at concentrations above 4×10^{-3} $mol.l^{-1}$ and by substrate with an inhibition constant of about 3 $mol.l^{-1}$ (Ramachandran and Perlmutter, 1976). Deactivation of urease has been attributed to oxidation of sulphydryl groups which can be reversed by treatment with dithiothreitol (Riddles et al, 1983).

The aim of this work was to investigate the kinetic behaviour of the urease-urea system in a constant flux hollow fibre membrane reactor. Experimental results were analysed by considering a CSTR kinetic model of the system and taking into account partial rejections of substrate and product.

MODEL DEVELOPMENT and SOLUTION

Background

A full analysis of an enzyme reaction occurring in an ultrafiltration apparatus such as this would require a model of the enzyme, substrate and product spatial distribution throughout the hollow fibres and all regions of the recycle tubing. The number of parameters required and the difficulty of solution of such a model would require a great deal of effort, both experimentally and computationally. Work by Turker (1985) and Gacesa et al (1983) on the residence time distribution in similar apparatus has indicated that the UF cell may be treated as a continuous stirred tank reactor (CSTR) when the recycle rate exceeds the feedrate. Here, the recycle rate was 150 $ml.min^{-1}$ whilst the maximum feedrate was 16 $ml.min^{-1}$, so the above condition was satisfied.

The material balances for a CSTR at steady state may be written (Fig 1):

Overall material balance: $$Q_f = Q_p \qquad ...1.$$

Substrate material balance: $$Q_f c_f^s = Q_p c_p^s + r_b v \qquad ...2.$$

Fig 1. Continuous Stirred Tank Reactor

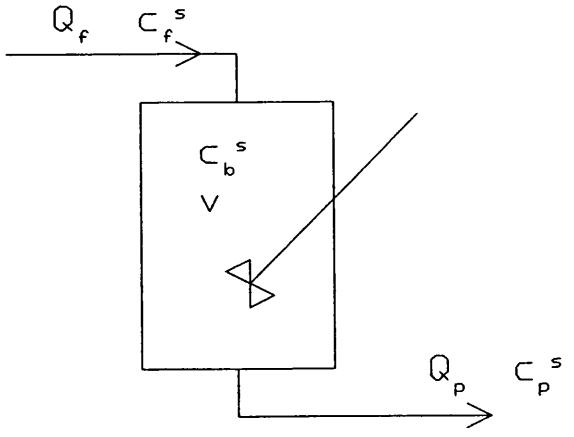

Effect of Concentration Polarisation

Use of the CSTR approximation requires that all solutes are homogeneously distributed throughout the recycle loop (including the hollow fibres). The presence of a transmembrane flux will, however, cause a degree of concentration polarisation of protein (enzyme) towards the membrane.

Concentration polarisation of BSA in the ultrafiltration apparatus used for this work has been measured for a range of fluxes and crossflow rates (Chapter 4). The degree of polarisation was modelled by considering an average polarisation layer protein concentration based on a boundary layer mass transfer correlation. Polarisation of enzyme was estimated using this model, and used to approximate the membrane reactor based on two well mixed regions: the bulk recycle volume and the polarised region. It was found that the small volume fraction of the ultrafiltration apparatus occupied by the polarised layer, together with the limited polarisation of enzyme under the conditions used, resulted in a negligible effect of enzyme polarisation on the model predictions. In addition, the high diffusivity of molecules such as urea will result in a low degree of polarisation, supporting the CSTR approximation. The model was therefore simplified to a single CSTR, as represented by Fig 1 and equations 1 and 2.

Model Development - Effect of Rejection

Work completed using the same constant flux ultrafiltration apparatus and membrane demonstrated that the rejection of a low molecular weight tracer by the membrane was significant (60%) when the membrane was fouled by protein (Chapter 5). It was therefore necessary to take substrate (and possibly product) rejection into account when modelling a reaction in the system. The simple case of constant rejection over the range of fluxes was used here. This approximation was justified by the work on rejection of adenosine 5′ monophosphate (5′AMP, MW 347.2) which indicated that the dependence of rejection upon flux was weak.

CSTR Enzyme Kinetic Model

The equations used to describe the system (in addition to equations 1 and 2) were:

Rejection of substrate: $$c_b^s = \frac{c_p^s}{1 - R^s} \quad ...3.$$

Rejection of product: $$c_b^p = \frac{c_p^p}{1 - R^p} \quad ...4.$$

Mass balance on product: $$c_p^p = 2(c_f^s - c_p^s) \quad ...5.$$

Reaction rate (based on substrate), Michaelis-Menten kinetics $$r_b = \frac{V_m c_b^e c_b^s}{K_m + c_b^s} \quad ...6a.$$

Reaction rate with uncompetitive substrate inhibition $$r_b = \frac{V_m c_b^e c_b^s}{K_m + c_b^s\left[1 + \frac{c_b^s}{K_1}\right]} \quad ...6b.$$

Reaction rate with uncompetitive substrate and competitive product inhibition $$r_b = \frac{V_m c_b^e c_b^s}{K_m\left[1 + \frac{c_b^p}{K_p}\right] + c_b^s\left[1 + \frac{c_b^s}{K_1}\right]} \quad ...6c.$$

Reaction rate with uncompetitive substrate and uncompetitive product inhibition $$r_b = \frac{V_m c_b^e c_b^s}{K_m + c_b^s\left[1 + \frac{c_b^s}{K_1} + \frac{c_b^p}{K_p}\right]} \quad ...6d.$$

Reaction rate with uncompetitive substrate and noncompetitive product inhibition $$r_b = \frac{V_m c_b^e c_b^s}{K_m\left[1 + \frac{c_b^p}{K_p}\right] + c_b^s\left[1 + \frac{c_b^s}{K_1} + \frac{c_b^p}{K_p}\right]} \quad ...6e.$$

The unknown parameters describing the system are the kinetic parameters V_m, K_m, K_1, K_p and the substrate and product rejections, R^s and R^p. Solution of the model was based on using estimated values of these parameters to calculate the permeate product concentration, and comparing this with the measured value. The solution algorithm for the above set of model equations is

shown in Fig 2. The algorithm uses the kinetic and rejection parameters together with a value of feedrate (Q_f) and feed substrate concentration (c_f^s) to simulate the steady state product concentration from the membrane reactor (c_p^s). The additional measured parameter is the reactor volume, v = 68 cm^3. The solution algorithm (Fig 2) may be used to investigate the effect of different kinetic parameters, feed flows and feed concentrations.

Fig 2. Algorithm for Solution of the CSTR Enzyme Kinetic Model

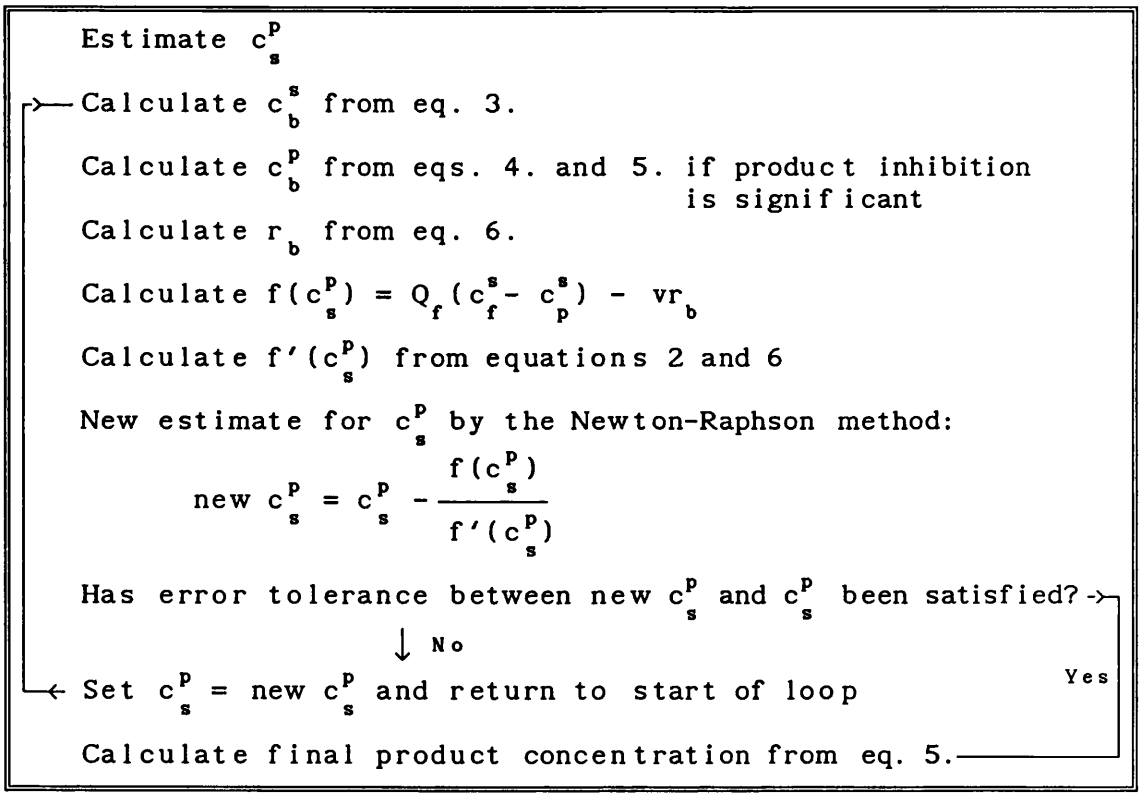

Parameter Estimation

Experimental data at 20 different sets of conditions were used to estimate the parameters in the CSTR enzyme kinetic model presented above. Experimental data required were the measured product concentration for different feedrates and feed substrate concentrations. The data were corrected for offsets in the product concentration measurements using information from the control experiments.

The model was solved as detailed in the above algorithm (Fig 2) using an estimated set of kinetic and rejection parameters, and the absolute error between the calculated product concentration (c_p^P) and the measured product concentration ($c_p^P|_m$) was calculated:

$$E = \left[1 - \frac{c_p^P}{c_p^P|_m}\right]^2 \quad \ldots 7.$$

The algorithm (Fig 2) was executed for each of the 20 sets of conditions and the 20 values of E obtained were added to form a total (S_E) for the whole data set. Thus S_E was a measure of the total difference between the model prediction and the experimental results over the range of conditions investigated. Equal weighting was given to all substrate concentrations and feedrates.

Fig 3. Algorithm for Parameter Estimation

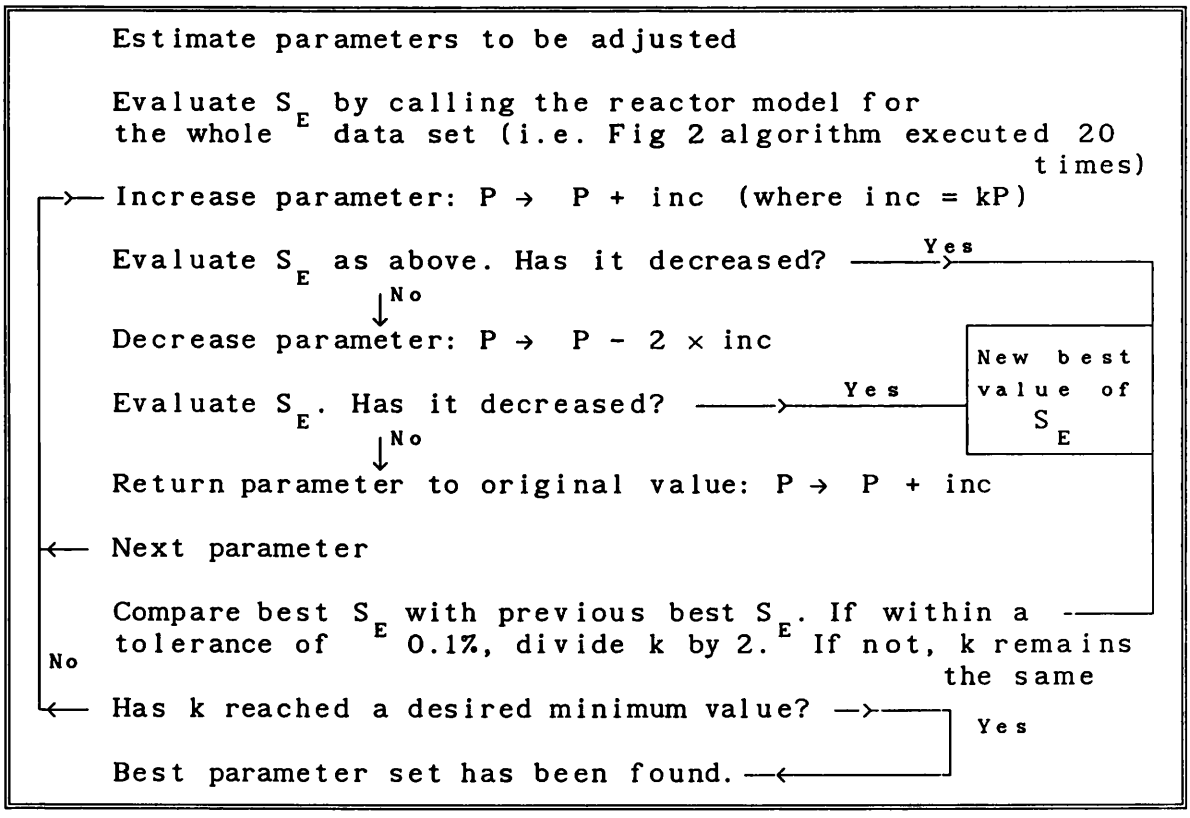

The parameters in the model were adjusted from the initial estimates to minimise the value of S_E using a simple exploratory

algorithm (Hooke and Jeeves, 1961)(Fig 3). The CSTR kinetic model was solved for each of the 20 sets of experimental conditions in order to determine each new value of S_E used in the parameter estimation algorithm. The parameter set remained the same during each new evaluation of S_E.

MATERIALS and METHODS

Apparatus

The constant flux ultrafiltration apparatus used for this study of urea hydrolysis was largely the same as that described in Chapter 2 (Fig 4). The membrane used was an Amicon H1P10-20 polysulphone hollow fibre cartridge of nominal molecular weight cutoff (nmwco) 10,000 and a nominal area of 600 cm^2. Product (NH_4^+) concentration in the permeate was measured with an NH_4^+ sensitive electrode (Kent Industrial Measurements 1057-200) and a reference electrode (Kent 1370-210). The electrodes were housed in glass flow cells and sealed by elastomer compression fittings. Electrode output was measured with a pH meter (Alpha 500).

Fig 4. Constant Flux Membrane Reactor

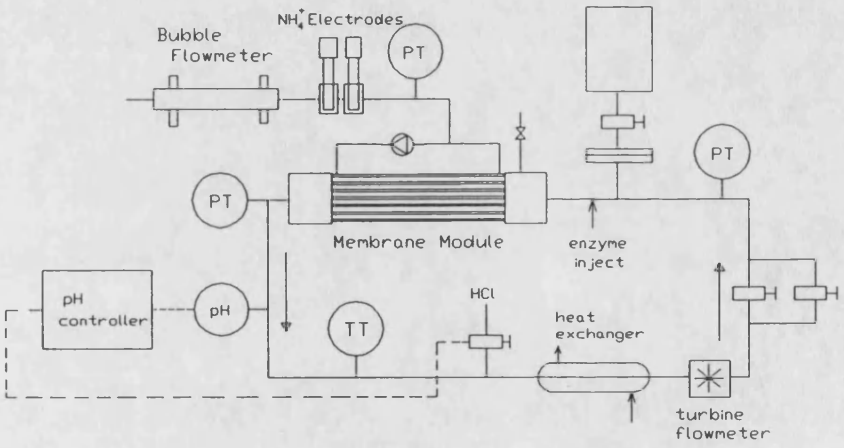

The reaction products resulted in a pH increase which could not be absorbed by the available buffer capacity, necessitating a pH control system. pH in the recycle loop was measured with a probe (Philips CE1) connected to a pH controller (LH Engineering 505). The pH controller was used to switch a peristaltic pump (Watson Marlow MHRE 22) via a relay in order to pump hydrochloric acid solution into the recycle loop. The use of small diameter pump tubing and an HCl concentration of 1M meant that the volume addition to the recycle loop was negligible.

Performance and Calibration of Ammonium Electrode

The ion specific electrode used was equally sensitive to ammonium and potassium ions, hence it was very important to keep the system free from potassium, especially when the measured product concentration was low. To this end, the reference electrode (which contained concentrated potassium chloride) was placed downstream of the ammonium electrode. The ion specific electrode also responded to sodium ions, although the sensitivity was a quarter of that for NH_4^+ or K^+. Changes in pH also affected the electrode response, as did temperature, and hence it was important to keep those as near constant as possible.

Calibration of the electrode was by once through flushing with ammonium chloride solution. A system of valves allowed the permeate stream to bypass the electrodes during calibration, so that calibration could be carried out during a run. The electrode output took about 30 min to stabilise, in accordance with the manufacturers' information (Kent Industrial Measurements, 1989). The calibration curve was determined using a range of NH_4Cl concentrations from 0.001M to 0.05M, and was found to conform to a log relationship (Fig 5):

$$\log(NH_4^+ \text{ conc}) = \text{constant} + 0.001862 \times (\text{probe output, mV} \times 10)$$

In order to minimise errors, the probes were calibrated in situ at intervals during experiments with NH_4Cl in buffer (pH 7.5) at a concentration close to that of the permeate solution being measured. The flowrate of solution through the electrode holders was found to have a negligible effect on the electrode output over the range 2 to 16 $ml.min^{-1}$ used in these experiments.

Fig 5. Ammonium Electrode Calibration

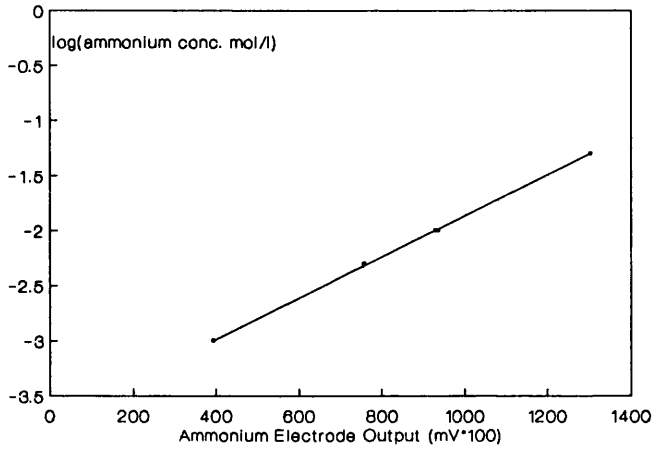

Reaction Conditions

Reaction experiments were performed in an 0.01M Tris-HCl buffer containing a small quantity of sodium azide to prevent microorganism growth and 0.001M Ethylenediaminetetraacetic acid (EDTA)(Sigma EDS) to reduce enzyme deactivation by heavy metal ions (Gacesa, 1977). The feed solution contained urea in concentrations varying from 0.001M to 0.025M. The enzyme used was urease isolated from Jack Beans (Sigma U-4002) with a quoted specific activity of 56,000 units.g^{-1} (where 1 unit liberates 1μmol NH_3 per min at pH 7.0 and 25°C). All the enzyme used in this work was taken from the same batch of solid urease which was kept in a freezer, minimising changes in activity over the series of experiments.

The pH in the recycle loop was controlled between limits of 7.45 and 7.55. The control action was optimised by adjusting the pH controller and the speed of the pH control pump. Drift of the recycle pH probe was compensated for by measuring the pH of the permeate stream and adjusting the pH controller accordingly.

Recycle loop temperature was maintained between 24 and 25°C by adjusting the temperature of the thermostatted water bath

supplying the recycle loop heat exchanger (Fig 4). The recycle flowrate (crossflow rate) was kept at 150 $ml.min^{-1}$ for all reaction experiments.

Reaction experiments were performed with a quantity of inert protein (BSA, Sigma A7906) present in the recycle loop to reduce deactivation by enzyme-membrane interaction. BSA and the accurately measured mass of enzyme were dissolved in buffer and injected directly into the recycle loop via a septum, allowing reproducible enzyme and BSA concentrations in the reactor.

Membrane Cleaning

Membrane cleaning was carried out according to the procedure described in Chapter 2.

RESULTS and DISCUSSION

General Discussion

The aim of the membrane reactor studies was to determine the performance for the urease-urea system at a variety of residence times and substrate concentrations. This data was then used to gain information on the reaction kinetics and other factors affecting the reactor performance.

It was desirable to obtain data whilst the system was at steady state, and also to investigate more than one operating condition in each experiment, in order to reduce the time spent cleaning the membrane and setting up the experiments. In order to achieve this, there had to be negligible decay of enzyme activity over the period necessary to achieve steady state several times after changes of operating conditions, or alternatively, a slow but quantifiable and repeatable decay over the same period. Experiments were conducted to determine the enzyme deactivation under typical system operating conditions.

Long-Term Deactivation Experiments

Several experiments were performed to examine enzyme deactivation over an extended period (8 to 46 hr). Most of these experiments were carried out using 4mg urease, 1g BSA, 0.01M urea and a feedrate of about 4.6 $ml.min^{-1}$. Buffer was pumped through the reactor; enzyme and inert protein were dissolved in a small volume of buffer and injected directly into the recycle loop. The feed was then changed to buffer with substrate (urea) at a known concentration, and the product concentration in the permeate was monitored with the ion selective electrode.

The product concentration in the permeate rose steeply at first, as the substrate reached the recycle loop and product began to pass through the membrane. A peak was reached, after which the product concentration decreased steadily. This was attributed to enzyme deactivation, resulting in lower conversion of the

(constant concentration) substrate feed. The time course of enzyme deactivation could easily be followed, analysed and plotted using the data logging and transfer system and a spreadsheet program (Figs 6 to 13, Table 1).

Table 1. Summary of Deactivation Experiments - Rate Constants

Fig N°	Mass Urease mg	Conditions	Rate Constant K_d (s) $\log(mol.l^{-1})$. $min^{-1} \times 10^3$
6	4.0	base case, buffer with 0.01M urea, 0.001M EDTA and azide. 4.6 $ml.min^{-1}$ feedrate.	1.11
7	4.0	no azide.	1.13
8	4.0	deoxygenated feed.	1.13
9	4.0	DL-dithiothreitol	0.775
10	10.0	longer term experiment	2.49 0.678 Note 3
11	10.4 +4.0	longer term experiment further 4mg enzyme	1.54 0.547 Note 3 1.36 0.425 Note 3
12	4.0	effect of flux: 18.3 $ml.min^{-1}$: first phase 4.4 $ml.min^{-1}$	2.52 1.03 Note 3 0.990
13	4.0	low substrate conc. 0.001M. 4.6 $ml.min^{-1}$ constant flux.	small

Note 1: The deactivation rate constants (K_d) were calculated from the slopes of the activity decline curves (e.g. Fig 6).

Note 2: The mass of BSA added was 1g for all experiments except N°10, in which only 0.25g was added.

Note 3: The additional values of K_d quoted in experiments 10 to 12 represent the second phase of deactivation, in which deactivation is slower.

The rate of deactivation was found to be quite rapid over the time course of the experiments (Fig 6). In this base case, product concentration declined from a peak of 0.017M (85% conversion) to 0.0089M (45%) in 8 hr. The results have been plotted as log(product concentration, $mol.l^{-1}$) vs. time, so that a straight line approximates a first order process with a decay constant (K_d) equal to the slope of the line. In the case of Fig 6 the decay constant remains the same over the time interval studied, suggesting that the mechanism of enzyme deactivation does not change over this interval.

Fig 6. Activity Decline, Base Case

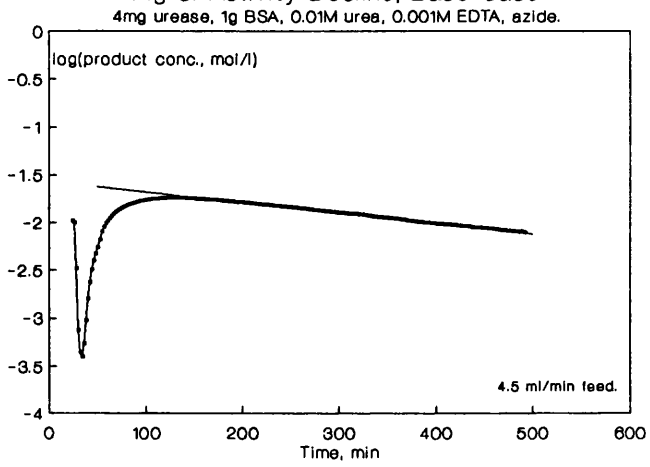

Causes of Enzyme Deactivation

Heavy metal ions have been cited as responsible for deactivation of enzymes (Gacesa et al, 1983). They found that the use of a chelating agent such as ethylenediaminetetraacetic acid (EDTA) considerably reduced deactivation. EDTA at a concentration of 0.001M was used in all this work, so that heavy metal ion deactivation effects should have been minimised.

Oxidation of sulphydryl groups has also been reported to cause enzyme deactivation (Gacesa and Hubble, 1987; Wiseman, 1978). Enzymes such as urease require these groups to remain in their reduced state, to maintain the catalytically important structure of the molecule. Deoxygenation of the system and/or the use of reducing agents may reduce deactivation by preventing or slowing

the oxidation of sulphydryl groups (Riddles et al, 1983). Investigation of these methods was undertaken and is discussed later.

Shear can contribute to enzyme deactivation (Charm and Wong, 1981). However Gacesa et al (1983) found that for experiments with urease conducted in a cone and plate viscometer, a range of shear strains (shear rate $\times$ time) from 0.02 to 3.2 $\times$ 10^7 had no effect on activity. The wall shear rate in the hollow fibres at the crossflow rate of 150 $ml.min^{-1}$ used here was about 815 s^{-1}, so the bulk enzyme shear strain in a long term experiment was unlikely to exceed the range studied by Gacesa et al (1983).

Interaction of enzyme with a surface such as the membrane may cause deactivation. Adsorption to the membrane is likely to result in denaturation of the enzyme molecule, reducing or destroying its catalytic activity (Huffman-Reichenbach and Harper, 1982). It is unlikely that activity would be fully recovered upon desorption. Dynamic exchange between adsorbed and dissolved states has been demonstrated, even when the total adsorbed amount of protein remains constant (Brash and Samak, 1978). This dynamic exchange might be expected to result in a steady loss of enzyme activity.

Further Deactivation Experiments

An experiment was performed under similar conditions to those previously mentioned, but in the absence of sodium azide (NaN_3) used to prevent microbial growth in buffer storage vessels and the apparatus (Fig 7). The decay constant was almost identical to that obtained with sodium azide present (Table 1), indicating that deactivation was not affected by sodium azide at this concentration.

Fig 7. Activity Decline, No Azide.

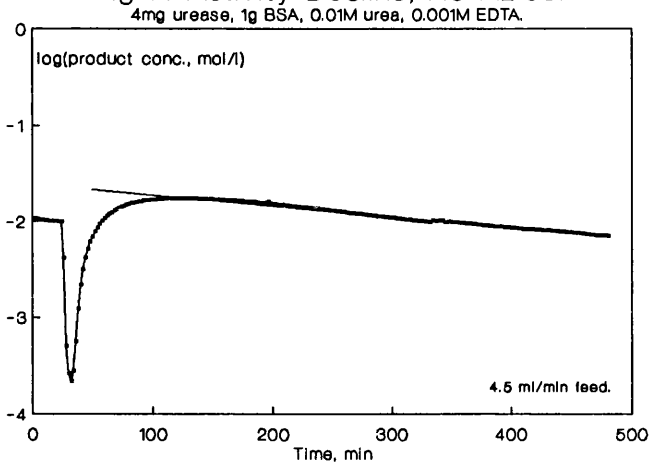

An experiment was performed to investigate the possibility of improving enzyme stability in the system by reducing the rate of oxidation of sulphydryl groups. In this experiment, the feed solution was deoxygenated by sparging the feed vessel with nitrogen for several hours before the experiment (Fig 8). Use of a deoxygenated feed had no effect on the decay constant (Table 1).

Fig 8. Activity Decline - Deoxygenated Feed.

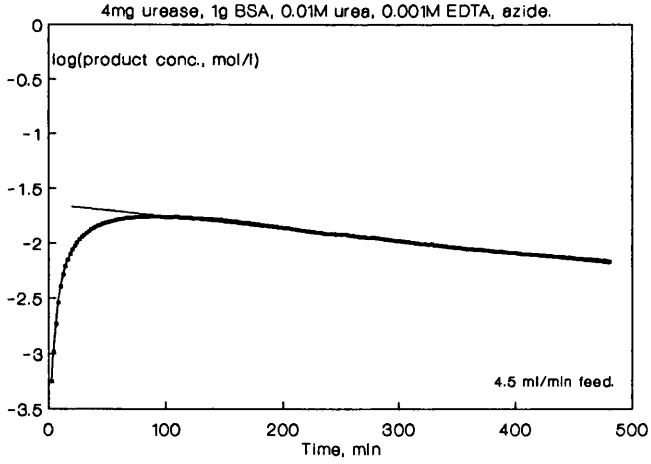

The use of reducing agents to prevent sulphydryl group oxidation was also investigated. L-cysteine and mercaptoethanol were found to have a time dependent effect on the output of the recycle pH

probe, thus preventing adequate pH control and rendering the reaction conditions uncertain.

A further experiment was performed with a feed solution containing 0.001M DL-dithiothreitol, a sulphydryl specific reducing agent (Riddles et al, 1983)(Fig 9). The presence of DL-dithiothreitol had a slight effect on the pH probe, but this was compensated for by measuring the pH of the permeate and adjusting the pH controller accordingly. DL-dithiothreitol was found to reduce enzyme deactivation over the 9 hr experiment performed, the decay constant decreasing by 32% from 0.0011 for the 'base case' to 0.00077 with DL-dithiothreitol (Table 1). However, the rate of deactivation was not reduced sufficiently to allow kinetic measurements over several sets of operating conditions in the same run, so the use of reducing agents and deoxygenated feeds was not investigated further.

Fig 9. Activity Decline - dithiothreitol.

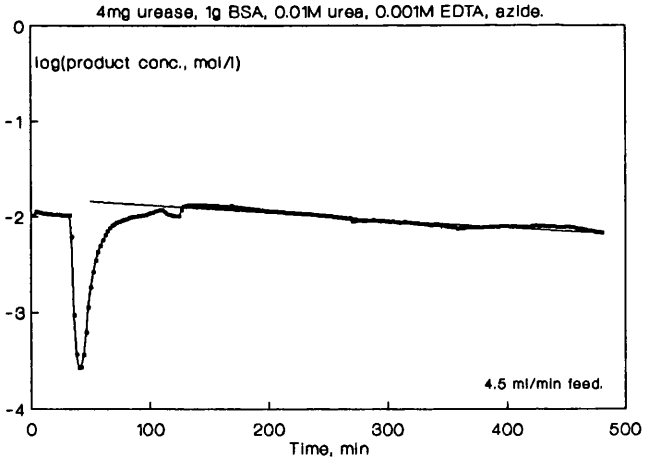

Very Long Term Deactivation Experiments

Work by Gacesa (1977) on long term monitoring of urease activity in a membrane reactor demonstrated that after an initial rapid decay during the first day of operation, the rate of activity decline approached a constant, lower value. With such behaviour it might be possible to obtain kinetic data by allowing the

activity to stabilise over a long period of time and then measuring pseudo steady state product concentrations over a range of conditions. The results could then be corrected for the (constant) activity decay over the period of the kinetic measurements, if the decay was not too rapid. To investigate the feasibility of this approach, an experiment was conducted at constant flux over a period of 22 hr using a higher initial charge of 10mg urease to compensate for the initial, rapid activity decline, and a smaller quantity of BSA (0.25g) in an attempt to reduce membrane fouling (Fig 10).

Fig 10. Activity Decline, Longer Term, Base Case.

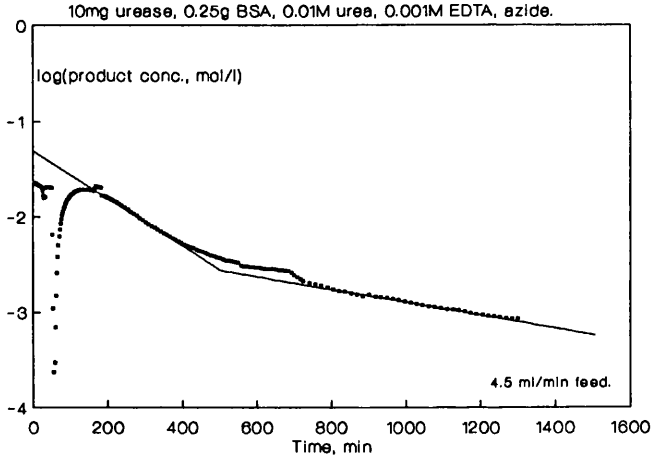

This experiment showed that the deactivation occurred in two distinct stages, the initial stage lasting for about 7 hr, after which the decay constant became smaller. Previous experiments had covered the first region only. The existence of two rates of deactivation suggests that the mechanism of deactivation changed, perhaps due to a reduction in the degree of enzyme-membrane interactions.

The initial decay constant was considerably higher with 10mg urease and only 0.25g BSA (0.0025) than with the previous experiments using 4mg urease and 1g BSA (0.0011). This could be due to increased enzyme-membrane interactions resulting from the

greater concentration of enzyme and/or the reduced concentration of inert protein.

A Second Addition of Enzyme

A long term constant flux experiment was conducted to determine the effect of a second addition of urease after the activity of the initial loading had decayed (Fig 11). It was found that deactivation of the second charge of enzyme was almost as rapid as that for the first charge (Table 1), suggesting that the mechanism of deactivation was not affected by time dependent fouling of the membrane. If the main mechanism of deactivation was by enzyme-membrane interactions, the interactions would have been of the continuous, dynamic exchange type proposed by Brash and Samak (1978).

Fig 11. Activity Decline, Second Enzyme Addition.

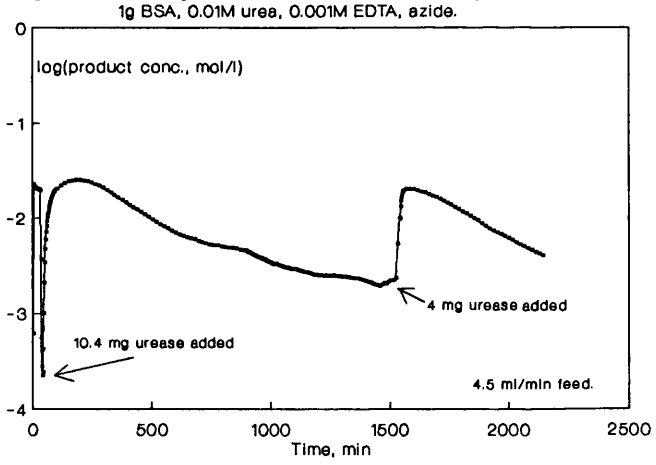

Membrane Resistance

Membrane resistance was found to increase with time during these experiments (Fig 12). The rate of increase was not significantly different during the experiment with 0.25g BSA when compared with the experiments with 1g BSA, suggesting that the increase in membrane resistance was not strongly dependent on the amount of BSA present. Membrane resistance seemed to increase more quickly at higher fluxes, at least initially. Membrane resistance has

been correlated with the amount of adsorbed protein (Matthiasson, 1983), thus the rise in membrane resistance and the activity decline may have both been due to a gradual increase in the amount of protein adsorbed to the membrane.

Fig 12. Activity Decline, Effect of Flux
1g BSA, 4mg urease, 0.01M urea, 0.001M EDTA, azide.

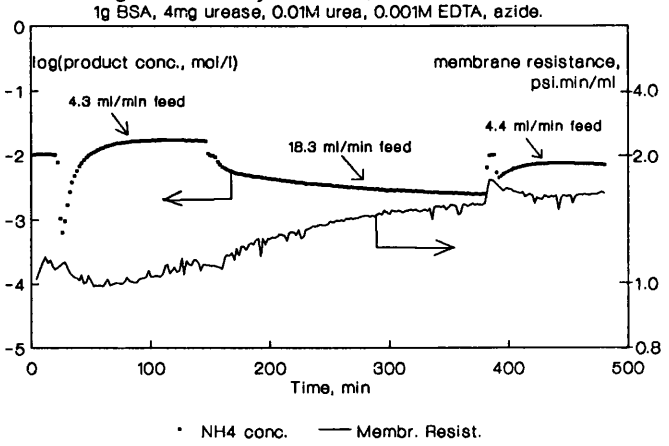

Effect of Flux on Deactivation

An experiment was conducted to determine the effect of flux on the rate of enzyme deactivation. After an initial period at 4.3 $ml.min^{-1}$, the feedrate (= permeate rate in the constant flux apparatus) was increased to 18.2 $ml.min^{-1}$ for 4 hr and then decreased to 4.4 $ml.min^{-1}$ (Fig 12, Table 1). At the higher flux, the decay constant was greater (0.0025 min^{-1}) for the first 2 hr than the standard value (0.0011 min^{-1}) obtained at the lower flux of about 4.5 $ml.min^{-1}$ in other experiments with otherwise similar conditions. After 2 hr at 18.2 $ml.min^{-1}$, the decay constant decreased to 0.0010 min^{-1} which is close to the value obtained at the lower flux. It seems that increasing the flux resulted in faster deactivation for a finite period, after which the decay constant returned to the 'base value'. This could have been due to the amount of adsorbed protein increasing to a new equilibrium value as the degree of concentration polarisation (and thus the protein concentration at the membrane) increased with flux.

Effect of Substrate Concentration on Deactivation

One long term deactivation experiment was carried out with a lower substrate concentration of 0.001M (Fig 13). Although the ammonium selective electrode response was rather uneven at these lower product concentrations, the practice of recalibration of the electrode during the run adds confidence to the results. The degree of deactivation at the lower substrate concentration (0.001M) was much less than that found from the work at 0.01M. In general, higher substrate concentrations are considered to have a stabilising effect on enzyme activity, but in this case the opposite effect seemed to occur. Substrate inhibition of urease does occur (Ramachandran and Perlmutter, 1976), and if irreversible substrate binding can destroy enzyme activity then this is likely to be more severe at higher substrate concentrations. Urease is reported to be resistant to denaturation in urea at concentrations up to 8M, so the urea concentrations used here are unlikely to have caused deactivation by enzyme denaturation.

Fig 13. Activity Decline, Low Substrate Concentration.

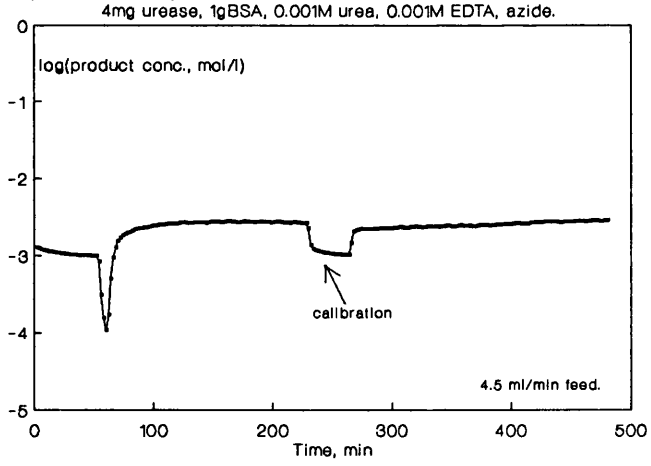

Summary of Urease Stability in the Membrane Reactor

Deactivation of urease in this membrane reactor system was quite rapid, such that it was impractical to obtain kinetic data at a number of operating conditions (flux, substrate concentration)

during a single run. Over the maximum period of constant conditions studied (22 hr), two different first order decay constants were observed, the first applying for around 7 hr. Deactivation was not affected by the presence of sodium azide, or by deoxygenating the feed solution. Deactivation rate was reduced by ≅ 30% by the use of DL-dithiothreitol, a reducing compound specific to sulphydryl groups, but it appeared that the main cause of deactivation was denaturation due to enzyme-membrane interactions. This has been observed by others (Kohlwey and Cheryan, 1981) working with the same membrane material. The effect of these interactions appeared to be reduced by the presence of inert protein (BSA), but was increased (for a period) on increasing transmembrane flux, possibly due to increased adsorption. The rate of deactivation did not significantly decrease even after more than 40 hr of operation, and a further addition of enzyme to the reactor decayed at the same rate as the initial addition. Deactivation was accompanied by a steady increase in membrane resistance, supporting the theory that deactivation is linked to a protein-membrane interaction process. Lower substrate concentrations seemed to result in markedly slower deactivation rates, although further work would be needed to confirm this.

Method for Obtaining Kinetic Data

In the light of the above conclusions, a short term or 'snapshot' approach to obtaining kinetic data was adopted. Buffer containing a fixed substrate concentration was fed into the ultrafiltration apparatus and the ammonium probe was calibrated at a concentration close to the expected product concentration. The dissolved urease (2mg) and BSA (0.25g) were injected directly into the recycle loop to start the reaction. This was done in order to minimise differences between experiments due to the mixing characteristics of the feed and recycle regions of the apparatus. The rise in product concentration was monitored and recorded. The concentration peak reached by the product in the permeate stream was then taken as representative of the steady concentration that

would be reached under constant operating conditions with no enzyme deactivation. Once the peak had been observed, the recycle loop was flushed out with buffer containing substrate at the concentration being used, and the experiment was repeated at a different feedrate, using a fresh enzyme charge. Thus four different feedrates (residence times) could be investigated in one days' experimentation. The membrane was cleaned after each day, and a different substrate concentration was used for the next series of experiments.

The residual enzyme activity remaining after rinsing the recycle loop was monitored by feeding substrate solution through the reactor before injecting the next charge of enzyme (Fig 14). The low level of activity remaining supports the proposal that adsorbed enzyme was denatured and retained little or no activity, and that desorbed enzyme (if any) was denatured to the point of inactivity.

Fig 14. Kinetic Experiment, Raw Data.

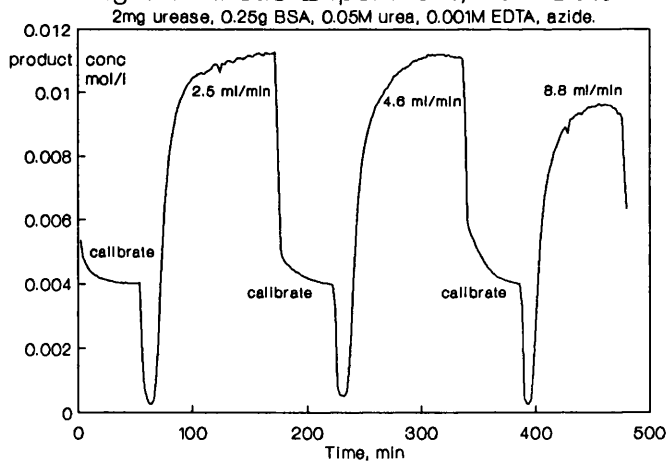

This approach to obtaining kinetic data was not ideal. Higher feedrates resulted in a faster approach to equilibrium in fluid dynamic terms, which would result in a higher concentration peak than lower feedrates if the deactivation rate was constant. However, initial decay constants have been shown to be greater at

higher fluxes. In these circumstances of fast enzyme deactivation, a compromise must be adopted and this technique produced internally consistent results.

Controls for Kinetic Experiments

The permeate product concentration from the membrane reactor (indicated by the ammonium selective electrode output) was sometimes found to exceed the theoretical maximum concentration corresponding to 100% conversion (e.g. Fig 14 where the feed substrate concentration is 0.005M, leading to a theoretical maximum product concentration of 0.01M). An investigation was undertaken to determine the cause of this, or at least to quantify the effect.

A series of batch reactions were carried out, covering the range of substrate concentrations (0.001M to 0.025M) used in the kinetic experiments. The same buffer composition was used as in all the enzyme reaction work (0.01M tris-HCl pH 7.5, with 0.001M EDTA and a small amount of sodium azide). Urease was added, and concentrated HCl was added as required to maintain the reaction pH close to 7.5. Once the pH had ceased to rise, a further addition of urease was made and the pH was monitored to ensure that the reaction was complete.

The reaction mixture was then fed into the membrane reactor, the recycle loop having been flushed through with the same solution. The ammonium electrode was precalibrated with ammonium chloride in buffer at the concentration corresponding to 100% conversion for the batch in question. BSA (0.25g) was injected into the recycle loop to simulate the conditions of the membrane reactor experiments. Permeate pH was monitored and the pH controller used to maintain this at pH 7.5 if necessary, again in order to simulate the conditions applied to the membrane reactor when performing kinetic experiments. Permeate product concentration was monitored as it increased and approached a steady state, thus determining the actual electrode reading at 100% conversion for

the range of substrate concentrations used. When a steady concentration reading had been reached, a portion of the batch reaction mixture was pumped directly through the ammonium electrode housing to check the extent of reaction.

The results (all at a feedrate of about 4.6 $ml.min^{-1}$) are summarised in Table 2 and show that the passage of the reaction products through the membrane resulted in an artificially high measurement of product concentration. At higher substrate concentrations, a small pH shift was observed between the feed solution (previously adjusted to pH 7.5) and the permeate. This indicated a selective retention of some ions more than others by the membrane, which may explain the observed effect on ammonium ion measurement.

Table 2. Control Experiments using a Fully Reacted Batch

substrate conc. $mol.l^{-1}$	theoretical product conc. @ 100% conversion. $mol.l^{-1}$	measured permeate conc. $mol.l^{-1}$	measured batch conc. $mol.l^{-1}$
0.0010	0.002	0.00290	0.00201
0.0025	0.005	0.00574	0.00497
0.0050	0.001	0.0112	0.01002
0.0100	0.020	0.0227	0.01990
0.0250	0.050	0.0570	≅ 0.05

As these control experiments were performed in the same way as the kinetic experiments, correction of the results of kinetic experiments by a factor indicated by Table 2 was considered to give valid data.

Effect of Flux on Concentration Measurement

The effect of feedrate (flux) on the ammonium electrode reading was also investigated in these control experiments. At the two extremes of substrate concentration (0.001M and 0.025M), the feedrate was increased from the base value of 4.6 $ml.min^{-1}$ to 9.3

$ml.min^{-1}$ and then 14.0 $ml.min^{-1}$. The electrode reading was allowed to stabilise between feedrates. The results are expressed as the concentration increase factor (CIF):

$$CIF = \frac{\text{measured } NH_4^+ \text{ concentration}}{\text{theoretical conc. @100\% conversion}}$$

Variation of the CIF with flux is shown in Table 3. The CIF was found to vary approximately linearly with feedrate over the range studied, and extrapolating to zero flux gave a factor of unity, suggesting that the ion retention effect was induced by flux.

Table 3. Variation of the Concentration Increase Factor with Flux

Substrate conc. 0.001M		Substrate conc. 0.0250M	
Flux $ml.min^{-1}$	Concentration Increase Factor	Flux $ml.min^{-1}$	Concentration Increase Factor (CIF)
4.15	1.25	4.6	1.30
9.1	1.30	9.6	1.31
14.0	1.50	14.0	≅ 1.5

Use of Data from Control Experiments

The above information allowed the product concentration measurements during kinetic experiments to be corrected at any feedrate. Maximum product concentrations were measured over a matrix of 5 different feed substrate concentrations (0.001M to 0.025M) and 4 feedrates (approx. 2 to 16 $ml.min^{-1}$). An example of the raw data is shown in Fig 14. Each of the concentration peak values was corrected using data from the control experiments, leading to a data set of 20 points describing product concentration variation with substrate concentration and feedrate (residence time). The results were then analysed in terms of the enzyme kinetics and rejection characteristics applicable in the system.

Results of Parameter Estimation

The CSTR enzyme kinetics model was applied to the corrected set of

20 points describing the experimental product concentration at various feedrates and substrate concentrations. The product concentrations predicted by the model were compared with the experimental concentrations and the total error for the 20 different conditions was used as a basis for parameter optimisation, as described previously under 'Model Development'. The best parameter sets obtained are summarised in Table 4 for several different kinetic models.

Table 4. Summary of Membrane Reactor Parameter Estimation Results

Subst Inhib	Prod Inhib	Subst Rej	V_m mol/g/s $\times 10^4$	K_m mol/l $\times 10^3$	K_i mol/l	Prod Rej	K_p mol/l $\times 10^3$	Error Sum
-	-	0.816	3.29	3.83	-	-	-	0.241
Uncomp	-	0.776	3.32	3.22	8.22	-	-	0.243
Uncomp	-	0	3.31	0.712	2.05	-	-	0.243
Uncomp	Comp	0.930	3.96	7.80	2.75	0.466	8.79	0.167
Uncomp	Uncomp	0.728	4.23	3.67	2.95	0.086	47.0	0.147
Uncomp	Noncomp	0.822	4.20	5.17	3.71	0.095	53.6	0.145

Use of the Michaelis - Menten Kinetic Model

The simplest model was based on Michaelis-Menten kinetics. There were three optimisable parameters: The Michaelis-Menten constants (V_m, K_m), and the substrate rejection coefficient (R^s). The results from this model are compared with the experimental data in Fig 15, which shows that the model was capable of a fair description of the system behaviour except at the highest substrate concentration and lowest feedrate.

Fig 15. Kinetic Data - Comparison with Michaelis Model.

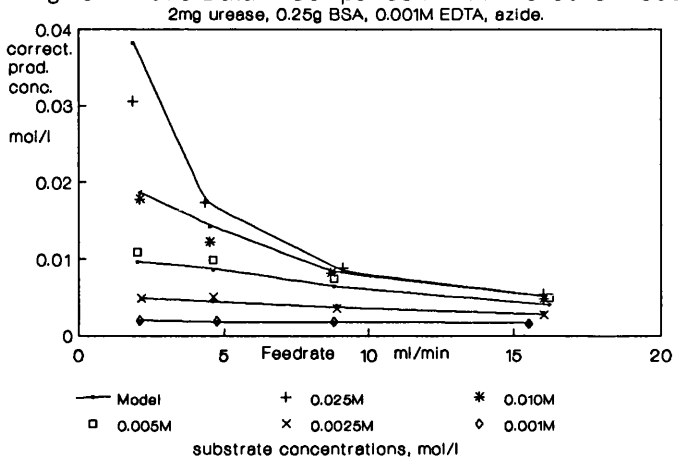

The estimated value for substrate rejection in this case was ≅ 81% which is a very high figure for such a small molecule (urea, MW 60) by a 10,000 nmwco membrane. However, fouling has been shown to cause up to 65% rejection of a small molecule (Chapter 5), which supports this value.

The estimated value of V_m was 3.3×10^{-4} mol(substr.).g(enz.)$^{-1}$.s^{-1}. The activity of 56,000 units.g(enz.)$^{-1}$ quoted by Sigma for the batch of urease used corresponds to $V_m = 4.7\times10^{-4}$ mol(substr.).g(enz.)$^{-1}$.s^{-1} (one unit liberates 1 μmol ammonia per min at pH 7.0 and 20 °C). The estimated and theoretical values compare well. It appears that the enzyme activity declined slightly from the 'as shipped' value, perhaps due to storage, adsorption or differences between the assay conditions and those in the membrane reactor.

The value of K_m of 3.8×10^{-3} mol(substrate).litre^{-1} is close to the usual value for urease-urea of ≅ 4×10^{-3}mol(substrate).litre^{-1} (Turker, 1985; Ramachandran and Perlmutter, 1976; Wall and Laidler, 1953; Reithel, 1971; Gacesa et al, 1983).

These results are therefore encouraging as the parameters obtained

agree closely with previous work, both in this thesis and by others, suggesting that the approach to modelling this system is valid.

Investigation of Substrate Inhibition

Urease has been shown to exhibit uncompetitive substrate inhibition (Ramachandran and Perlmutter, 1976) with an inhibition constant of about 3 $mol.l^{-1}$. Investigation of an uncompetitive substrate inhibition model yielded similar values of R^s, V_m and K_m to the Michaelis-Menten model, with a K_1 rather higher than that of Ramachandran and Perlmutter (1976) of 8.2 $mol.l^{-1}$ (Table 4). The fit to experimental data was very similar to that obtained with Michaelis-Menten kinetics. Substrate inhibition may have occurred in this system, but it was not significant at the concentrations used here.

The Case of No Substrate Rejection

If substrate rejection was assumed to be zero, the predicted values of the remaining parameters would be different. Investigation of zero substrate rejection with an uncompetitive substrate inhibition model resulted in little change to V_m, a value of K_1 closer to that of Ramachandran and Perlmutter (1976), and a substantially decreased value of K_m (Table 4). This low value of K_m does not seem valid when compared to other work, and supports the proposal that considerable substrate rejection occurred in this system.

Product Inhibition

Product inhibition of urease activity occurs at concentrations above 4×10^{-3} $mol.l^{-1}$ (Ramachandran and Perlmutter, 1976; Laidler and Hoare, 1949). Even with zero rejection of product, the concentration of ammonium ions will approach 5×10^{-2} $mol.l^{-1}$ under the conditions used in this work. It appears likely that some rejection of ammonium ions took place, although their charge reduces the confidence with which rejection can be estimated from rejection of similarly sized molecules. Data for product

inhibition is scarce, but Turker (1985) estimated product inhibition constants of 5.5×10^{-3} $mol.l^{-1}$ for a competitive product inhibition model, and 8.9×10^{-2} $mol.l^{-1}$ for an uncompetitive model.

Investigation of combined product inhibition and uncompetitive substrate inhibition models was undertaken, with product rejection as a separate parameter (Fig 16, Table 4). The fit to experimental data was better than with Michaelis-Menten kinetics or a substrate inhibition model only, although this was to be expected with the larger number of parameters. The experimental data was too limited to make a selection between the three product inhibition mechanisms, but the uncompetitive and noncompetitive models give similar results, differing from the competitive mechanism (Table 4). The total error (S_E) for the three models is similar. It should be noted that the minimum estimated value for product rejection (R_p) is ≅ 9% and the maximum is as high as 47% for the competitive product inhibition model, indicating that rejection of the small product ion NH_4^+ was significant.

Fig 16. Uncomp. Substr. and Comp. Prod. Inhibition.

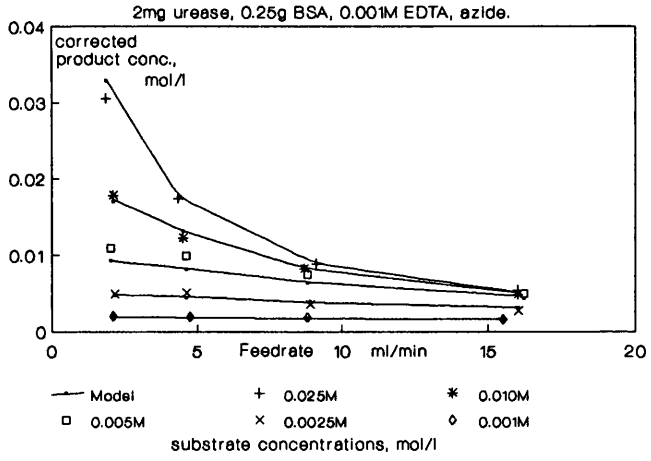

Summary of the Kinetic Work

Due to the quite rapid enzyme deactivation in the reactor, a technique was developed to estimate the kinetic behaviour of the enzyme in this system based on short term reaction experiments

using a fresh charge of enzyme for each change of process conditions (feed rate and substrate concentration). Peak values of permeate product concentration were taken as representative of the steady value which would exist under conditions of zero deactivation. The data obtained was found to be internally consistent.

Passage of the product mixture through the membrane caused a quantifiable shift in product (ammonium ion) measurement using an ion sensitive electrode, suggesting that some ions were retained more than others by the fouled membrane.

The system was adequately described over a range of substrate concentrations of 0.001M to 0.025M and feedrates from 2 $ml.min^{-1}$ to 16 $ml.min^{-1}$ by a CSTR enzyme kinetics model, taking into account constant rejections of substrate and product. A parameter optimisation technique applied to different kinetic mechanisms and rejection scenarios allowed the following conclusions to be drawn:

Substrate rejection was significant at around 75% and although uncompetitive substrate inhibition is indicated in the literature for this system, it was not significant at the concentrations used here.

Product inhibition occurred and product rejection of between 9% and 47% was indicated by parameter optimisation. There was insufficient data to determine the mechanism of product inhibition. To determine the mechanism with confidence, further work would be necessary to measure product rejection, preferably under reaction conditions.

Under the conditions of flux and crossflow applied here, polarisation of enzyme did not significantly change reactor performance from that of a CSTR, and hence the main influence of membrane fouling in this enzyme reactor was to cause variations in the rejection of substrate and product.

CONCLUSIONS

Rapid enzyme deactivation occurred in this system, possibly due to a dynamic exchange between adsorbed and dissolved enzyme, with denaturation upon adsorption and/or desorption. As expected, deactivation was slower in the presence of inert protein, presumably due to reduced enzyme-membrane interactions.

A simple CSTR enzyme kinetics model with substrate and product rejection adequately described the system under the conditions used. Enzyme polarisation did not significantly affect the performance of the membrane reactor. A parameter optimisation approach to the solution of the model for the whole experimental data set yielded values for kinetic constants and solute rejections in agreement with the literature values and with rejection measurements presented in Chapter 5.

Substrate inhibition occurs in the urease-urea system, but it was not significant at the at the concentrations used here. Product inhibition was significant, but the mechanism could not be determined with confidence from the experimental data available.

The modelling approach has illustrated the importance of substrate and product rejection in determining the performance of a membrane reactor.

REFERENCES

Alfani, F.; Gallifuoco, A.; Cantarella, M.
"Study of Michaelis-Menten kinetics with linear type product inhibition in ultrafiltration membrane reactors: Mathematical model, experimental and data correlation".
The Chem. Eng. J., 43 (1990) B43-B51.

Bossow, B.; Wandrey, C.
"Continuous enzymatically catalyzed production of L-leucine from the corresponding racemic hydroxy acid".
Ann. N.Y. Acad. Sci., 506 (Enzyme Eng 5) ed Shuler, M.L.; Weigand, W.A. (1987) 325-336.

Boudrant, J.; Cheftel, C.
"Continuous proteolysis with a stabilised protease. II. Continuous experiments".
Biotechnol. Bioeng., 18 (1976) 1735-1749.

Bowski, L.; Shah, P.M.; Ryu, D.Y.; Vieth, W.R.
"Process simulation of sucrose hydrolysis on invertase in a continuous flow stirred tank/UF system".
Biotechnol. Bioeng. Symp. Series, 3 (1972) 229-239.

Brash, J.L.; Samak, Q.M.
"Dynamics of interactions between human albumin and polyethylene surface".
J. Colloid Interface Sci., 65 (1978) 495-504.

Bresollier, Ph.; Petit, J.M.; Julien, R.
"Enzyme hydrolysis of plasma proteins in a CSTR ultrafiltration reactor: Performances and modelling".
Biotechnol. Bioeng., 31 (1988) 650-658.

Charm, S.E.; Wong, B.L.
"Shear effects on enzymes".
Enzyme. Microb. Technol., 3 (1981) 111-118.

Cheryan, M.; Deeslie, W.D.
"Soy protein hydrolysis in membrane reactors".
J. Am. Oil Chem. Soc., 60 (1983) 1112-1115.

Frennesson, I.; Trägårdh, G.; Hahn-Hägerdal, B.
"An ultrafiltration membrane reactor for obtaining experimental reaction rates at defined concentrations of inhibiting sugars during enzymatic saccharification of alkali-pretreated sallow: Formulation of a simple empirical rate equation".
Biotechnol. Bioeng., 27 (1985) 1328-1334.

Gacesa, P.
"Catalytic reactors using soluble enzymes".
PhD thesis, University of Bath, (1977).

Gacesa, P.; Eisenthal, R.; England, R.
"Immobilization of urease within a thin channel ultrafiltration cell".
Enzyme. Microb. Technol., 5 (1983) 191-195.

Gacesa, P.; Hubble, J.
"Enzyme Technology".
Open University Press, Milton Keynes, (1987).

Hong, G.; Tsao, G.T.; Wankat, P.C.
"Membrane reactor for enzymatic hydrolysis of cellobiose".
Biotechnol. Bioeng., 23 (1981) 1501-1516.

Hooke, R.; Jeeves, T.A.
"'Direct search' solution of numerical and statistical problems".
J. Assoc. Comp. Machin., 8 (1961) 212-229.

Huffman-Reichenbach, L.; Harper, W.J.
"Beta-galactosidase retention by hollow fiber membranes".
J. Dairy Sci., 65 (1982) 887-898.

Katoh, S.; Yanagida, T.; Sada, E.
"Performance of a membrane type enzyme reactor utilizing ultrafiltration".
J. Chem. Eng. Japan, 11 (1978) 143-146.

Kent Industrial Measurements Ltd
"Performance and specification for the ammonium-potassium ion selective electrode model 1057-200".
Publication of Kent Industral Measurements Ltd., Stonehouse, UK (1989).

Kohlwey, D.E.; Cheryan, M.
"Performance of a β-D-galactosidase hollow fibre reactor".
Enzyme Microb. Technol., 3 (1981) 64-68.

Laidler, K.J.; Hoare, J.P.
"The molecular kinetics of the urease-urea system. I. The kinetic laws".
J. Am. Chem. Soc., 71 (1949) 2699-2702.

Luchini, P.; Pozzi, A.
"Unsteady-state behaviour of enzyme membrane reactors with substrate rejection".
J. Membrane Sci., 27 (1986) 263-274.

Matthiasson, E.
"The role of macromolecular adsorption in fouling of ultrafiltration membranes".
J. Membr. Sci., 16 (1983) 23-26.

Miyawaki, O.; Nakamour, K.; Yano, T.
"Theoretical study of continuous NAD recycling by conjugated enzymes immobilized in ultrafiltration hollow fiber".
J. Chem. Eng. Japan, 15 (1982) 142-147.

Ramachandran, K.B.; Perlmutter, D.D.
"Effects of immobilization on the kinetics of enzyme catalysed reactions. II. Urease in a packed column differential reactor system".
Biotechnol. Bioeng., 18 (1976) 685-699.

Reithel, F.J.
"Ureases".
in "The Enzymes", 3ed, vol. 4. Ed. Boyer, P.D., Academic, New York, (1971).

Riddles, P.W.; Andrews, R.K.; Blakeley, R.L.; Zerner, B.
"Jack bean urease. VI. Determination of thiol and disulphide content. Reversible inactivation of the enzyme by blocking of the unique cysteine residue".
Biochimica et Biophysica Acta, 743 (1983) 115-120.

Ryu, D.Y.; Bruno, C.F.; Lee, B.K.; Venkatasubramanian, K.
"Microbial penicillin amidohydrolase and the performance of a continuous enzyme reactor system".
Proc. IFS: Ferment. Technol. Today, (1972) 307-314.

Shah, Y.T.; Remmen, T.
"Radial mass transfer effects in a porous wall tubular reactor".
Int. J. Heat Mass Transfer, 14 (1971) 2109-2124.

Turker, M.
"A study of concentration polarisation in a hollow fibre membrane reactor".
MSc thesis, University of Wales (1985).

Wall, M.C.; Laidler, K.J.
"The molecular kinetics of the urease-urea system. IV. The reaction in an inert buffer".
Arch. Biochem. Biophys., 43 (1953) 299-306.

Wandrey, C.; Flaschel, E.; Schugerl, K.
"Problems in extrapolation of enzymatic kinetic measurements to reactor design using hog kidney acylase as an example".
Biotechnol. Bioeng., 21 (1979) 1649-1670.

Wiseman, A.
"Stabilisation of Enzymes".
in "Topics in enzyme and fermentation biotechnology", 2 (1978) 280-303.

Last Page of Chapter 6

CHAPTER 7

TWO DIMENSIONAL MODELLING of SOLUTE DISTRIBUTION and ENZYME REACTION in an ULTRAFILTRATION HOLLOW FIBRE

ABSTRACT

A hollow fibre ultrafiltration membrane was modelled in two dimensions by developing and solving equations describing solute convection and diffusion into and out of a differential element of the fibre. Analytical solutions of the axial and radial velocity profiles in a permeating tube permitted solution of the partial differential equations (PDEs) describing the system. The model was developed to describe an enzyme membrane reactor, with three coupled PDEs describing the distribution, rejection and reaction of enzyme, substrate and product. Constant membrane resistance, solute diffusivities and fluid properties were assumed. Flux variations due to the pressure drop down the fibre lumen were considered. A restricted solution of the equations was obtained by the application of an explicit finite difference scheme (discretisation) to the equations which were decoupled by setting the reaction rate to zero. The model describes polarisation of the rejected solute, and predicted an increase in the concentration and thickness of the polarisation layer from the inlet to the outlet of the fibre, in agreement with the work of others. An implicit (Crank-Nicolson) finite difference solution scheme would be needed to solve the equations for a reacting system. Such a solution would be potentially useful in investigating the effect of solute rejection and polarisation on the performance of a membrane reactor.

NOMENCLATURE

Sub and Superscripts

E	Enzyme
i	Component label (superscript), radial mesh label (subscript)
P	Product
r	Radial distance
R	At wall of fibre
S	Substrate
x	Axial distance
X	Dimensionless axial distance
Y	Dimensionless radial distance
0	At entrance of fibre

Symbol	Dimensions	Description
b	-	Ratio of fibre length to radius, = L/R
$\mathbb{B}$	-	Dimensionless lumped parameter in pressure drop equations, $= L\sqrt{\beta}$
$C^i_{X,Y}$	-	Dimensionless concentration of component i at position X,Y, where $C^E = c^E_{X,Y}/c^E_0$; $C^S = c^S_{X,Y}/c^S_0$; $C^P = c^P_{X,Y}/c^S_0$
$c^i_{x,r}$	ML^{-3}	Concentration of component i in fluid element at point x,r
d	-	Ratio of initial radial wall velocity to initial average axial velocity, $= v_{0,R} / \bar{u}_0$
D^i	L^2T^{-1}	Diffusivity of component i
h	-	Dimensionless axial step size in finite difference mesh
k	-	Dimensionless radial step size in finite difference mesh
k_m	-	Dimensionless Michaelis constant, $= K_m/c^S_{0,r}$
k_1	-	Dimensionless inhibition constant, $= K_1/c^S_{0,r}$

K_I	ML^{-3}	Product inhibition constant - kinetic
K_m	ML^{-3}	Michaelis constant - kinetic
L	L	Fibre length
M_F	-	Mass of product per unit mass of substrate reacted
p_x	$ML^{-1}T^{-2}$	Absolute pressure at point x in fibre
p_{perm}	$ML^{-1}T^{-2}$	Absolute pressure in permeate region
P_X	-	Dimensionless pressure at point X in fibre, $= p_x / p_0$
P_{perm}	-	Dimensionless pressure in permeate region, $= p_{perm} / p_0$
Q_x	L^3T^{-1}	Total axial volumetric flowrate at point x in fibre
r	L	Radial distance from centre of fibre
r^I	-	Dimensionless reaction rate, $= R_I R / v_{0,R} c^S_{0,r}$
R	L	Fibre radius
Re	-	Axial Reynolds number, $= 2R\rho\bar{u}_x / \mu$
R_I	$ML^{-3}T^{-1}$	Rate of reaction of component i (+ve is formation)
R_m	$ML^{-2}T^{-1}$	Membrane resistance
$u_{x,r}$	LT^{-1}	Axial velocity in fluid element at point x,r
$\bar{u}_x$	LT^{-1}	Average axial velocity at point x
$U_{X,Y}$	-	Dimensionless axial velocity at point X,Y; $= u_{x,r} / \bar{u}_0$
$\bar{U}_X$	-	Dimensionless average axial velocity at point X, $= \bar{u}_x / \bar{u}_0$
$v_{x,r}$	LT^{-1}	Radial velocity in fluid element at point x,r
V_m	$M(s)M(e)^{-1}T^{-1}$	Maximum reaction rate - kinetic constant
$V_{X,Y}$	-	Dimensionless radial velocity at point X,Y; $= v_{x,r} / v_{0,R}$
x	L	Axial distance along fibre
X	-	Dimensionless axial distance, = x/L
Y	-	Dimensionless radial distance, = r/R

α^1	-	Dimensionless diffusivity of component i, $= D_1/(V_{0,R}\ R)$
β	L^{-2}	Lumped parameter in pressure drop equations, $= 16\mu\ /\ R^3R_m$
γ^1	-	Real rejection of component i (γ=1 total rejection)
λ	-	Radial Reynolds number, $= R\rho v_{x,R}/\ \mu$
μ	$ML^{-1}T^{-1}$	Dynamic viscosity of fluid in fibre
ν	L^2T^{-1}	Kinematic viscosity of fluid in fibre, $= \mu/\rho$
ρ	ML^{-3}	Density of fluid in fibre

INTRODUCTION

Modelling of fluid flow and solute distribution in membrane filtration has received considerable attention in the literature. Many of these models have been based on the existence of boundary layers for mass transfer between the bulk solution and the membrane, the thickness of which is estimated using laminar or turbulent flow mass transfer correlations (Porter and Michaels, 1971). A more complex class of model considers a polarisation layer thickness dependent on the wall concentration gradient, using an osmotic pressure model for the permeation rate (Leung and Probstein, 1979; Clifton et al, 1984; Aimar et al, 1989). Work has also been published on more complete two dimensional descriptions of solute distribution in ultrafiltration, in laminar flow modules where the fluid flows are relatively easy to calculate.

Feasibility of a 'Complete' Description of Laminar Membrane Filtration

In principle, the values of the solute concentration and velocity components at any point in a laminar flow membrane channel can be described by solving the convection/diffusion equations for the channel simultaneously with the momentum (Navier Stokes) equations. In real membrane systems, the convection/diffusion and momentum equations will be coupled, presenting a problem that is very difficult to solve. The momentum equations are dependent on the membrane resistance and the fluid viscosity at the point considered. However the membrane resistance and fluid viscosity are affected by the solute concentration, which is in turn dependent on the velocity components through the phenomenon of concentration polarisation. Solute rejection may also be affected by solute concentration at the membrane surface, which has important implications for the system performance. There are also likely to be time dependent changes of membrane resistance and solute rejection, and these parameters may be different at different points along the membrane channel. A full description of laminar flow membrane filtration is therefore a very complex,

interacting problem requiring a great deal of information on the effects of fouling on membrane resistance and solute rejection.

Practical Modelling of Laminar Flow Membrane Filtration

Practical attempts at modelling by the approach described above have required assumptions in order to simplify the problem. Time dependent changes in membrane resistance and solute rejection are usually ignored, and frequently these properties are assumed invariant with position in the membrane channel. The assumption of constant membrane resistance allows separate solution of the momentum equations (velocity profiles) from the convection/ diffusion equations.

Analytical and numerical solutions for velocity profiles in porous walled ducts are summarised by Belfort and Nagata (1985). For circular ducts, the solution of Yuan and Finkelstein (1956) provides convenient analytical expressions for the axial and radial velocity profiles in the case of relatively low permeation (radial Reynolds number < 1) and constant wall velocity (constant flux). Representation of the velocity profiles as analytical expressions allows the convection/diffusion equations to be solved to give the solute concentration at any point in the membrane channel.

Fig 1. Schematic of Hollow Fibre Showing Differential Element

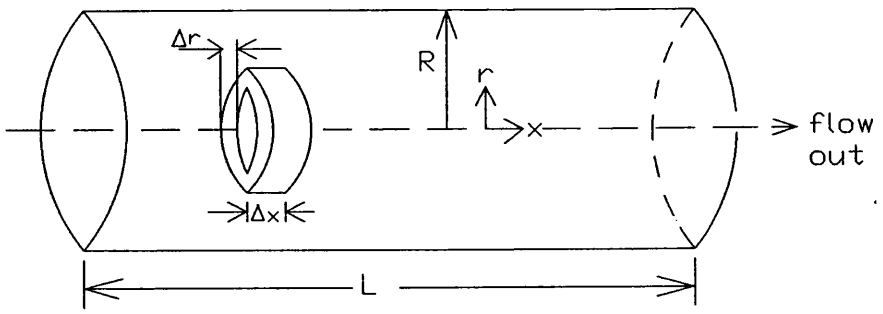

For tubular channels the convection diffusion equation is derived by taking mass balances over a hollow cylindrical element (Fig 1). Solutions based on this approach, usually using analytical velocity profiles, have been presented by several authors, and are summarised below:

Bhattacharyya et al (1990) - reverse osmosis - finite element analysis using the velocity profile equations of Berman (1953) for rectangular channels. The model includes variation of solute diffusivity with concentration and a Bingham plastic viscosity model.

Shah (1971) - reverse osmosis - flat, wide channel, Berman velocity profiles, diffusivity a function of concentration.

Merson and Ginette (1970) - reverse osmosis - power law viscosity model.

Carter and Hasting (1980) - reverse osmosis - rectangular channel with alternating permeable and impermeable sections, Berman velocity profiles.

Kleinstreuer and Belfort (1984) - a general paper on modelling of fluid flow and solute distribution in membrane filtration.

Kleinstreuer and Paller (1983) - ultrafiltration - rectangular channels, velocity profiles after Green (1979), stepwise change in membrane permeability from section to section, flux varies with permeability and wall concentration according to an osmotic pressure model.

The problem of describing fluid flow and solute distribution in membrane channels has thus been tackled for single solutes, although time dependent fouling and variation of membrane properties with position have usually been neglected. An example of a proposed use of such models is for the optimisation of channel length in ultrafiltration (Aimar et al, 1989).

Application to Reaction Systems

A logical extension of the modelling approach described above is its application to a reacting system. A practical example of a permeating channel with reaction is a membrane bioreactor with

enzyme in solution. The distributed parameter approach (in which two dimensional variation in solute concentration is considered) is particularly appropriate in this case because of the likelihood of significant polarisation of enzyme, and possible partial rejection of substrate and/or product. Consideration of the spatial variation of the enzyme, substrate and product will allow these factors to be taken into account. Previous investigations of reaction in permeating channels include:

Shah and Remmen (1971) considered a first order irreversible reaction in a tubular permeating channel, using the velocity profiles of Yuan and Finkelstein (1956) and assuming constant wall velocity (flux) and rejection.

Katoh et al (1978) performed a similar analysis for an enzyme reaction with Michaelis-Menten kinetics in a tubular membrane reactor. The model results were generally found to agree with experimental data. Slightly simplified forms of the convection/diffusion/reaction equations and the velocity profile equations were used.

The work undertaken here was a development of the approaches of Shah and Remmen (1971) and Katoh et al (1978). A product inhibited enzyme reaction in a hollow fibre was modelled, and an approximate consideration of the variation in transmembrane flux due to the pressure drop in the fibre lumen was considered.

A Single Pass Hollow Fibre Enzyme Membrane Reactor Model

The hollow fibre membrane reactor model presented here was based on a finite difference solution of the convection/diffusion/reaction equations for enzyme, substrate and product. Analytical approximations to the axial and radial velocity profiles of Yuan and Finkelstein (1956) were used. It was assumed that the velocity profile equations were applicable to the small channel diameter of a hollow fibre. This should be a valid assumption as the requirement that the fluid behaves as a continuum is still satisfied (channel diameter at least one to two orders of magnitude greater than the molecule size). The model was based on a single hollow fibre, with the inherent assumption that the

situation in all fibres in a membrane module was the same. In practice, this has been shown to be untrue under some circumstances (Park and Chang, 1986).

The small diameter of hollow fibres means that their pressure drop is significant, resulting in a decreasing transmembrane pressure difference with increasing distance down the fibre. The laminar flow pressure drop equation can be integrated with a differential mass balance over an element of the fibre length, assuming a constant membrane resistance. This gives the wall velocity (flux) at any axial position in the fibre (Bruining, 1989). One implication of this approach is that although the analysis is potentially more realistic, the total transmembrane flow becomes a dependent variable, and the transmembrane pressure at the inlet to the fibre is the independent variable. This may necessitate an iterative approach for constant flux systems.

Membrane resistance was assumed constant throughout the fibre, as were fluid viscosity, the solute diffusivities and the reaction parameters. The initial conditions were based on the entrance to the permeating region of the fibre. As the hollow fibre cartridge was constructed by sealing the ends (15mm) of the fibres in epoxy, there was an 'entrance length' of about 30 diameters before the permeating section was reached. The axial velocity profile was therefore assumed to be that for fully developed laminar flow at the entrance of the region to be modelled. The concentration profile was assumed to be flat at the entrance.

Boundary conditions were defined at the wall and the centre of the fibre. The three dimensional hollow fibre was reduced to a two dimensional problem by assuming that the fibre behaved axisymmetrically, i.e. that the conditions were the same at any point with the same axial and radial coordinates. At the wall, the boundary condition was derived by taking a mass balance across the thin separating skin of the membrane, which incorporated the solute rejection coefficients. Diffusive transport across the separating skin was neglected, as was reaction on the surface and

inside the membrane. The assumption of no reaction on the surface was justified by the fact that adsorbed enzyme was likely to be denatured and hence inactive (Chapter 6). At the centre of the fibre, the boundary condition was that the radial velocity was zero, and the concentration and axial velocity gradients (in the radial direction) were zero.

When deriving the equations describing convection, diffusion and reaction of the three solutes, radial convection and diffusion and axial convection into and out of the differential volume element (Fig 1) were considered. Axial diffusion was neglected as axial convection is controlling in crossflow filtration. The reaction rate was assumed to be constant throughout the differential element. A partial differential equation (PDE) was obtained for each of the three solutes (enzyme, substrate and product). The introduction of a reaction term meant that the three PDEs were coupled.

Solution of PDEs can be by implicit or explicit schemes. Implicit schemes require solution of a set of simultaneous equations for each PDE at each axial step, and hence for coupled systems of PDEs the solution becomes much more complicated. Explicit solutions are obtained by discretising the PDEs in one direction, thus obtaining sets of ordinary differential equations (ODEs). The ODEs can then be solved by conventional finite difference methods. Explicit schemes can be applied with little modification to coupled systems of PDEs, but in order to maintain stability, the axial step length is severely restricted by the radial step length, so a very large number of steps may be required. Nevertheless, an explicit scheme was applied in the work reported here.

Use of the Model

A practical enzyme membrane reactor is likely to be of the recycle type, where the outflow from the membrane module is recycled to a continuous stirred tank reactor (CSTR), plug flow reactor (PFR) or, in the simplest case, to the inlet of the membrane module.

Depending on the relative volumes of the different parts of the system and the degree of concentration polarisation of enzyme, the reaction occurring within the membrane module may or may not contribute significantly to the overall reaction rate. In at least one system, the contribution of the membrane module was found to be negligible (Ryu et al, 1972), making a permeation/reaction model unnecessary. If the contribution of the membrane module is significant, the model must consider all the regions in the system. For example, a hollow fibre model as described above might be combined with a CSTR model. Recycle systems will complicate the solution and may require an iterative approach, with the hollow fibre and other models being solved several times.

MODEL DEVELOPMENT

The equations governing the concentrations of the three components (enzyme, substrate and product) at all points in the hollow fibre are derived by considering steady state mass balances over a fluid element (Fig 1) in axial and radial directions:

Radial Convection for Component i:

$$2\pi r\,\Delta x\, v_{x,r}\, c^{1}_{x,r} \quad - \quad 2\pi\,(r+\Delta r)\,\Delta x\, v_{x,(r+\Delta r)}\, c^{1}_{x,(r+\Delta r)}$$

$$\text{(in)} \quad - \quad \text{(out)}$$

$$\therefore \text{(in-out)} \cong \quad -2\pi\,\Delta x\,\Delta r\,\frac{\partial}{\partial r}\left[rvc^{1}\right]_{x,r}$$

Radial Diffusion:

$$-2\pi\,\Delta x\, D^{1}\left[r\frac{\partial c^{1}}{\partial r}\right]_{x,r} \quad - \quad -2\pi\,\Delta x\, D^{1}\left[r\frac{\partial c^{1}}{\partial r}\right]_{x,(r+\Delta r)}$$

$$\therefore \text{(in-out)} \cong \quad 2\pi\,\Delta x\,\Delta r\, D^{1}\,\frac{\partial}{\partial r}\left[r\frac{\partial c^{1}}{\partial r}\right]_{x,r}$$

Axial Convection:

$$2\pi r\,\Delta r\, u_{x,r}\, c^{1}_{x,r} \quad - \quad 2\pi r\,\Delta r\, u_{x+\Delta x,r}\, c^{1}_{x+\Delta x,r}$$

$$\therefore \text{(in-out)} \cong \quad 2\pi r\,\Delta x\,\Delta r\,\frac{\partial}{\partial x}\left[uc^{1}\right]_{x,r}$$

Axial diffusion: assumed negligible compared to axial convection

Reaction: $2\pi r\,\Delta r\,\Delta x\, R_1$

At steady state, the sum of the (in-out) terms together with the reaction equation is zero:

$$D^{1}\frac{\partial}{\partial r}\left[r\frac{\partial c^{1}}{\partial r}\right]_{x,r} - \frac{\partial}{\partial r}\left[rvc^{1}\right]_{x,r} - r\frac{\partial}{\partial x}\left[uc^{1}\right]_{x,r} + rR_1 = 0$$

which can be simplified to give:

$$D^{1}\frac{\partial^{2}c^{1}}{\partial r^{2}} + \frac{D^{1}}{r}\frac{\partial c^{1}}{\delta r} - \frac{\partial}{\partial x}\left[uc^{1}\right] - \frac{\partial}{\partial r}\left[vc^{1}\right] + R_1 = 0 \qquad \ldots 1.$$

Initial conditions: (at the entrance of the fibre)

$x = 0$

$c^1_{0,r} = c^1_0$ for all r.

$v_{0,r}$ = f(r) given by velocity profiles.

$u_{0,r}$ = g(r) given by velocity profiles.

$R_i = h(c^1_0)$ for all components i = 1 to n

Boundary Conditions:

at the centre of the fibre $r = 0$

$$\left.\frac{\partial c^1}{\partial r}\right|_{x,0} = 0 \text{ for all i,x}$$

$$v_{x,0} = 0 \text{ for all x}$$

at the wall of the fibre $r = R$

$$u_{x,R} = 0 \text{ for all x}$$

mass balance over the wall for a short element of axial length Δx:

$$2\pi r\ \Delta x\ v_{x,R}\ c^1_{x,R} - 2\pi r\ \Delta x\ v_{x,R}\ c^1_{x,R}(1-\gamma^1) = 2\pi r\ \Delta x\ D^1\left[\frac{\partial c^1}{\partial r}\right]_{x,R}$$

which simplifies to:

$$v_{x,R}\ c^1_{x,R}\ \gamma_1 = D^1\left[\frac{\partial c^1}{\partial r}\right]_{x,R} \qquad \ldots 2.$$

Reaction rate expression:

Product inhibition enzyme kinetic model:

$$R_S = \frac{V_m c^S c^E}{c^S + K_m\left[1 + \frac{c^P}{K_1}\right]} \qquad \ldots 3.$$

Pressure and Flux Variation Along the Fibre

As hollow fibres are long, thin tubes, the pressure drop from entrance to exit is relatively large. The operating pressure differential between the retentate and permeate of hollow fibre cartridges is low - around 2 bar. Therefore the fibre lumen pressure drop can result in a significant reduction in transmembrane pressure drop from entrance to exit of the fibres.

This effect was considered when developing the hollow fibre model. The pressure drop along the fibre is approximated by the laminar flow pressure drop equation. Assuming a constant membrane resistance, the flux at each point along the fibre is calculated by integrating the pressure drop and mass balance equations (Bruining, 1989). It should be noted that this development assumes a negligible effect of polarisation upon the fluid viscosity. This assumption should be valid for low degrees of polarisation.

Laminar flow pressure drop along the fibre:

$$\frac{\partial p_x}{\partial x} = -\frac{8\mu Q}{\pi R^4} \qquad ...4.$$

A mass balance over a short element of the fibre length gives:

$$\frac{\partial Q_x}{\partial x} = -2\pi R\, v_{x,R} \qquad ...5.$$

Flow through the membrane:

$$v_{x,R} = \frac{p_x - p_{perm}}{R_m} \qquad ...6.$$

Differentiating eq. 4 with respect to x and substituting:

$$\frac{\partial^2 p_x}{\partial x^2} = \frac{16\,\mu}{R^3\, R_m}\left[p_x - p_{perm}\right]$$

Analytical solution for p gives: $\left[\text{setting } \beta = \frac{16\,\mu}{R^3\, R_m}\right]$

$$p_x = \left[\frac{p_0 - p_{perm}}{2} - \frac{4\mu\,\bar{u}_0}{R^2\sqrt{\beta}}\right] e^{x\sqrt{\beta}} + \left[\frac{p_0 - p_{perm}}{2} + \frac{4\mu\,\bar{u}_0}{R^2\sqrt{\beta}}\right] e^{-x\sqrt{\beta}} + p_{perm} \qquad ...7.$$

Substituting for p_x into eqs. 5 and 6 and integrating allows the axial velocity at any point in the fibre to be calculated:

$$\bar{u}_x = \bar{u}_0 - \frac{2}{R\,R_m\sqrt{\beta}}\left[\left[\frac{p_0 - p_{perm}}{2} - \frac{4\mu\,\bar{u}_0}{R^2\sqrt{b}}\right] e^{x\sqrt{\beta}}\right.$$

$$\left. - \left[\frac{p_0 - p_{perm}}{2} + \frac{4\mu\,\bar{u}_0}{R^2\sqrt{\beta}}\right] e^{-x\sqrt{\beta}} + \frac{8\mu\,\bar{u}_0}{R^2\sqrt{\beta}}\right] \quad ...8.$$

The radial velocity at the wall (i.e. the flux) is given by equation 6. Equations 6, 7 and 8 give the fibre lumen pressure, average axial velocity and radial wall velocity (flux) at any position along the fibre.

Velocity Profiles

Yuan and Finkelstein (1956) presented analytical solutions to the Navier Stokes equations for laminar pipe flow with injection or suction through a porous wall. They assumed a constant wall velocity and presented solutions for small radial flow Reynolds numbers (less than 1). The velocity profile equations of Yuan and Finkelstein (1956) have been adapted to take into account the varying transmembrane pressure drop (and hence wall velocity) due to the pressure drop down the fibre lumen.

Axial Velocity Profile: (Yuan and Finkelstein, 1956), $\lambda < 1$

$$\frac{u_{x,r}}{\bar{u}_0} = 2\left[\frac{1}{1 - \frac{\lambda}{18} + \frac{83\,\lambda^2}{5400}} + 2\,\frac{\lambda}{Re}\,\frac{x}{R}\right]\left[1 - Y^2\right.$$

$$+ \frac{\lambda}{36}\left[2 + 9Y^2 - 9Y^4 + 2Y^6\right] +$$

$$\left.\frac{\lambda^2}{10{,}800}\left[166 - 760Y^2 + 825Y^4 - 300Y^6 + 75Y^8 - 6Y^{10}\right]\right] \quad ...9.$$

The maximum value of the radial Reynolds number, λ, in this system has been calculated to be $\cong 3\times10^{-3}$, which means that the assumption of Yuan and Finkelstein (1956) - ($\lambda<1$) remains valid.

The term $1 - \frac{\lambda}{18} + \frac{83\ \lambda^2}{5400}$

is very close to 1 under the conditions applied here, and has been set equal to 1.0 in this model. The term

$1 + 2\frac{\lambda}{Re}\frac{x}{R}$ is then equal to $\frac{\bar{u}_x}{\bar{u}_0}$ and represents the reduction in average axial velocity due to permeation. The second term in the equation represents the variation in the axial velocity as a function of the radial position and the radial Reynolds number. If the equation describing the variation in average axial velocity with axial position (eq. 8) is substituted into eq. 10, the analysis can be adapted to approximate the situation where the wall velocity (flux) varies with axial position.

Radial Velocity Profile: (Yuan and Finkelstein, 1956)

$$v_r = 2v_R Y \left[1 - \frac{Y^2}{2} + \frac{\lambda}{72}\left[-4 + 9Y^2 - 6Y^4 + Y^6\right] + \frac{\lambda^2}{10,800}\left[166 - 760Y^2 + 825Y^4 - 300Y^6 + 75Y^8 - 6Y^{10}\right]\right] \quad ...10.$$

The radial velocity profile presented above will take into account variation of the wall velocity with axial position if the appropriate values of v_R and λ are substituted at each axial position.

The above equations 1 to 10 (plus the boundary and initial conditions) complete a mathematical description of a single pass hollow fibre with chemical reaction and permeation/rejection of enzyme, substrate and product.

Non-Dimensionalisation of the Model Equations

It is desirable to convert the equations to dimensionless form prior to solution. The convection/diffusion equation for enzyme (eq. 1) can be rewritten as:

$$\alpha^E \frac{\partial^2 C^E}{\partial Y^2} + \frac{\alpha^E}{Y}\frac{\partial C^E}{\partial Y} - \frac{1}{db}\frac{\partial}{\partial X}\left[UC^E\right] - \frac{\partial}{\partial Y}\left[VC^E\right] - \frac{VC^E}{Y} = 0 \quad \ldots 11a.$$

and those for the substrate and product can be rewritten:

$$\alpha^1 \frac{\partial^2 C^1}{\partial Y^2} + \frac{\alpha^1}{Y}\frac{\partial C^1}{\partial Y} - \frac{1}{db}\frac{\partial}{\partial X}\left[UC^1\right] - \frac{\partial}{\partial Y}\left[VC^1\right] - \frac{VC^1}{Y} + r^1 = 0 \quad \ldots 11b.$$

The boundary conditions become:

$$\left.\frac{\partial C^1}{\partial Y}\right|_{X,Y=1} = 0 \ldots 12.$$ for all X at the centre of the fibre, and

$$V_{X,Y=1}\, C^1_{X,Y=1}\, \gamma^1 = \alpha^1 \left[\frac{\partial C^1}{\partial Y}\right]_{X,Y=1} \quad \ldots 13.$$ at the wall of the fibre

The reaction equations becomes:

for substrate, $$r^S = - \frac{C^S C^E}{C^S + k_M\left[1 + \frac{C^P}{k_1}\right]} \frac{V_m R\, C^E_0}{V_{0,R}\, C^S_0} \quad ..14a.$$

and for product, $$r^P = - M_F\, r^S \quad ..14b.$$

The pressure and velocity variation equations become:

$$P_X = P_{perm} + \left[\frac{1}{2} - \frac{P_{perm}}{2} - \frac{4\mu\bar{u}_0 L}{R^2 \mathbb{B} p_0}\right] e^{x\mathbb{B}} + \left[\frac{1}{2} - \frac{P_{perm}}{2} + \frac{4\mu\bar{u}_0 L}{R^2 \mathbb{B} p_0}\right] e^{-x\mathbb{B}} \quad \ldots 15.$$

$$\bar{U}_X = 1 - \frac{2p_0 L}{R R_m \mathbb{B} \bar{u}_0}\left[\left[\frac{1}{2} - \frac{P_{perm}}{2} - \frac{4\mu\bar{u}_0 L}{R^2 \mathbb{B} p_0}\right] e^{x\mathbb{B}} - \left[\frac{1}{2} - \frac{P_{perm}}{2} + \frac{4\mu\bar{u}_0 L}{R^2 \mathbb{B} p_0}\right] e^{-x\mathbb{B}} + \frac{8\mu\bar{u}_0 L}{R^2 \mathbb{B} p_0}\right] \quad \ldots 16.$$

The dimensionless wall velocity can be calculated from:

→ 7.17 ←

$$V_{X,Y=1} = \frac{\left[P_X - P_{perm}\right] p_0}{R_m V_{0,R}} \quad ...17.$$

In dimensionless form the axial velocity profile is given by:

$$\bar{U}_{X,Y} = 2\bar{U}_X \left[1 - Y^2 + \frac{\lambda}{36}\left[-2 + 9Y^2 - 9Y^4 + 2Y^6\right] + \frac{\lambda^2}{10,800}\left[166 - 760Y^2 + 825Y^4 - 300Y^6 + 75Y^8 - 6Y^{10}\right]\right] ...18.$$

and the radial velocity profile becomes:

$$V_{X,Y} = 2V_{X,Y=1}Y\left[1 - \frac{Y^2}{2} + \frac{\lambda}{72}\left[-4 + 9Y^2 - 6Y^4 + Y^6\right] + \frac{\lambda^2}{10,800}\left[166 - 380Y^2 + 275Y^4 - 75Y^6 + 15Y^8 - Y^{10}\right]\right] ...19.$$

These equations complete the dimensionless description of the system.

Solution of the Equations

The model development gives three parabolic partial differential equations (PDEs), one each for enzyme, substrate and product. Partial differential equations are obtained because the system is described in both axial and radial directions. The three PDEs must be solved simultaneously to describe the concentrations of the three components at any point in the fibre, as a function of the fibre geometry, flowrates, and physical and kinetic parameters. Parabolic PDEs may be solved by an explicit method (discretisation) or by an implicit method (e.g. Crank-Nicolson (1947); Smith, 1985). Here, the explicit method has been adopted initially as it is simpler to program. However, explicit methods have inherent disadvantages which are discussed later.

The Discretisation Method of Solution

The PDEs describe a continuous variation of the concentrations of the three components in the axial and radial directions. In this

method of solution, the PDEs are 'discretised' in one direction (in this case in the radial direction) so that the variation in that direction is approximated at discrete mesh points (Fig 2). In this way a PDE is represented by an ordinary differential equation (ODE) at each of the mesh points. In this case, there are three sets of ODEs describing changes in the axial direction, one for each component.

It should be noted that there is a serious drawback to the discretisation method. The axial step must be small because the stability criterion for this method of solution states that:
$h \leq 0.5\ k^2$, where h is the axial step length and k is the radial step length.

Derivatives in the radial direction are written as finite difference approximations using central difference formulae:

$$\left.\frac{\partial C}{\partial Y}\right|_i \cong \frac{C_{i+1} - C_{i-1}}{2k} \quad ; \quad \left.\frac{\partial^2 C}{\partial Y^2}\right|_i \cong \frac{C_{i+1} - 2C_i + C_{i-1}}{k^2}$$

where the subscripts denote the mesh point in the radial direction:

Fig 2. Mesh for Finite Difference Solution of Model Equations

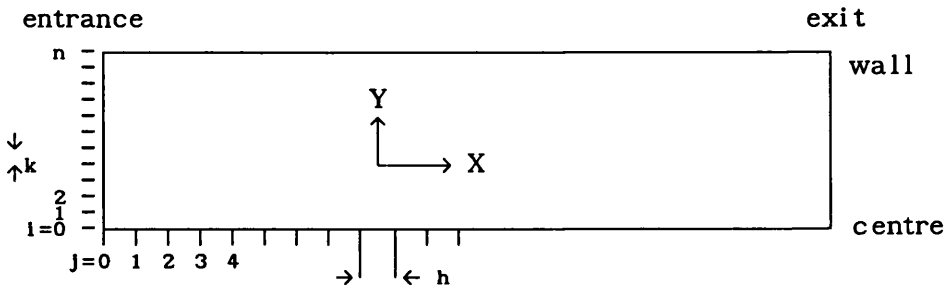

The set of equations representing the variation in the concentrations of the three components in the axial direction at each of the radial mesh points can be written as:

$$\left.\frac{dC^J}{dX}\right|_1 = \frac{db}{U_1}\left[\alpha^J \left.\frac{d^2C^J}{dY^2}\right|_1 + \frac{\alpha^J}{Y_1}\left.\frac{dC^J}{dY}\right|_1 - V_1 \left.\frac{dC^J}{dY}\right|_1 - C_1^J\left[\frac{1}{db}\left.\frac{dU}{dX}\right|_1 + \left.\frac{dV}{dY}\right|_1 + \frac{V_1}{Y_1}\right] + r_1^J\right]$$

where the superscript j (=0 to 2) represents the component and the subscript i (=1 to n-1) represents the radial mesh point.

Introducing finite difference approximations:

$$\left.\frac{dC^J}{dX}\right|_1 = \frac{db}{U_1}\left[\alpha^J\left[\frac{C_{1+1}^J - 2C_1^J + C_{1-1}^J}{k^2}\right] + \left[\frac{\alpha^J}{Y_1} - V_1\right]\left[\frac{C_{1+1}^J - C_{1-1}^J}{2k}\right] - C_1^J\left[\frac{1}{db}\left.\frac{dU}{dX}\right|_1 + \left.\frac{dV}{dY}\right|_1 + \frac{V_1}{Y_1}\right] + r_1^J\right] \quad \ldots 20.$$

The boundary conditions are approximated by finite difference as follows:

At the centre of the fibre, a backward difference approximation to eq. 12 gives:

$$C_{1=0}^J \cong C_{1-1}^J \quad \ldots 21.$$

which allows the centre concentrations to be estimated from the adjacent values.

At the wall of the fibre, a forward difference approximation to eq. 13 gives:

$$C_{1=n}^J = \frac{C_{1=n-1}^J \alpha^J}{\alpha^J - V_{Y=1}\gamma^J k} \quad \ldots 22.$$

which allows the wall concentration to be estimated from the adjacent value.

Derivatives of the Velocity Profiles

These must be calculated at each mesh point. From the dimensionless velocity profile equations 18 and 19, the following are obtained:

$$\frac{dU_{X,Y}}{dX} = -4\,V_{X,Y=1}db\left[1 - Y^2 + \frac{\lambda}{36}\left[-2 + 9Y^2 - 9Y^4 + 2Y^6\right] + \frac{\lambda^2}{10,800}\left[166 - 760Y^2 + 825Y^4 - 300Y^6 + 75Y^8 - 6Y^{10}\right]\right] \quad \ldots 23.$$

$$\frac{dV_{X,Y}}{dY} = 2\,V_{X,Y=1}\left[1 - \frac{3Y^2}{2} + \frac{\lambda}{72}\left[-4 + 27Y^2 - 30Y^4 + 7Y^6\right] + \frac{\lambda^2}{10,800}\left[166 - 1140Y^2 + 1375Y^4 - 525Y^6 + 135Y^8 - 11Y^{10}\right]\right] \quad \ldots 24.$$

Solution of the ODEs

The set of ODEs represented by eq. 20 must be solved for each mesh point along the fibre in the axial direction. Many numerical methods are available for solving sets of ODEs. The Backward Euler method has been used here. The derivative is approximated implicitly and solved iteratively, such that:

$$\left.\frac{dC}{dX}\right|_j \cong \frac{C_j - C_{j-1}}{h}$$

where the subscript j represents the axial mesh point. The Backward Euler method was found to give the same results at the same step lengths as a 4^{th} order Runge-Kutta method, but was considerably faster.

Solution of the Model Equations

The finite difference method of solving the non dimensional model equations set out above was solved using a computer. The initial programming was carried out in Borland 'Turbo Basic' on an IBM PC clone with a maths co-processor. Subsequently the program was transferred in Fortran to a Gould mainframe computer. The

solution algorithm is outlined in the following flowcharts:

Fig 3. Algorithm for Solution of the Model

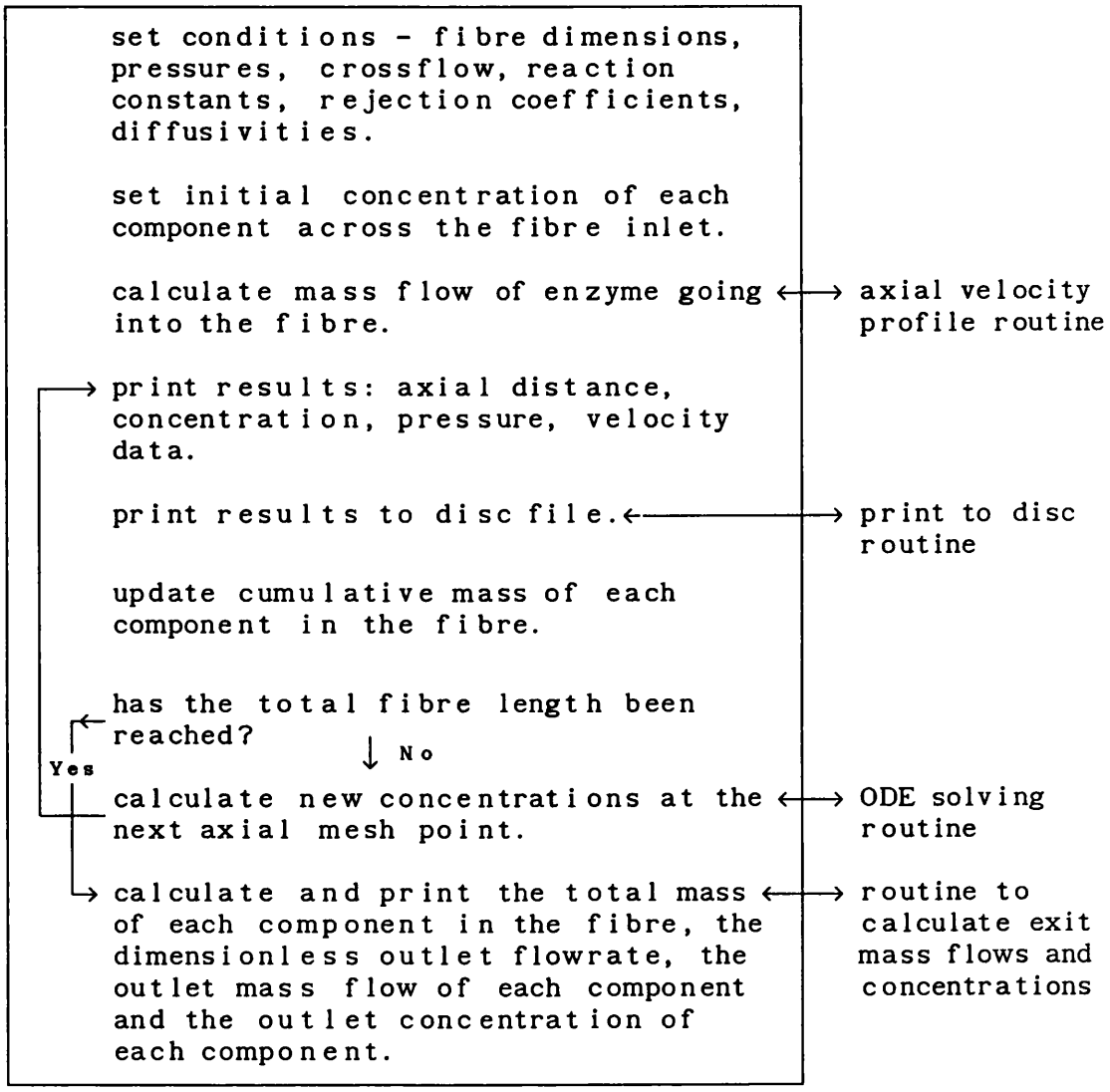

Fig 4. Flowchart Showing Structure of Subroutines

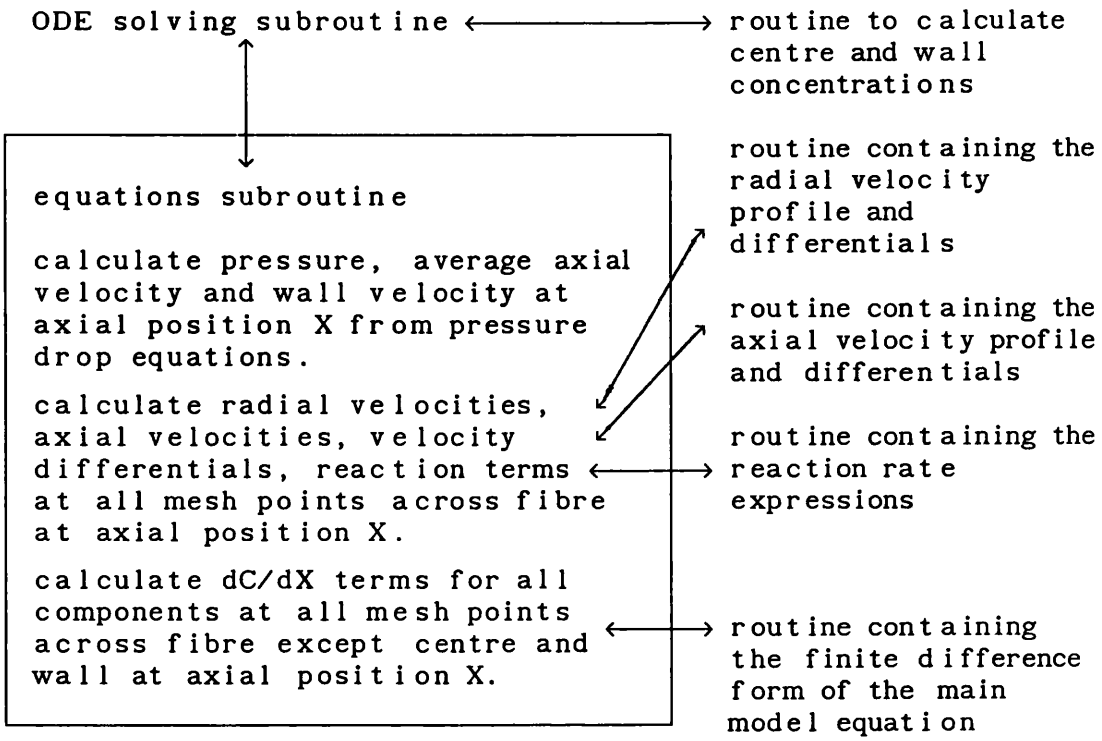

RESULTS and DISCUSSION

The two dimensional hollow fibre model was solved using an explicit finite difference scheme produced by discretising the partial differential equations (PDEs) in the radial direction. The number of ordinary differential equations (ODEs) to be solved for each component was equal to the number of mesh points in the radial direction. The results were calculated in the form of solute concentrations at each radial mesh point. As the solution advanced down the fibre, new sets of solute concentrations were calculated at each axial mesh point. In this way the two dimensional description of the hollow fibre was expressed in terms of a grid, where the solute concentrations were calculated at each node (Fig 5 shows results corresponding to the model parameters described in Table 1).

Table 1. Model Parameters for Example Plot

model run with zero reaction rate so that problem is reduced to enzyme polarisation		
Parameter	Value	Units
fibre radius	2.5×10^{-4}	m
fibre length	0.16	m
inlet pressure (abs)	1.38×10^{5}	$N.m^{-2}$
permeate pressure (abs)	1.01×10^{5}	$N.m^{-2}$
membrane resistance	0.0175	$Ns.m^{-3}$
average inlet velocity	0.1131	$m.s^{-1}$
rejection - enzyme	1.0	-
substrate	0.0	-
product	0.0	-
kinematic viscosity	1.0×10^{-6}	$m^2.s^{-1}$
enzyme diffusivity	3.46×10^{-11}	$m^2.s^{-1}$
number of radial steps	90	-
number of axial steps	200	-

As a first step, the problem was simplified by setting the rate term in the reaction equation (Eq 14a) to zero, implying no reaction. This reduced the problem to one of calculation of the concentration profiles for enzyme, in this case assuming total rejection of enzyme and no rejection of substrate and product. The calculated concentration of substrate and product at all the

points in the fibre served as a check on the accuracy of the solution; the dimensionless substrate concentration must remain equal to one (i.e. no change in substrate concentration) and the dimensionless product concentration must remain equal to zero (i.e. no product formed under zero rate conditions).

Table 2. Summary of Model Output for the Parameters Shown in Table 1. Includes Variations in Pressure, Axial Velocity and Wall Velocity

X	Dimensionless Enzyme Concentrations at X, Y=						Press	Axial Vel	Wall Vel
	.000	.956	.967	.978	.989	1.00	P_X	$\bar{U}_X$	$V_{X,Y=1}$
0.00	1.00	1.00	1.00	1.00	1.00	1.00	1.000	1.000	1.000
0.05	1.00	1.00	1.02	1.10	1.35	1.80	0.999	0.999	0.997
0.10	1.00	1.01	1.07	1.23	1.56	2.08	0.998	0.998	0.994
0.15	1.00	1.04	1.13	1.34	1.73	2.31	0.998	0.997	0.991
0.25	1.00	1.10	1.25	1.54	2.01	2.68	0.996	0.994	0.985
0.50	1.00	1.28	1.54	1.97	2.59	3.42	0.992	0.988	0.969
0.75	1.00	1.46	1.81	2.33	3.07	4.04	0.988	0.983	0.953
1.00	1.00	1.64	2.06	2.67	3.50	4.58	0.983	0.977	0.938

Table 3. Summary of Model Output for Conditions of Lower Flux

Parameters as Table 1 except inlet press = 1.083×10^5 $N.m^{-2}$									
X	Dimensionless Enzyme Concentrations at X, Y=						Press	Axial Vel	Wall Vel
	.000	.956	.967	.978	.989	1.00	P_X	$\bar{U}_X$	$V_{X,Y=1}$
0.00	1.00	1.00	1.00	1.00	1.00	1.00	1.000	1.000	1.000
0.05	1.00	1.00	1.00	1.02	1.05	1.10	0.999	1.000	0.985
0.10	1.00	1.00	1.01	1.04	1.08	1.13	0.998	1.000	0.968
0.15	1.00	1.01	1.02	1.05	1.10	1.15	0.997	0.999	0.951
0.25	1.00	1.02	1.04	1.08	1.12	1.17	0.995	0.999	0.918
0.50	1.00	1.04	1.07	1.11	1.16	1.20	0.989	0.998	0.834
0.75	1.00	1.07	1.10	1.13	1.18	1.22	0.984	0.997	0.750
1.00	1.00	1.08	1.11	1.15	1.18	1.22	0.979	0.996	0.666

Additional checks were carried out on this non reacting form of the model, to verify the solution. As the enzyme was assumed to be totally rejected, the mass flowrate of enzyme leaving the fibre should have been equal to that entering the fibre. The exit mass flowrate of enzyme was calculated by numerical integration of the

concentration and velocity profiles at the fibre exit, based on annuli at each of the radial mesh points. The comparison between inlet and exit mass flows of enzyme was used to assess the accuracy of the calculation. Agreement to within 1% was deemed acceptable.

Fig 5. Example Model Results for Protein Polarisation

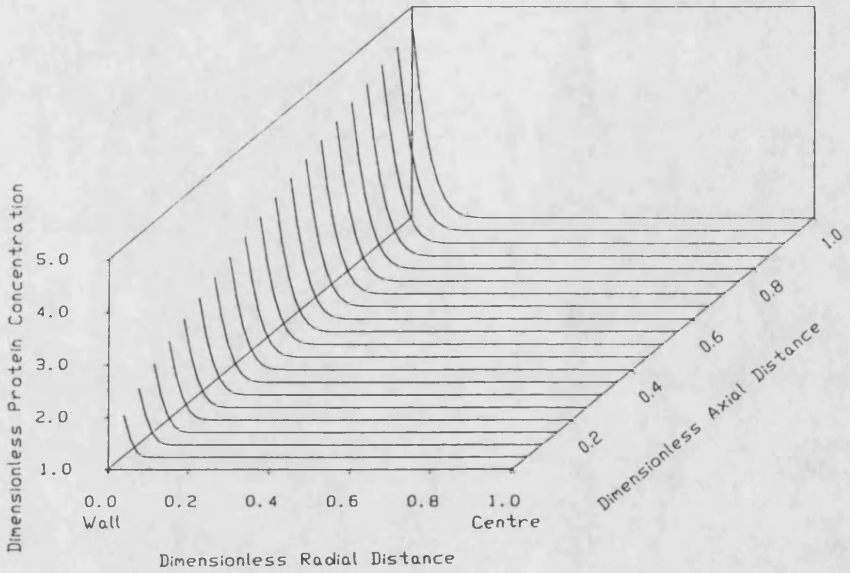

The number of radial steps was found to strongly influence the accuracy of the solution. A large number of steps were required in order to satisfy the mass balance mentioned above. Unfortunately, reduction of the radial step size required a corresponding reduction in the axial step size, according to the stability criterion $h \leq 0.5k^2$. Improvement in the accuracy of the solution by reduction of the radial step size therefore carried a severe penalty in the form of the number of calculations required and the associated rounding errors.

The results for the non reacting system (Fig 5) showed a gradual development of the concentration polarisation from the inlet to the exit of the fibre, a phenomenon which has been predicted by others for crossflow membrane filtration (Aimar et al, 1989). This has implications for the design of membrane systems, in that shorter channels will result in lower overall polarisation, producing greater fluxes and possibly reducing fouling due to lower wall concentrations. Prediction of wall concentrations by

this type of model may allow correlation of wall concentration with fouling effects.

The present work was not extended to investigation of a reacting system. 'Turning on' the reaction by setting V_m to a non zero value gave a less stable system of equations. Reduction of the step sizes in an attempt to obtain a solution resulted in unacceptably large requirements for computer time, even when using a mainframe.

Implicit methods of solution of PDEs such as the Crank-Nicolson (1947) method are not subject to the same stability restrictions as the explicit method used here, so small radial steps can be used to cope with steep radial concentration gradients, without reducing the axial step size too severely. The Crank-Nicolson method is based on approximating derivatives in the axial and radial directions by central difference around a point halfway between two mesh points (Smith, 1985). This approach tends to reduce the errors introduced by the approximations, but requires solution of a set of $\mathbb{N}$ simultaneous equations at each axial step (where $\mathbb{N}$ is the number of internal radial mesh points). The Crank-Nicolson method is computationally more complex than the explicit method used here, especially when there is a set of coupled PDEs. However, it seems that in order to proceed with this work an implicit solution method such as Crank-Nicolson must be adopted. It might be possible to reduce the amount of computation by introducing a variable step size in the radial (and possibly axial) direction. Small steps would be used near the wall where concentration changes steeply with radius, and larger steps would be used near the centre of the fibre where the concentration profile is quite flat.

This type of modelling of crossflow membrane filtration is computationally intensive, and requires considerable effort for model development and solution. So far, time dependent fouling has not been included in this type of model, not only because of complexity of solution, but also due to the lack of predictive

models for such effects. The use of two dimensional models such as those discussed here for predicting the behaviour of ultrafiltration systems is therefore limited, as time dependent fouling effects often control the system performance. However, extension of two dimensional models to reacting systems may be of greater use, as membrane reactors may be more strongly affected by solute rejection and polarisation than by changes in membrane resistance. Two dimensional modelling could allow a qualitative investigation of the effect of these phenomena, promoting a greater understanding of the operation of membrane reactors. Inaccuracies due to failure to incorporate time or position dependent variations in membrane properties may be less significant for qualitative investigations of membrane reactors.

CONCLUSIONS

It was possible to model two dimensional solute distribution in a hollow fibre membrane by developing and solving equations describing convective and diffusive mass transport into and out of a differential element of the fibre. In order to solve the equations, solutions developed by other workers for the velocity profiles in a permeating channel were used.

For a rejected macromolecular solute, the model described a developing concentration polarisation region from entrance to exit of the fibre, suggesting that polarisation and associated fouling problems may be reduced by using shorter membrane channels.

It was necessary to assume constant membrane resistance, both with position and time, in order to solve the model. This reduced the relevance of the model, as fouling is often the controlling factor in membrane performance. In the light of these limitations it seems that for *polarisation* studies, the cost of the above modelling approach in both development and computer time, is large compared to the benefits.

The convection diffusion model was adapted by including reaction terms so that an enzyme membrane reactor was represented. The solution of such a model was more complex than for the non reacting case as a system of coupled partial differential equations (PDEs) had to be solved, as opposed to uncoupled PDEs for non interacting solutes.

An explicit solution scheme was used to solve coupled systems of PDEs with relatively little additional complication. However the explicit approach suffered from stability restrictions and was not capable of solving the coupled equations describing the enzyme membrane reactor. It would be necessary to use an implicit scheme such as the Crank-Nicolson method for the reacting system.

The convection/diffusion/reaction model for a membrane channel

could be a potentially valuable tool for studying enzyme membrane reactors, because if solved the model would be capable of describing the effects of solute rejection and polarisation which are likely to be important in determining reactor performance.

REFERENCES

Aimar, P.; Howell, J.A.; Turner, M.
"Effects of concentration boundary layer development on the flux limitations in ultrafiltration".
Chem. Eng. Res. Des., 67 (1989) 255-261.

Berman, A.S.
"Laminar flow in channels with porous walls".
J. Appl. Phys., 24 (1953) 1232-1235.

Bhattacharyya, D.; Back, S.L.; Kermode, R.I.; Roco, M.
"Prediction of concentration polarisation and flux behaviour in reverse osmosis by numerical analysis".
J. Membr. Sci., 48 (1990) 231-262.

Belfort, G.; Nagata, N.
"Fluid mechanics and cross-flow filtration: Some thoughts".
Desalination, 53 (1985) 57-79.

Bruining, W.J.
"A general description of flows and pressures in hollow fiber membrane modules".
Chem. Eng. Sci., 44 (1989) 1441-1447.

Carter, J.W.; Hasting, A.P.M.
"The reduction of concentration polarisation by the use of impermeable or fully permeable membrane sections".
IChemE North Western Branch Papers, No 4 (1980) 6.1-6.18.

Clifton, M.J.; Abidine, N.; Aptel, P.; Sanchez, V.
"Growth of the polarization layer in ultrafiltration with hollow-fibre membranes".
J. Membr. Sci., 21 (1984) 233-246.

Crank, J.; Nicolson, P.
"A practical method for numerical evaluation of solutions of partial differential equations of the heat conduction type".
Proc. Camb. Phil. Soc., 43 (1947) 50-67.

Green, G.A.
"Laminar flow through a channel with one porous wall".
Course Project in Adv. F. M., Dept. Chem. and Env. Eng., RPI, Troy, NY (1979).

Katoh, S.; Yanagida, T.; Sada, E.
"Performance of a membrane-type enzyme reactor utilizing ultrafiltration".
J. Chem. Eng. Japan, 11 (1978) 143-146.

Kleinstreuer, C.; Belfort, G.
"Mathematical modeling of fluid flow and solute distribution in pressure driven membrane modules".
Synthetic Membrane Processes - Fundamentals and Water Applications, ed. Belfort, G., Academic, Orlando, (1984).

Kleinstreuer, C.; Paller, M.S.
"Laminar dilute suspension flows in plate-and-frame ultrafiltration units".
AIChE J., 29 (1983) 529-533.

Leung, W-F.; Probstein, R.F.
"Low polarization in laminar ultrafiltration of macromolecular solutions".
Ind. Eng. Chem. Fundam., 18 (1979) 274-278.

Merson, R.L.; Ginette, L.F.
"Improved processing of foods by reverse osmosis".
Applied Polymer Symp., 13 (1970) 309-322.

Park, J.K.; Chang, H.N.
"Flow distribution in the fiber lumen side of a hollow fiber module".
AIChE J., 32 (1986) 1937-1947.

Porter, M.C.; Michaels, A.S.
"Membrane ultrafiltration".
Chem. Technol., 1971, 258-254.

Ryu, D.Y.; Bruno, C.F.; Lee, B.K.; Venkatasubramanian, K.
"Microbial penicillin amidohydrolase and the performance of a continuous enzyme reactor system".
Proc. IFS: Ferment. Technol. Today (1972) 307-314.

Shah, Y.T.
"Mass transport in reverse osmosis in case of variable diffusivity".
Int. J. Heat Mass Transfer, 14 (1971) 921-930.

Shah, Y.T.; Remmen, T.
"Radial mass transfer effects in a porous wall tubular reactor".
Int. J. Heat Mass Transfer, 14 (1971) 2109-2124.

Smith, G.D.
"Numerical solution of partial differential equations: Finite difference methods".
3ed, Clarendon Press, Oxford (1985).

Yuan, S.W.; Finkelstein, A.B.
"Laminar pipe flow with injection and suction through a porous wall".
Trans. A.S.M.E., 78 (1956) 719-724.

APPENDIX to CHAPTER 7

Listing of the Turbo Basic computer program to solve the two dimensional membrane reactor model using an explicit (discretisation) method.

```
'hollow fibre reactor model, Neil Sanders 18th Aug 1989
'accounts for pressure variation along fibre
'parameters representative of large fibre deposition experiments


'double precision all variables
      defdbl a-z
      cls
      n=1000
      dim  y0(n),  y(n),  y1(n),  y2(n),  d(n),  d1(n),  a(3),  u(n),
           du(n), v(n), dv(n), r(n),g(3)
      dim  k1(n),  k2(n),  k3(n),  k4(n),  c0(3),  mass(3),  ci(3),  co(3),
           mfo(3)
      dim c(3), newc(3)

'fibre radius, cm
      rr=0.025
'fibre length, cm
      l=16.0
'plug flow reactor volume, cm^3
      vol=58
'area for flow, cm^2
      area=4*atn(1)*rr^2*1000
'inlet pressure (absolute), mg/cm.s^2
      pi=1.379e9                          '20*6895*1e4
'permeate pressure (absolute), mg/cm.s^2
      pperm=14.7*6895*1e4
'membrane resistance, mg/s.cm^2
      rm=1.75e12
'calculate initial wall velocity, cm/s
      vwi=(pi-pperm)/rm
      print "vwi="vwi
'calculate dimensionless permeate pressure
      pp=pperm/pi
'inlet velocity, cm/s
      uav0=11.31
'rejection coefficients
      g(0)=1.0
      g(1)=0.0
      g(2)=0.0
'kinematic viscosity, cm^2/s
      visc=1.0e-2
'dynamic viscosity, mg/cm.s
      dvisc=visc*1e3
'dimensionless constants for pressure - crossflow equations
      bb=l*(16*dvisc/(rm*rr^3))^0.5
      dd=4*dvisc*uav0*l/(pi*bb*rr^2)
      e=2*pi*l/(uav0*rr*rm*bb)
'initial concentrations, mg/cm3
      ci(0)=0.144                         'enzyme
      ci(1)=15.0                          'substrate
      ci(2)=0.0                           'product
'diffusivities, cm2/s
      de=3.46e-7
      ds=1.37e-5
      dp=2.0e-5
```

```
'kinetic parameters
      km=0.03                                  'mg(s)/cm3
      ki=0.094                                 'mg(p)/cm3
      vm=0.089                                 'mg(s)/mg(e).s
'mass correction factor, mg product per mg substrate
      mf=0.5667
'wall / axial velocity factor
      d=vwi/uav0
'length / radius factor
      b=l/rr
'number of divisions across fibre*3
      nn=180
'calc nondimensional reaction parameters
      vmn=0 'vm*rr*ci(0)/(vwi*ci(1))
      kmn=km/ci(1)
      kin=ki/ci(1)
'calc nondimensional diffusivities
      a(0)=de/(vwi*rr)
      a(1)=ds/(vwi*rr)
      a(2)=dp/(vwi*rr)
'calc mesh interval across fibre
      kk=3/nn
'initialise at x=0
      x=0
      vw=1
      ux=1
      for i=3 to nn+3 step 3
            y0(i)=1
            y0(i+1)=1
            y0(i+2)=0
      'set up radial grid
            y(i)=(i-3)*kk/3
      next i
'calc mass flow of enzyme into fibre
      tmfi=0
      qi=0
      'velocities across fibre
      for i=3 to nn+3 step 3
            gosub axial
      next i
      for i=3 to nn step 3
      qi=qi+(y(i+3)^2-y(i)^2)*(u(i+3)+u(i))/2
      'mass flow of enzyme
      mfi=((u(i)+u(i+3))/2)*((y0(i)+y0(i+3))/2)*(y(i+3)^2-y(i)^2)
      tmfi=tmfi+mfi
      next i
      ci=tmfi/ux
      print "vol. flow in ="qi
      print "enzyme flow in ="tmfi
      print "enzyme conc. in ="ci
'integration step length
      h=0.005
'print step size and number of discretization points
      print "step="h, "nn="nn
'print column headings
      print"     X";"        CENTRE";"     WALL";"      PRESS";
```

```
      "       FLOW";"       PERM"
'set interval for writing to file
      c=1/(100*h)
'set axial distance counter
      count=-1
      dcount=1
'integrate!
      j=0
'print heading to disc file
      chop=len(str$(dcount))-1
      n$="c:dat"+right$(str$(dcount),chop)+".prn"
      open n$ for output as #1
      print #1, 31
      print #1, x
      for i = 3 to nn+3 step 3
            print #1, 1-(i-3)*kk/3, y0(i+j)
      next i
      close #1
200   j=0
'print data to screen
      count=count+1
      if count < 10 then 201
      print using "##.###^^^^";x,y0(3+j),y0(nn+3+j),p,ux,vw
      count=0
      dcount=dcount+1
'print data to disc file
      chop=len(str$(dcount))-1
      n$="c:dat"+right$(str$(dcount),chop)+".prn"
      open n$ for output as #1
      print #1, 31
      print #1, x
      for i = 3 to nn+3 step 3
            print #1, 1-(i-3)*kk/3, y0(i+j)
      next i
      close #1
201   'calculation of total mass of components in fibre
      for j=0 to 2
            stepmass=0
            for i=3 to nn step 3
                  stepmass=stepmass+(y(i+3)^2-y(i)^2)*(y0(i+3+j)
                        +y0(i+j))/2
            next i
            mass(j)=mass(j)+stepmass*4*atn(1)*rr^2*1*ci(j)*h*1000
      next j
      m=m+1
      if x >= 1.0  goto 100
      gosub rungekut
      goto 200

100   'on completion of calculations along the fibre
'output total mass of components in fibre
      for j=0 to 2
            print
            print"Mass"j"in Fibre is"mass(j)"mg"
      next j
'calculate dimensionless outlet vol. flowrate
```

```
      qo=0
      for i=3 to nn step 3
            qo=qo+(y(i+3)^2-y(i)^2)*(u(i+3)+u(i))/2
      next i
      print
      print "Vol. flow out ="qo
      print
      gosub excond
      end

excond:   'calc fibre exit conditions
      print"Fibre Exit Conditions"
      print
'calculate dimensionless exit mass flows and concentrations
      for j=0 to 2
            mfo(j)=0
            for i=3 to nn step 3
                  mfo(j)=mfo(j)+(y(i+3)^2-y(i)^2)*(u(i+3)+u(i))
                        *(y0(i+3+j)+y0(i+j))/4
            next i
            co(j)=mfo(j)/ux
            print"Mass Flow"j"="mfo(j);"Conc"j"="co(j)
            print
      next j
      return

eqns:'the differential equations - not including centre or wall
'calculate pressure and average crossflow velocity at x
      p=(0.5-pp/2-dd)*exp(x*bb)+(0.5-pp/2+dd)*exp(-x*bb)+pp
      ux=1-e*((0.5-pp/2-dd)*exp(x*bb)-(0.5-pp/2+dd)*exp(-x*bb)
            +2*dd)
'calculate wall velocity at x
      vw=(p-pp)*pi/(vwi*rm)
      for i=6 to nn step 3
      'calculate radial velocity profile and differentials
            gosub radial
      'evaluate reaction terms
            gosub reaction
      'calculate axial velocity profile
            gosub axial
      'evaluate  concentration differentials
            gosub model
      next i
      return

model:    'mass balance equations
      for j=0 to 2
            d(i+j)=(a(j)/kk^2)*(y0(i+j-3)-2*y0(i+j)+y0(i+j+3))
            d(i+j)=d(i+j)-y0(i+j)*((v(i)/y(i))+dv(i)+(du(i)/(d*b)))
            d(i+j)=d(i+j)-((v(i)-(a(j)/y(i)))/(2*kk))
                  *(y0(i+j+3)-y0(i+j-3))
            d(i+j)=d(i+j)+r(i+j)
            d(i+j)=d(i+j)*d*b/u(i)
      next j
      return
```

```
reaction:  'reaction terms for the three components
      r(i)=0
      r(i+1)=-vmn*y0(i)*y0(i+1)/(y0(i+1)+kmn*(1+(y0(i+2)/kin)))
      r(i+2)=-mf*r(i+1)
      return

radial:     'radial velocity profile and differential
      rer=vw*vwi*rr/visc
      v(i)=1-((y(i)^2)/2)-(rer/72)*(-4+9*y(i)^2-6*y(i)^4+y(i)^6)
      v(i)=v(i)+(rer^2/10800)*(166-380*y(i)^2+275*y(i)^4-75*y(i)^6+
           15*y(i)^8-y(i)^10)
      v(i)=v(i)*2*vw*y(i)
      dv1=2-3*y(i)^2
      dv2=(rer/72)*(-8+54*y(i)^2-60*y(i)^4+14*y(i)^6)
      dv3=(rer^2/10800)*(332-2280*y(i)^2+2750*y(i)^4-1050*y(i)^6+27
           0*y(i)^8-22*y(i)^10)
      dv(i)=vw*(dv1-dv2+dv3)
      return

axial:      'axial velocity profile and differential
      rer=vw*vwi*rr/visc
      u2=1-(y(i)^2)-(rer/36)*(-2+(9*y(i)^2)-(9*y(i)^4)+(2*y(i)^6))
      u3=((rer^2)/10800)*(166-(760*y(i)^2)+(825*y(i)^4)-(300*y(i)^6
           )+(75*y(i)^8)-(6*y(i)^10))
      u(i)=2*ux*(u2+u3)
      du(i)=-4*vw*d*b*(u2+u3)
      return

rungekut:

      'this subroutine integrates the equations using backward
      'euler with Newton-Raphson convergence acceleration.
      for ii=6 to nn+2
           y1(ii)=y0(ii)
      next ii
      do
           ytest=y1(6)
           gosub eqns
           for ii=6 to nn+2
                d1(ii)=(d(ii)-d1(ii))
                y2(ii)=y1(ii)-(1/(1-h*d1(ii)))*(y1(ii)-y0(ii)
                     -h*d(ii))
                y1(ii)=y2(ii)
           next ii
      loop until abs((ytest-y1(6))/y1(6))<=1e-6
      for ii=6 to nn+2
           y0(ii)=y1(ii)
           d1(ii)=d(ii)
      next ii
      x=x+h
      gosub centrewall
      return

centrewall:      'estimates new centre and wall concentrations
                 'from updated adjacent values
      for j=0 to 2
```

```
      y0(3+j)=y0(6+j)
      y0(nn+3+j)=y0(nn+j)*a(j)/(a(j)-(kk*g(j)*vw))
next j
return
```

CHAPTER 8

CONCLUSIONS - IMPLICATIONS for the OPERATION of an ENZYME MEMBRANE REACTOR

The use of membrane filtration as a downstream processing step in biotransformations can sometimes be eliminated by including the membrane in the reactor system, allowing operation as a combined reactor/separator. Although membranes may be used as novel supports for immobilised enzymes in catalysis, the use of dissolved enzymes in membrane reactors avoids the cost of chemical immobilisation, and this type of reactor has been used successfully for industrially important reactions (Leuchtenberger et al, 1983). Work describing the application of results of membrane separation research to modelling and prediction of membrane reactor performance is rather limited.

The aim of the experimental study presented in this thesis was to carry out a systematic investigation of some of the aspects of membrane separation which significantly influence the performance of an enzyme membrane reactor. In the reactor configuration chosen, a dissolved enzyme preparation was retained in a reactor by an appropriate semipermeable membrane. Solvent was forced through the membrane convectively, carrying with it the dissolved product. The reactor was expected to show performance changes resulting from a number of phenomena known to occur during membrane filtration, namely:

(a) Changes in fouling (adsorbed protein).
(b) Changes in rejection of solutes.
(c) Concentration polarisation of solutes.

The aim was to quantify these effects in isolation (where possible) and then to assess systematically their contribution to the observed reactor performance using a model enzyme system.

The constant flux ultrafiltration apparatus (Turker and Hubble,

1987) was used to study the phenomena of protein adsorption and polarisation in isolation. The use of constant flux (c.f. constant pressure) eliminated the effect of time dependent changes in membrane resistance on the degree of polarisation. The studies of adsorption and polarisation were followed by an investigation of their effects on solute rejection. The fouling studies were then related to reactor performance by using the constant flux apparatus as a membrane reactor.

Adsorption

The constant flux ultrafiltration apparatus was used at zero feedrate so that there was no net transmembrane flux. Under these conditions, there was no polarisation and so the protein (BSA) concentration at the membrane surface was equal to the bulk concentration. The amount of membrane associated protein was determined as a function of protein concentration by measuring reductions in bulk protein concentration. The technique was useful as it measured adsorption under operating conditions. As hollow fibre membranes were used for this work, it should be noted that pressure drop between the inlet and the outlet of the fibre lumen can be significant at higher crossflows, possibly resulting in local transmembrane flux (and hence polarisation) at some points in the fibres. Calculations showed that this effect was not significant with the short fibre Amicon H1P10-20 module used here.

The amount of protein adsorbed to polysulphone membranes was found to be about 1.5 g per m^2 of membrane area at an equilibrium protein concentration of about 25 $g.l^{-1}$, in agreement with the work of others (Hanemaaijer et al, 1989). This amount was too great to be explained by monolayer adsorption to the nominal surface area of the membrane, and further experiments suggested that the high adsorbed amounts were due to a combination of multilayer adsorption and migration of protein through to the porous support structure of the anisotropic membranes. Migration of protein through the thin separating skin of the membranes might result in loss of enzyme during operation of a membrane reactor,

although in this work migration appeared to stop when a pseudo equilibrium occurred at fixed protein concentration.

Adsorbed amounts have been reported to increase with equilibrium protein concentration even at concentrations above the maximum of 25 $g.l^{-1}$ used in this work (Matthiasson et al, 1989). As protein adsorption is essentially irreversible (Norde, 1986), concentration polarisation will result in increased adsorption due to increased protein concentration at the membrane surface. Denaturation of enzyme may well take place upon adsorption, so that the adsorbed enzyme in a membrane reactor is likely to exhibit low (or zero) activity. The large amounts of protein that can be adsorbed may therefore significantly reduce membrane reactor performance.

It may be possible to select the degree of purity of an enzyme used in a membrane reactor. If so, there will clearly be a trade-off between highly active, pure samples which may lose large proportions of the enzyme mass (and therefore activity) to adsorption, and crude preparations where large amounts of protein are needed for the same activity. In the case of crude preparations, fouling problems may be increased due to the higher concentration of protein.

Dynamic exchange between adsorbed and dissolved protein appeared to occur with the polysulphone membranes used in this study. If such an exchange takes place, then in addition to the initial loss of activity upon enzyme addition and polarisation, a gradual loss of activity may be observed due to exchange of active enzyme in solution for denatured, inactive adsorbed enzyme.

In view of the above considerations, it is clearly desirable to minimise adsorption in order to reduce activity loss in an enzyme membrane reactor. Operating conditions were found to affect protein adsorption, such that adsorption:

(a) Increased towards the isoelectric point of the protein.

(b) Increased with increasing crossflow velocity (with polysulphone membranes).

(c) Decreased with increasing ionic strength (although this may depend on the solution pH relative to the isoelectric point of the protein).

The operating regime for a membrane reactor could be chosen to minimise protein adsorption, for instance by the use of low fluxes to reduce polarisation, and/or constant flux to prevent very high polarisation occurring when the membranes are new. The choice of membrane material will also have a considerable influence on adsorption. It is widely reported that hydrophobic membranes adsorb more protein than membranes made of hydrophilic materials. In this work, hydrophobic polysulphone membranes were found to retain their high adsorption capacity even after many cycles of use and cleaning. However, a 'low protein binding' (more hydrophilic) regenerated cellulose membrane showed a considerable drop in adsorption capacity after some use. The choice of membrane material may represent a compromise between fouling properties and usable lifetime, as 'low fouling' membranes are often less resistant to cleaning regimes.

It may be possible to pretreat membranes to reduce adsorption capacity. Investigation of pretreatments would have to include considerations of the effectiveness, economics, longevity and product compatibility of possible materials.

Modelling of protein adsorption to membranes requires that all the following observed phenomena are accounted for:

(a) Increase of equilibrium adsorbed amount with concentration.

(b) Slow reversibility.

(c) Dynamic exchange between adsorbed and dissolved protein.

(d) Multilayer and support side adsorption.

The literature search presented in this thesis has not identified a model which satisfies all these requirements. Clearly development of a suitable model must remain a major goal of work

in this area.

Polarisation

The constant flux ultrafiltration apparatus was used to measure the decrease in bulk protein (BSA) concentration occurring when a transmembrane flux was applied. The adsorbed amount was greater after polarisation, supporting the conclusion from the forgoing work that adsorption is essentially irreversible, and increases with concentration even at high protein concentrations. Increased crossflow rates resulted in decreased concentration polarisation, in accordance with established theory. After many use and cleaning cycles, increases in adsorption after polarisation were no longer observed. This shows that time dependent changes in membrane properties occur.

As well as affecting enzyme activity, the increase in fouling due to polarisation will affect membrane resistance. If fouling is severe enough, the desired permeate flux for a membrane reactor may not be obtainable within the pressure rating of the membrane, leading to over long residence times. Addition of membrane area to solve this problem obviously provides a greater area for protein adsorption, thus possibly causing greater loss of enzyme activity. In the case of macromolecular substrates, fouling problems will be even greater, but there may be a (desirable) reduction in enzyme-membrane interactions due to the reduced opportunity for enzyme-membrane contact at the necessary adsorption sites.

It seems that reduction of fouling due to polarisation is desirable in an enzyme membrane reactor. This could be achieved by pretreatment, choice of membrane material or constant flux regimes as discussed earlier, and also by reduction of the degree of polarisation by hydrodynamics.

A model describing the change in bulk protein concentration due to polarisation was developed. It allowed the bulk enzyme

concentration to be estimated in order to calculate reactor performance. The model was based on approximating the polarised layer as a region of uniform concentration and constant thickness. Mass balances over the regions of the recycle loop were combined with the approximation of the polarisation layer to complete the description of the constant flux apparatus. Although this was clearly a major simplification of the true situation where polarisation develops over the length of the permeating channel, the model was capable of describing changes in bulk protein concentration with flux and crossflow. The model could also be used to estimate the average concentration at the membrane surface (wall concentration) in order to correlate this concentration with adsorbed amount under polarisation conditions.

A rigorous approach to modelling concentration polarisation in a permeating channel requires solution of the partial differential equations describing the concentration and velocity profiles in two dimensions. In addition, the time dependent relationships between wall concentration and adsorption, rejection and membrane permeability must be known. In practice, these relationships are not directly measurable and cannot at present be predicted accurately. Therefore the computational cost of rigorous models is of doubtful benefit.

The work showed that changes in bulk protein concentration can be described by a simple model capable of analytical solution using parameters that were estimated empirically. Although in this work changes in bulk enzyme concentration due to polarisation proved to be of less significance to reactor performance than the effects of enzyme adsorption and solute rejection, this might not be so in all cases. The simple analytical model whose parameters can be empirically estimated should be of use in preliminary assessments of membrane configurations and operating regimes for membrane reactors.

Rejection

Observed rejection of a tracer molecule (adenosine 5′ monophosphate, 5′AMP) was measured in the constant flux ultrafiltration apparatus by spectrophotometric determination of retentate and permeate tracer concentrations. Rejection of molecules of this size may affect the performance of enzyme membrane reactors, as the products (and sometimes substrates) may be of approximately this size. The rejection of substrate and product molecules will determine the operating conditions in the reactor, and hence affect reaction rate and conversion.

Membrane fouling was found to significantly affect tracer rejection although the tracer (molecular weight 347.2) was much smaller than the nominal molecular weight cutoff of the membrane (10,000). Tracer rejection by the fouled membrane was as great as 60%, in contrast to rejections of 15% by a clean (not new) membrane. The cleaning regime (consisting of backflushing the hollow fibre membrane with 0.1M NaOH) reduced rejection from the fouled value, but was not able to return the rejection to the value of 15% observed *before* fouling.

The presence of polarised protein was found to have little additional effect on tracer rejection over the case of adsorbed protein only. However in the hollow fibre system used, the maximum polarisation obtainable was limited by the pressure rating of the membrane and it was unlikely that boundary layer protein concentrations were particularly high. Others have reported that very high boundary layer concentrations can affect rejection of small molecules (Ingham et al, 1980).

It has often been assumed that the rejection of small molecules by membranes used in enzyme reactors remains constant, but this may not always be true. Increased rejection of smaller molecules may have several implications for membrane reactors. Stability of enzymes has been found to depend on substrate and product concentrations (Vasudevan et al, 1990), and so variations in

operating concentrations due to rejection changes may affect enzyme stability as well as reaction rate. In addition to increased substrate and product concentrations leading to different reaction conditions, it may be possible to achieve desirably high rejections of native cofactors. Alternatively, if high rejections of smaller molecules must be avoided, it may be possible to use membranes of a higher molecular weight cutoff than would normally be specified, so that the modified rejection properties after fouling correspond to those required for operation of the membrane reactor.

Reaction

A model reacting system (urease-urea) was used to study the effects of fouling and polarisation in the constant flux apparatus. Loss of enzyme activity was rapid, necessitating a 'snapshot' or non steady state approach to obtaining kinetic data. Deactivation in this system seemed to be attributable mainly to denaturation of the enzyme by interaction with the membrane. Other common causes of deactivation such as sulphydryl group oxidation or presence of heavy metal ions were less significant.

Long term operation of a membrane reactor is likely to require lower rates of enzyme deactivation than those found in this work. Strategies intended to reduce protein adsorption to membranes may be beneficial in this situation. Although enzyme deactivation by adsorption has been observed by others (Ohlson et al, 1983), protein adsorption to membranes is a very system dependent phenomenon and the problem may be less severe with other enzymes or membranes.

Urea hydrolysis by urease was investigated as a function of flux (residence time) and feed substrate concentration in a constant flux ultrafiltration apparatus. A simple model considering the system as a continuous stirred tank reactor (CSTR) is valid hydrodynamically (Gacesa, 1977) and was successfully applied to this system. The CSTR model was combined with a kinetic

expression, and consideration of substrate and product rejection was included. The use of the CSTR approximation was further validated by the low degree of concentration polarisation in the hollow fibre module, which resulted in a negligible effect of enzyme distribution on reactor performance in this case.

Kinetic and rejection parameters were estimated using a parameter optimisation routine in which the error between the model and experimental results was systematically minimised. Kinetic parameters estimated in this way were similar to literature values (Ramachandran and Perlmutter, 1976), which suggests that the experimental technique and modelling approach used were valid. Estimates of the rejections of substrate and product were quite high at about 80% for substrate (urea) and between 9% and 47% for product (ammonium ions). The experimental data was insufficient to determine the rejections with certainty, and these should ideally be measured directly under reaction conditions.

Modelling

Modelling of concentration polarisation in a membrane channel was discussed earlier in this chapter, the main conclusion being that lack of information on the effect of wall concentration on adsorption, rejection and membrane resistance renders a rigorous solution impossible at present. It was, however, possible to model the spatial variation of solute concentration and velocity in a membrane channel in two dimensions. This was facilitated by assuming constant membrane permeability and by using analytical approximations for the velocity profiles in permeating flow. These assumptions mean the model was of little use for ultrafiltration processes, as it did not consider the time dependent nature of membrane fouling, and in fact required information on membrane fouling to be supplied. However it was possible to extend the distributed parameter model to describe a reacting enzyme system.

In this work the equations describing a distributed parameter

model of a hollow fibre membrane reactor with a product inhibited enzyme reaction were derived. Equations for enzyme, substrate and product were required, including reaction terms where appropriate. The model was solved using an explicit (discretisation) technique for the case of zero reaction rate, and the results showed the development of protein polarisation from the entrance to the exit of the fibre. The 'no reaction' solution was verified by mass balance. Attempts to solve the model under reaction conditions encountered stability problems, and it seems that an implicit technique would be necessary in this case.

The distributed parameter membrane reactor model developed here may be of use in determining the effect of concentration polarisation on a membrane reactor, as the model takes into account solute distribution in the membrane channel. Such a model might be used to determine the conditions under which polarisation significantly affects reactor performance. The model might be particularly useful for scaleup of membrane reactors, where the effects of enzyme-membrane interactions are known from small scale experiments, but the effects of greater size and volume are unknown. However, application of a distributed parameter model to a recycle membrane reactor would require simultaneous solution of models describing reaction in the other regions of the system, thus complicating the solution.

Summary

Enzyme membrane reactors are affected by solute polarisation, rejection and adsorption. In the case of moderate polarisation applying to this work, adsorption and rejection were the most significant factors controlling reactor performance. Quite large quantities of protein were adsorbed to the membrane and adsorption seemed to result in deactivation through denaturation. Significant enzyme deactivation occurred in the system studied here, leading to a long term decline in performance. Dynamic exchange of enzyme between adsorbed and dissolved states seemed to contribute to long term loss of enzyme activity. It therefore

seems desirable to minimise adsorption in a membrane reactor system if such deactivation occurs.

Fouling of membranes by proteins (i.e. protein adsorption) caused high rejections of a molecule which was much smaller than the nominal molecular weight cutoff of the membrane. This indicated that the operating concentrations in a reactor may change as the membrane fouls, and this should be considered when evaluating a membrane reactor system.

Concentration polarisation affected membrane fouling by changing the solute concentration at the membrane surface, and was therefore important in determining reactor performance. In addition, more severe polarisation might affect the performance of a membrane reactor by changing the spatial enzyme distribution. Understanding of the effects of polarisation might be improved by further development of distributed parameter models of membrane reactors capable of accounting for solute distribution.

REFERENCES

Brash, J.L.; Samak, Q.M.
"Dynamics of interactions between human albumin and polyethylene surface".
J. Colloid Interface Sci., 65 (1978) 495-504.

Gacesa, P
"Catalytic reactors using soluble enzymes".
PhD Thesis, University of Bath, (1977).

Hanemaaijer, J.H.; Robbertsen, T.; Boomgaard, T.; Gunnink, J.W.
"Fouling of ultrafiltration membranes. The role of protein adsorption and salt precipitation".
J. Membr. Sci., 40 (1989) 199-217.

Ingham, K.C.; Busby, T.F.; Sahlestrom, Y.; Castino, F.
"Separation of macromolecules by ultrafiltration: Influence of protein adsorption, protein-protein interactions, and concentration polarisation".
Ultrafiltration Membranes and Applications, ed Cooper, A.R. (1980)

Leuchtenberger, W.; Karrenbauer, M.; Plocker, U.
"Scale-up of an enzyme membrane reactor process for the manufacture of L-enantiomeric compounds".
Ann. N.Y. Acad. Sci., 434 (1983) 78-86.

Matthiasson, E.; Hallstrom, B.; Sivik, B.
"Adsorption phenomena in fouling of ultrafiltration membranes".
Engineering Sciences in the Food Industry, ed. McKenna, B.M. (1989).

Norde, W.
"Adsorption of proteins from solution at the solid-liquid interface".
Adv. Colloid Interface Sci., 25 (1986) 267-340.

Ohlson, I.; Tragardh, G.; Hahn-Hagerdal, B.
"Recirculation of cellulolytic enzymes in an ultrafiltration membrane reactor".
Acta Chemica Scandinavica, 37 (1983) 737-738.

Ramachandran, K.B.; Perlmutter, D.D.
"Effects of immobilization on the kinetics of enzyme catalysed reactions. II. Urease in a packed column differential reactor system".
Biotechnol. Bioeng., 18 (1976) 685-699.

Turker, M.; Hubble, J.
"Membrane fouling in a constant flux ultrafiltration cell".
J. Membrane Sci., 34 (1987) 267-281.

Vasudevan, P.T.; Ruggiano, L.; Weiland, R.H.
"Studies on the deactivation of immobilized urease".
Biotechnol. Bioeng., 35 (1990) 1145-1149.

Last Page of Chapter 8